School of Doctoral Studies in Biological Sciences

University of South Bohemia in České Budějovice
Faculty of Science

Stability and dynamics of size-structured freshwater communities along environmental gradients

Ph.D. Thesis

MSc. Samuel Dijoux

Supervisor: doc. Ing. MgA David Boukal, Ph.D.
Department of Ecosystem Biology, University of South Bohemia
Institute of Entomology, Biology Centre of the Czech Academy of Science

České Budějovice 2023

This thesis should be cited as:

Dijoux S., 2023: Stability and dynamics of size-structured freshwater communities along environmental gradients. Ph.D. Thesis Series, No. 4. University of South Bohemia, Faculty of Science, School of Doctoral Studies in Biological Sciences, České Budějovice, Czech Republic, 2023 190 pp.

Annotation

This thesis focuses on the dynamics and stability of size-structured communities in freshwater in response to environmental stressors. It reviews the influences of anthropogenic stressors on the stability, structure and diversity of freshwater communities, with a particular focus on the multiscale influences of rising temperature and nutrient enrichment. The three main chapters use recent advances in food web theory to explore the dynamics, stability and structure of communities under multiple threats (species invasions, nutrient enrichment and warming). The theoretical outcomes provide robust predictions for ecologists to link individual-level responses to global patterns observed at community scale. This thesis demonstrates the importance of considering species traits (body size, trophic position, performance of vital rates) and life histories to improve predictions on future responses to environmental stressors and to develop appropriate conservation measures.

Declaration

I hereby declare that I am the author of this dissertation and that I have used only those sources and literature detailed in the list of references.

České Buějovice, 06.04.2023

……

Samuel Dijoux

This thesis is originated from a partnership of Faculty of Science, University of South Bohemia, and Institute of Entomology Biology Centre CAS, supporting doctoral studies in the Ecosystems Biology study program.

Financial support

The studies were financially supported by the Czech Science Foundation (GAČR no. 17-15480S, 21-29169S) and the Grant Agency of the University of South Bohemia in České Budějovice (GAJU no. 158/2016/P and 116/2019/P). The funders had no role in conducting the research and/or during the preparation of the article.

Ker la Fournaise, Ker Flamboyant
Out flam' ka vassiyé mé zamé ka fanné.

Acknowledgements

This thesis would never have reached its completion without the help and motivational supports from many persons I met along the path.

I would like to first express my respects and gratitude toward my supervisor David Boukal, for his continuous and patient guidance all along my research. His endless "*Rule Number One*" have paved a long road toward the improvement of my research and writings.

I would like to thank all my collaborators, Arnaud Sentis, Noémie A. Pichon, Raul Primicerio and Aslak Smalås, for our beautiful collaborations, the exciting discussions that gave birth to countless project ideas and for the warm welcome I received during my visits at the INRAE (Aix-en-Provence) and at UiT (Tromsø).

Work would not have been possible without releasing some pressure. Many thanks go to my lab mates, Derya, Andrea LD, Claire, Julien, András, Vojta and Joacim, for the countless pivocytosis, the cheers and talks around the coffee machine. I wish to personally thank Julien, Joacim, Claire and Andrea LD for their good vibes and precious advices which help me shape the path of researcher I would like to become.

I would also like to thank all the friends and colleagues who voluntarily dedicated a bit of their time to talk and exchange about academia and science through all the *Academic coffee meetings* sessions, and those who make the *Academic Research Network* a reality for the time being. Sophie, Andrea LD, Lobsang, Derya, Noelia, Sonia, Andrea K, Patrick, Edu, Felipe, Miguel, just to name a few, thank you for all for this fantastic experience.

Mille mercis to Andreja & Vincent, my crazy rescuers between the Master and PhD. *Sans vous, cette thèse n'aurait jamais pu commencer sur de bonnes voies*. To Andrea LD, Derya, Sonia, Somi and Massoud for making the life around a bit brighter.

To all my family, ma mère, Natacha, Eddie, Sébastien, and Julie. Thank you to fuel me up with all the strength, hope and determination I needed when I felt weaken. This thesis is a token of my proudness and gratitude toward each of you.

And finally and above all, I deeply thank my fiancée Sophie for her everlasting love. Your never-ending trust and support were my lighthouse during all these stormy ups and downs.

In memory of my father to whom this thesis is dedicated.

List of papers and author's contribution

The thesis is based on the following papers:

I. **Dijoux, Samuel**; Pichon, Noémie A.; Sentis, Arnaud; Boukal David S. Body size and trophic position determine the outcomes of species invasions along temperature and productivity gradients. (Manuscript).

SD was involved in the design of the study (40%), wrote the code (90%), performed the numerical analyses (100%), led the data analysis (80%) and writing of the first draft (70%).

II. **Dijoux, Samuel**; Boukal, David S. (2021), Community structure and collapses in multichannel food webs: Role of consumer body sizes and mesohabitat productivities. Ecology Letters, 24: 1607-1618 (IF = 11.274).

SD was involved in the design of the study (50%), wrote the code (100%), performed the numerical analyses (100%), led the data analysis (80%) and writing of the first draft (70%).

III. **Dijoux, Samuel**; Smalås, Aslak; Primicerio Raul; Boukal, David. S. Temperature-dependent consumer growth rates, rather than temperature-size rule, determine the propensity for catastrophic collapses of top predators at suboptimal temperatures (Manuscript).

SD led the design of the study (70%), wrote the code (100%), performed the numerical analyses (100%), led the data analyses (80%) and co-led writing of the first draft (50%).

Co-author agreement

David Boukal, the supervisor of this Ph.D. thesis and co-author of papers I., II, III., fully acknowledges the stated contribution of Samuel Dijoux and his status of the first author in these manuscripts.

……

David S. Boukal

Content

Introduction ……..…….……1

Freshwater communities in the Anthropocene ……3
Effects of warming & nutrient enrichment: from individuals to communities ……..……..…….4
Study of food webs as a tool to predict community responses to global change ……7
Trophic modules and drivers of species coexistence ……8
Size and temperature dependence of vital rates: the role of metabolic ecology ……..10
The interplay between species life histories and environmental changes ……..11
Aim and scope of this thesis ……..……14
Chapter overview ……..…….....15
References ……..…20

Chapter I. ……..……29
Supplementary information ……..…65

Chapter II. ……...……103
Supplementary information ……117

Chapter III. ……..……..…….133
Supplementary information ……163

Summary ……..……..……175
Take-home messages and future directions ……..……...180

Curriculum vitae ……183

~ Introduction ~

~ Thesis Introduction ~

Stability and dynamics of size-structured freshwater communities along environmental gradients

Freshwater communities in the Anthropocene

Freshwater ecosystems include a wide range of habitats including standing waters (puddles, bogs, ponds, wetlands, lakes, and reservoirs) and running waters (streams to rivers) that differ in their chemical and physical properties. Freshwater ecosystems therefore cover large environmental gradients that shape local communities (Wellborn et al. 1996). These ecosystems cover only 0.8% of the Earth's surface but harbour more than 10% of the animal biodiversity (Stendera et al. 2012; Darwall et al. 2018). Freshwater communities are dominated by ectotherms from different phyla—ranging from zooplankton to macroinvertebrates, molluscs and fish—that occupy different trophic levels and feeding guilds and are linked by trophic interactions.

These ecosystems have been undergoing unprecedented changes during the Anthropocene. Freshwater species are subject to multiple stressors (Dudgeon et al. 2006): habitat alterations and destruction, pollution (microplastics, chemical, heavy metals, and agricultural runoffs), nutrient enrichment, global warming, overharvesting and species invasions (Young et al. 2016; Isbell et al. 2017; IPBES 2019). These stressors impact freshwater biota stronger than terrestrial and marine biota (Forster et al. 2012). Since 1900, the global surface area of freshwater systems has declined by 64–71% (Davidson 2014), which lead to a 76% decline in biodiversity only since 1970 (McLellan et al. 2014). This represents the highest rate of defaunation and the highest proportion of threatened animal species in freshwater habitats compared to other biomes (Young et al. 2016).

The rising multiplicity of threats to freshwater communities requires novel approaches in order to understand how species and entire communities will respond to human-induced global changes. The impact of multiple drivers on freshwater communities is particularly complex to disentangle due to three main reasons: 1) each driver can act on one or multiple scales of organization (from cells to ecosystem levels); 2) their impact can be simultaneously direct and indirect (i.e., through feedback effects or other processes). Finally, 3) individual drivers can interact through additive, antagonistic or synergistic effects (Galic et al. 2018).

Effects of warming & nutrient enrichment: from individuals to communities

Environmental changes driven by temperature and nutrient enrichment influence food webs at multiple scales through mechanisms ranging from altered individual metabolic rates to changed interspecific interactions (Binzer et al. 2012, 2016; Sentis et al. 2014). Global temperatures are predicted to increase by 1.4–4.4°C by the end of the 21st century (IPCC 2022). Such increase will have profound effects on ecosystems, impacting every level ranging from individual metabolism to community structure (Sala et al. 2000). Increasing temperatures influence aquatic communities more than terrestrial ones given the dominance of ectotherms in aquatic habitats (Young et al. 2016).

Three general "rules" have been proposed to describe the impact of global warming on biota. First, warming induces shifts of species ranges toward higher latitudes and altitudes (Parmesan & Yohe 2003; Sunday et al. 2012). The arrival of new species more acclimated to warmer temperatures in higher latitudes (Bellard et al. 2013; Seebens et al. 2021) will further induce more pressure on cold-tolerant species that might be less competitive and resilient to invasions (Bellard et al. 2016; Sentis et al. 2021). These migrations from tropical and temperate to Arctic areas will simultaneously result in loss of ecosystem diversity and functions, making the communities more vulnerable to collapse (Walther et al. 2002; Wardle et al. 2011).

Second, warming impacts food webs by inducing changes in the phenology of the constituent species, which may result in synchronous or asynchronous temporal shifts of prey and their predators during the season. This effect, termed the match-mismatch hypothesis, may have profound effects on trophic interactions and lead to the loss of some consumers (Johansson et al. 2015; Reinhardt et al. 2015).

Third, the so-called "temperature-size rule" (TSR) predicts the reduction of body size of ectotherms with warming (Gardner et al. 2011). TSR seems to be particularly prominent and widespread in aquatic ectotherms (Sheridan & Bickford 2011; Lavin et al. 2022). On an individual level, TSR may result from a mismatch between individual growth and development rates with warming (Atkinson 1994; Angilletta 2004; Brown et al. 2004; Kingsolver & Huey 2008) causing individuals to grow faster and maturate at smaller sizes when developing under warmer conditions (Atkinson 1994; Forster et al. 2012). On the community level, TSR can increase community persistence by modifying predator-prey mass ratio and altering the interaction strengths and energetic efficiency of trophic transfer (Sentis et al. 2017). The main drivers responsible for warming-induced size reduction have been under debate for three decades, either explained by the increasing metabolic demands in oxygen with warming (Atkinson 1994; Verberk et al. 2021) or due to increasing allocation costs in gonadic growth with warming (Audzijonyte & Richards 2018; Wootton et al. 2022). The observed reductions in mean species body size at the community level can also be explained by demographic effects: the increase of abundance of small species and decrease in body size at the population level as a result of increased juvenile abundance and decreased individual body sizes (Daufresne et al. 2009; Forster et al. 2012). Increased abundance and reduced body size might be advantageous for species that invade new habitats (Sentis et al. 2021), for example through higher capacity to exploit resources via exploitative competition (Reuman et al. 2014; Dijoux et al. 2023 (Chapter I)).

Despite these "rules", the implications of the relationships between individual body mass, temperature and many individual-level processes and species interactions for the community structure and persistence are

still not fully explored. Recent studies showed that warming can enhance community stability by decreasing interaction strengths between trophic levels (Rall et al. 2010; Fussmann et al. 2014; Sentis et al. 2014, 2015) that lead, e.g. to smaller amplitudes of cycling populations in a food chain model (Binzer et al. 2012). Metabolic rates tend to increase faster with temperature than feeding rates, which can cause species starvation, especially at higher trophic levels (Rall et al. 2012; Seifert et al. 2014, 2015; Lindmark et al. 2019). In consequence, warming is expected to rewire food webs, selecting for shorter food webs with smaller predators in lower trophic positions (Brose et al. 2012; Boukal et al. 2019).

Together with warming, eutrophication of freshwater habitats represents another main driver of environmental change that affects communities (Schindler 2006). Nutrient availability plays a key role in the synthesis and repair of biomolecules that are vital for individual growth, somatic maintenance and survival (Elser et al. 1996). In food webs, the highest amount of energy that basal resources can convert from nutrients to biomass is estimated by their carrying capacity and represents the habitat productivity. At the community scale, increases in habitat productivity lead to a proportional increase of primary producers or higher trophic levels depending on the structure of the food web (Fretwell 1987). However, nutrient enrichment in freshwaters induced by increasing amounts of wastewater, more intensive land use and fertilizer consumption (McCann 2020) can destabilise communities via the "paradox of enrichment", in which stable population equilibria become unstable and give rise to increasing oscillations until reaching extinction boundaries (Rosenzweig 1971; Oksanen et al. 1981). Habitats subject to nutrient enrichment are therefore expected to be most impacted in term of biodiversity loss (Isbell et al. 2013), making communities more vulnerable to collapses and loss of ecosystem functions. Some of these effects lead to strong regime shifts at the level of entire ecosystems. For example, the loss of water transparency in shallow lakes during a shift from a clearwater state dominated by macrophytes to a turbid state dominated by phytoplankton and algal blooms (Scheffer et al. 1993, 2001; Janssen et al. 2014) typically causes not only the loss of vegetation but can also lead to more frequent anoxic condition and loss of oxygen-sensitive species in the animal community.

Warming can catalyse the destabilising influences of eutrophication on the community structure through its multiple effects ranging from individual organisms to community structure (Binzer et al. 2012; Rodgers 2021). Warming notably enables the strengthening of the trophic cascade from fish to primary producers (Kratina et al. 2012) by inducing increased predation pressure on zooplankton populations, which releases the pressure on phytoplankton and in turn leads to higher assimilation of excess nutrients (Shurin et al. 2012).

Study of food webs as a tool to predict community responses to global change

The study of food webs offers a robust solution to study the effects of novel stressors on freshwater communities. Food webs describe the flows of energy within the community from basal resources towards upper trophic levels through grazing and predation. The structure of food webs can range from simple trophic chains to highly complex, modular networks (Schoener 1989; Holt et al. 1994; Wollrab et al. 2012). Complex food webs, characterized by high connectance and non-random distribution of trophic links, are often more resilient to species extinctions and environmental change than simple or random structures (May 1974). Redundant trophic links therefore enable species turnover and prevent the collapse of food webs (Dunne et al. 2002; Allesina et al. 2009; Bascompte & Stouffer 2009). The relationships between food web structure and community dynamics highlight how changes at a population scale (e.g. changes in survival and reproduction) influence the community composition through top-down and bottom-up effects and energy flows (Oksanen et al. 1981; Fretwell 1987; Wollrab et al. 2012). For example, food web models predict that warming can counterbalance the destabilising effect of nutrient enrichment on communities, which leads to lower efficiency of the consumers and thus weakens the trophic links (Binzer et al. 2012; Sentis et al. 2014). Moreoever, these models predict that higher predator-prey mass ratios might counter the effects of enrichment and stabilise the dynamics at low temperatures (Binzer et al. 2012, 2016; Wollrab et al. 2012).

Research on food web structure and dynamics has been transformed by recent emphasis on the role of species traits (Boukal 2014; Brose et al. 2019; Wootton et al. 2021). Indeed, freshwater food webs are strongly size-structured. They include small organisms with usually low dispersal abilities at low trophic levels and larger organisms with usually higher dispersal abilities occupying higher trophic levels (Rooney et al. 2008). Larger species therefore tend to link mesohabitats across spatial and time scales and connect different energy pathways that rely on the photosynthetic activity by phytoplankton in pelagic mesohabitat and on the decomposition of allochtonous matter by decomposers in benthic mesohabitat (Schindler & Scheuerell 2002; Vander Zanden et al. 2002; McCann & Rooney 2009). The linkage of 'fast' and 'slow' energy transfer relying on asymmetric turnover rates between mesohabitats enables the persistence of large predators in freshwater systems (Rooney et al. 2006) and the maintenance of a large biomass of the top predator (McCauley et al. 2018). Such biomass structure in freshwaters thus follows an inverted pyramid (or 'top-heavy' pyramid), which contrasts with the 'bottom-heavy' pyramids, described by Elton (1927) as a gradual decrease of the large biomass produced by primary resources towards higher trophic levels due to metabolic and other losses (McCauley et al. 2018).

Trophic modules and drivers of species coexistence

Trophic modules are the building blocks of food webs (McCann 2011) and constitute case studies to investigate how environmental changes affect the dynamics and stability of simple communities. A small number of food web modules including three species describes all possible direct and indirect pairwise interactions between these species: apparent competition of species sharing a common predator, exploitative competition of species sharing common resources, tri-trophic chain in the absence of such competing interactions (with a top predator, intermediate consumer, and basal resource), and intraguild predation combining competition and predation. In the latter module, the community is composed of an omnivorous top predator that competes with the intermediate prey species for basal resources (Wootton 2017). Studies of these trophic modules have

enabled us to understand mechanisms driving species coexistence in natural systems. Models of exploitative competition predict that the species or life stage able to reduce the amounts of available resources in the system dominates the competition (Persson et al. 1998), as described by the resource-ratio hypothesis (stated as the R* rule) (Tilman 1985). As an analogous rule to R* rule, the P* rule predicts that the prey species that enables higher increase in predator population dominates in apparent competition (Holt et al. 1994). Both apparent and exploitative competition can operate jointly; the lack of available resources and increased predation pressure then become the two determining factors that can drive the less efficient species to extinction (Holt et al. 1994). In intraguild predation, species can coexist under the condition that the intraguild prey is a better competitor than the intraguild predator, while simultaneously resisting predation-induced mortality to avoid its exclusion (Holt & Polis 1997; Wootton 2017).

These classical food web modules and the mechanisms that drive species coexistence or exclusion enable us to explore and understand how communities may respond to species invasions induced by global change scenario. The arrival of a new species can influence the structure and dynamics of resident community through dynamic processes driven by the interplay between the local abiotic filter and the performance of resident and invading species in the system (Chesson 2000; Kraft et al. 2015). Species invasions can shift communities away from their initial equilibrium state, perturb species interactions, suppress less resilient species, and cause cascading effects through the entire food web (Gallardo et al. 2016; Reynolds & Aldridge 2021). Incoming species, however, do not always negatively influence resident communities. They can be perceived as a biodiversity source that can fuel ecosystem resilience to destabilizing environmental stressors. For example, invading species can serve redundant functions that help prevent potential community collapse; they can also occupy empty niches vacated by extinct species and hence restore previously lost ecosystem functions (Herbold & Moyle 1986; Moyle & Light 1996; Dijoux et al. 2023 (Chapter I)).

Size and temperature dependence of vital rates: the role of metabolic ecology

More recently, food web studies have begun to shift from describing processes at the population level to processes at the individual level to provide more mechanistic descriptions of food webs. This approach is based on the observation that key phenotypic traits such as body size, foraging behaviour and habitat use drive individual life histories, i.e., growth, development, survival and fecundity, which in turn give rise to population- and community-level patterns (de Roos et al. 2003, 2013; Gårdmark et al. 2015).

Many recent papers on food web structure and dynamics rely on the principles of metabolic ecology. They unite two universal and ecologically relevant dependencies: the temperature and size dependence of vital rates. It implies that larger organisms have a slower mass-specific metabolic rate than smaller organisms, have a longer lifespan, but require more resources to sustain themselves than smaller organisms (Brown et al. 2004). Higher temperatures increase individual metabolic demands and, within a certain thermal range, lead to faster vital rates (Gillooly et al. 2002). Size- and temperature-dependent metabolism therefore plays crucial role in individual energy budgets (Gillooly et al. 2002; Brown et al. 2004; Woodward et al. 2005), with cascading effects on higher levels of biological organization. Bio-energetic and biomass-based models (e.g., Yodzis & Innes, 1992) link individuals to populations and communities that use the principles of metabolic ecology are necessarily more complex than classical models based on population size, such as Lotka-Volterra models (May 1974; McCann 2011). On the other hand, they lead to new insights into community functioning (Rall et al. 2012; Dell et al. 2014; Fussmann et al. 2014; Gounand et al. 2016) and biomass distributions within food webs (Bideault et al. 2021; Synodinos et al. 2021; Sentis et al. 2022) by using allometric scaling rules (Petchey et al. 2008).

The interplay between species life histories and environmental changes

Individuals and their interactions with the environment change substantially through ontogeny, especially in taxa that grow multiple orders of magnitude during their life, such as most fish species (de Roos et al. 2013). The inherent ontogenetic asymmetry in individual life histories can affect the structure and stability of populations, which can have profound cascading consequences for food webs (Fig. 1a). Three aspects determine the relationship between individual life history and population cycles: the delay between birth and first reproduction, size allometries of vital rates (e.g., increase in food intake efficiency with body size) and environmental feedbacks on individual life histories. Changes in environmental conditions can also have different repercussions on population dynamics depending on the nature of ontogenetic asymmetry (de Roos et al. 2013; Persson & de Roos 2013). Accounting for species life histories appears crucial to investigate mechanisms and intriguing phenomena that cannot be described by classic approaches treating individuals within populations as identical or reducing species to a set of constant traits (e.g., fixed body mass, trophic position, or feeding strategy). Studies focusing on size- or stage-dependent life histories can explain how novel patterns at the population level arise from the interplay between environmental conditions and species traits. For example, an emergent Allee effect can arise in a predator population when the biomass of juvenile prey, driven by decreasing habitat productivity, becomes insufficient to maintain predator biomass, which in turn collapses (Fig. 1b; de Roos & Persson 2002; de Roos et al. 2003). Sudden population collapses can trigger further shifts in the community structure, characterized by the simultaneous presence of two stable equilibria for a given range of environmental conditions (Fig. 1c; de Roos & Persson 2002; de Roos et al. 2003; Lindmark et al. 2019; Dijoux & Boukal 2021 (Chapter II)).

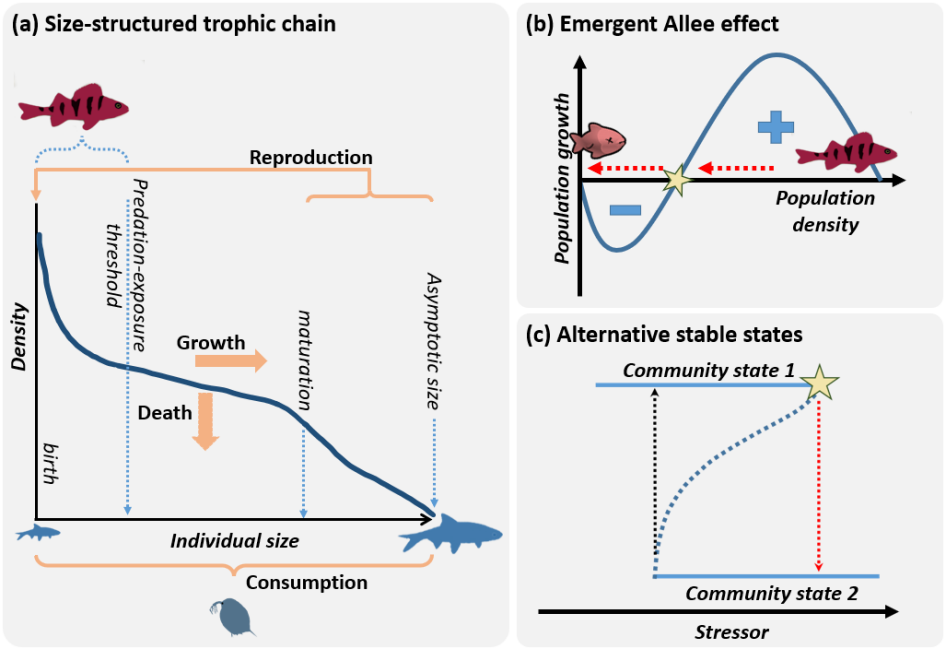

Figure 1. Schematic description of (a) size-structured life history of an intermediate consumer in a trophic chain leading to emergent phenomena (b) in top predator population (i.e., emergent Allee effect) and (c) in community transitions along the gradient of a stressor. Core model of a size-structured trophic chain, as described in de Roos & Persson (2002), Dijoux & Boukal (2021) (Chapter II), and in Chapter III. The trophic chain is composed of an unstructured population of the basal resource (cladoceran *Daphnia* sp.) and an unstructured population of perch as the top predator (*Perca fluviatilis*) that prey upon a size-structured population of European roach (*Rutilus rutilus*). Consumer population is characterized by a strong intraspecific competition between juveniles and adults for common resources, resulting in density-dependent growth and recruitment. Only small juvenile consumers are vulnerable to predation. (b) The 'cultivation effect' of the predator on juvenile consumer biomass means that predator population growth rate can become negative and the population collapse when it decreases below an Allee effect threshold (yellow star). (c) Such extinction marks a sudden shift in the community state (from state 1 to state 2) along a stressor gradient, with alternative stable states (superposition of two states at equilibria) between the threshold values denoting predator invasion (upward arrow) and collapse (downward arrow) along the stressor gradient.

Physiologically structured population models account for individual life histories and enable to investigate the feedbacks between individual life histories and the environment (de Roos 2020, 2021). Compared to classic abundance or biomass-based models (e.g. Yodzis & Innes (1992)), the inclusion of individual state into population-dynamic models requires additional equations that describe individual-level processes such as fecundity, survival and growth. As a minimum, the individual state can be described by age, size and/or developmental stage (de Roos et al. 2003), but additional traits such as boldness/shyness (Réale et al. 2010) can increase the realism of such models. These models are particularly useful to study the effects of anthropogenic stressors on freshwater biota as they enable to directly link the impacts of anthropogenic stressors from individual traits and life histories to the community scale. For example, they can enable to investigate the joint effects of temperature-size rule and temperature-dependencies of species vital rates (growth, reproduction, ingestion) in size-structured population, their impact on predator population persistence, and community transition along environmental gradients (de Roos & Persson 2002; Lindmark et al. 2019; Chapter III).

Disentangling the multiple effects of environmental change driven by temperature and nutrient enrichment on aquatic biota is a challenging task. Food web models have proven to be useful to tackle those challenges when experimental approaches are time and resource demanding. Models can conveniently test various scenarios, such as switching on and off different mechanisms and comparing the outcomes to observed patterns. Developing suitable models can thus improve our understanding of the implications of environmental change that influences freshwater communities, and more generally, to understand how individual-level responses to these changes influence food web structure and persistence.

~ Aim and scope of this thesis ~

In this thesis, I studied selected impacts of anthropogenic environmental change on freshwater populations and communities. I asked the following questions:

Q1) How do body size and habitat niche influence population dynamics, species coexistence, and freshwater community structure?
Q2) Does body size and trophic position matter when we investigate community responses to invading species along key axes of environmental change?
Q3) *How do environmental conditions affect size-dependent life histories and their impact on food web structure and persistence?*

I have addressed these questions in the three chapters of this thesis, using biomass-based models of population dynamics and physiologically structured population models accounting for the commonly observed size- and temperature-dependent biological rates.

~ Chapter overview ~

Chapter I. Body size and trophic position determine the outcomes of species invasions along temperature and productivity gradients. [Manuscript under review in *Ecology Letters*]

Chapter I focuses on how simple communities respond to species invasions along gradients of temperature and nutrients. I develop a set of bioenergetic models accounting for mass- and temperature-dependent biological rates and two key invader traits (trophic position and body mass) to analyse the changes induced by an invading species in a resident community in terms of community composition, diversity and stability. The five trophic modules covered in this chapter, i.e., apparent competition, exploitative competition, trophic chain and intraguild predation with the invading species playing the role of the intraguild prey or intraguild predator, enabled me to 1) synthesize all trophic interactions between the resident and invading species, and 2) determine the conditions underlying invasion success and failure in a changing world.

In this chapter, I highlight how species invasions lead to a variety of outcomes in communities along environmental gradients. I identify cases where the invading species could either mitigate or enhance the impact of global change on community diversity and stability. While invasions of smaller competing consumer often enhance the risk of community collapse due to eutrophication in cold habitats, invasions of larger invaders can prevent (at least partially) such collapses induced by eutrophication by either rescuing some species that were prone to extinction in absence of the invasion event, or by restoring some of the ecosystem function that was lost through species extinction (i.e., by filling new vacant niches).

I show that the changes induced by invading species on local communities are driven by the interplay between the abiotic conditions, resident size structure and the interactions formed between resident and invading species. Using pre-established principles of community coexistence/exclusion, I predict that smaller species will be more successful than larger resident species in communities subject to warming

and nutrient scarcity, while larger invading predator will be more successful in communities subject to cold temperatures and nutrient enrichment.

Chapter II. Community structure and collapses in multichannel food webs: Role of consumer body sizes and mesohabitat productivities. [published in *Ecology Letters* (2021), 24: 1607-1618]

Chapter II focuses on how the combination of symmetries and asymmetries in mesohabitat productivities and consumer size jointly influence the community structure and stability of multichannel food webs.

I develop a physiologically structured population model (PSPM) representing a "minimal" multichannel food webs with five species across three trophic levels: a mobile unstructured top predator population (such as perch, *Perca fluviatilis*), preying on the early juvenile stages of two structured consumer populations (such as roach, *Rutilus rutilus*) each inhabiting pelagic and benthic mesohabitat and relying on its own resource (such as *Daphnia*). I vary the body size of the benthic consumer relative to its pelagic counterpart, i.e., by integrating a size ratio in individual length at birth, at maturation and asymptotic length, under gradients of mesohabitats resource productivities. I investigate how 1) consumer sizes influence their life history traits (development, birth and growth rates and generation time) under varying predation exposure and mesohabitat productivities; 2) these traits influence the communities size structure and persistence at both mesohabitat scale with a local predator (a trophic chain), and 3) multichannel food web scale when predator feed on both pelagic and benthic populations. The highlights of this study are threefold and improve our understanding of the dynamic structure and persistence of multichannel food webs, by linking consumer size, resource productivity and exposure of the consumers to predation in both mesohabitats.

At the population level, a larger consumer species has a higher growth rate, but a lower birth rate due to high intraspecific competition with juveniles,

than a smaller consumer in the absence of predation. However, the larger species benefits from predation mortality due to a release from intraspecific competition, which enables a higher birth rate compared to the smaller consumer.

At the mesohabitat scale (in a trophic chain), increasing consumer body size does not (measurably) affect its minimum resource requirements but increases habitat productivity thresholds required for predator persistence and invasion. This is explained by an emergent Allee effect in the predator population when reduced prey availability (due to decreased predation exposure of juvenile consumers) leads to a negative depensatory population growth. When such persistence threshold is reached, predator population collapses and the community state suddenly shift from a trophic chain to a consumer-resource system. Through the influence on predator invasion and persistence, larger consumer sizes increase the range of mesohabitat productivities with a bistability regime, i.e., two alternative equilibria (consumer-resource and trophic chain) separated by an unstable equilibrium.

At the multichannel food web scale, the linkage of mesohabitats differing in their productivity and consumer size can alter and disrupt the whole community structure by affecting both predator and consumer species. The coexistence or exclusion of pelagic and benthic consumers involved in apparent competition due to the mobile top predator are driven by the energy balance between both mesohabitat pathways and follows predictions of the P* rule, stipulating that the preyed species able to sustain the highest predator biomass wins and dominates the competition. This shows why multichannel food webs occur in natural systems despite the asymmetries in consumer sizes and mesohabitat productivities: thee rely on a compensation effect of these two types of asymmetries. In other words, freshwater multichannel food webs remain stable due to an energy balance between pelagic and benthic system, with the more productive pelagic habitat feeding smaller pelagic consumers and less productive benthic habitat sustaining larger consumer. In the absence of such compensatory mechanisms, the community structure would be disrupted and likely collapse. Such habitat linkage also offers additional community

transitions that lead to the emergent Allee effect in predator population. Moreover, I also predict that such community shift can be followed by a sudden loss of the lesser competitive consumer, a novel phenomenon named *Cascading Emergent Allee effect*. This effect appears when both asymmetries, instead of compensating each other, act synergistically: the mesohabitat with low resource productivity is inhabited by a smaller consumer, while the other mesohabitat with higher productivity has large consumers. The population of the smaller, competitively inferior consumers therefore collapses as soon as the top predator population establishes in the system, e.g., when the overall levels of habitat productivity increase.

The homogenization of freshwater habitats induced by habitat degradation and eutrophication are likely to either disrupt the energy pathways within multichannel food webs through the loss of less resilient species, or to reduce the disparities between mesohabitats and tend to select species with similar traits. This will in consequence simplify the structure of freshwater food webs, characterised by a decreased biodiversity and ecosystem services, and make the system more prone to collapse under further stressors (e.g., species invasions, pollution, warming).

Chapter III. Temperature-dependent consumer growth rates, rather than temperature-size rule, determine the propensity for catastrophic collapses of top predators at suboptimal temperatures. [Manuscript].

Chapter III focuses on the relative contribution of food and temperature dependence of vital rates and the temperature-size rule for the structure of a tri-trophic chain along gradients of habitat productivity and temperature. Here I focus on the emergent Allee effect in the top predator covered also in Chapter II, where I only considered the role of body size and habitat productivity.

Using the same core model as in Chapter II, I extend the physiologically structured population model describing the trophic chain composed of unstructured populations of basal resource and top predator and size-

structured consumer. To this model I add two common responses of species to warming: size reduction of the consumer and/or top predator population (by varying the size threshold of predation exposure, size at maturation and asymptotic size of the consumers) and temperature-dependent consumer life history and predator mortality and foraging efficiency. This allows a detailed investigation of the role of direct and indirect influences of temperature on species in shaping community structure. I explore multiple scenarios in which I test the influence of each type of species response at the community level alone or in combination. I also consider temperature dependence only in consumer or in both consumers and the top predator.

My results show that the consequences of the direct and indirect species responses to warming (temperature-dependent vital rates and TSR) at the community level differ. I observe that the community structure along the gradients of habitat productivity and temperature is nearly identical when the model includes both temperature-dependent vital rates and TSR in the consumer as compared to a scenario that includes only temperature-dependent consumer vital rates, especially individual growth. This suggests that the direct effects of temperature-dependent somatic growth outperform those of temperature-size rule at the community level.

References

Allesina, S., Bodini, A. & Pascual, M. (2009). Functional links and robustness in food webs. *Philos T Roy Soc B*, 364, 1701–1709.

Angilletta, M.J. (2004). Temperature, Growth Rate, and Body Size in Ectotherms: Fitting Pieces of a Life-History Puzzle. *Integr Comp Biol*, 44, 498–509.

Atkinson, D. (1994). Temperature and Organism Size-A Biological Law for Ectotherms? *Adv Ecol Res*, 25, 1–58.

Audzijonyte, A. & Richards, S.A. (2018). The energetic cost of reproduction and its effect on optimal life-history strategies. *Am Nat*, 192, 150–162.

Bascompte, J. & Stouffer, D.B. (2009). The assembly and disassembly of ecological networks. *Philos T Roy Soc B*, 364, 1781–1787.

Bellard, C., Cassey, P. & Blackburn, T.M. (2016). Alien species as a driver of recent extinctions. *Biol Lett*, 12, 24–27.

Bellard, C., Thuiller, W., Leroy, B., Genovesi, P., Bakkenes, M. & Courchamp, F. (2013). Will climate change promote future invasions? *Glob Chang Biol*, 19, 3740–3748.

Bideault, A., Galiana, N., Zelnik, Y.R., Gravel, D., Loreau, M., Barbier, M., *et al.* (2021). Thermal mismatches in biological rates determine trophic control and biomass distribution under warming. *Glob Chang Biol*, 27, 257–269.

Binzer, A., Guill, C., Brose, U. & Rall, B.C. (2012). The dynamics of food chains under climate change and nutrient enrichment. *Philos T Roy Soc B*, 367, 2935–2944.

Binzer, A., Guill, C., Rall, B.C. & Brose, U. (2016). Interactive effects of warming, eutrophication and size structure: Impacts on biodiversity and food-web structure. *Glob Chang Biol*, 22, 220–227.

Boukal, D.S. (2014). Trait- and size-based descriptions of trophic links in freshwater food webs: current status and perspectives. *J Limnol*, 73, 171–185.

Boukal, D.S., Bideault, A., Carreira, B.M. & Sentis, A. (2019). Species interactions under climate change: connecting kinetic effects of

temperature on individuals to community dynamics. *Curr Opin Insect Sci*, 35, 88–95.

Brose, U., Archambault, P., Barnes, A.D., Bersier, L.F., Boy, T., Canning-Clode, J., *et al.* (2019). Predator traits determine food-web architecture across ecosystems. *Nat Ecol Evol*, 3, 919–927.

Brose, U., Dunne, J.A., Montoya, J.M., Petchey, O.L., Schneider, F.D. & Jacob, U. (2012). Climate change in size-structured ecosystems. *Philos T Roy Soc B*, 367, 2903–2912.

Brown, J.H., Gillooly, J.F., Allen, A.P., Savage, V.M. & Geoffrey, B. (2004). Toward a Metabolic Theory of Ecology. *Ecology*, 85, 1771–1789.

Chesson, P. (2000). Mechanisms of Maintenance of Species Diversity. *Annu Rev Ecol Syst*, 31, 343–366.

Darwall, W., Bremerich, V., De Wever, A., Dell, A.I., Freyhof, J., Gessner, M.O., *et al.* (2018). The Alliance for freshwater life: A global call to unite efforts for freshwater biodiversity science and conservation. *Aquat Conserv*, 28, 1015–1022.

Daufresne, M., Lengfellner, K. & Sommer, U. (2009). Global warming benefits the small in aquatic ecosystems. *P Natl Acad Sci USA*, 106, 12788–93.

Davidson, N.C. (2014). How much wetland has the world lost? Long-term and recent trends in global wetland area. *Mar Freshw Res*, 65, 934–941.

Dell, A.I., Pawar, S. & Savage, V.M. (2014). Temperature dependence of trophic interactions are driven by asymmetry of species responses and foraging strategy. *J Anim Ecol*, 83, 70–84.

Dijoux, S. & Boukal, D.S. (2021). Community structure and collapses in multichannel food webs: Role of consumer body sizes and mesohabitat productivities. *Ecol Lett*, 24, 1607–1618.

Dijoux, S., Pichon, N.A., Sentis, A. & Boukal, D.S. (2023). Body size and trophic position determine the outcomes of species invasions along temperature and productivity gradients. *Authorea*.

Dudgeon, D., Arthington, A.H., Gessner, M.O., Kawabata, Z.I., Knowler, D.J., Lévêque, C., *et al.* (2006). Freshwater biodiversity: Importance, threats, status and conservation challenges. *Biol Rev Camb Philos*, 81, 163–182.

Dunne, J.A., Williams, R.J. & Martinez, N.D. (2002). Network structure and biodiversity loss in food webs: robustness increases with connectance. *Ecol Lett*, 5, 558–567.

Elser, J.J., Dobberfubl, D.R., Mackay, N.A. & Schampel, J.H. (1996). Organism size, life history, and N:P Stoichiometry. Toward a unified view of cellular and ecosystem processes. *Bioscience*, 46, 674–683.

Elton, C.S. (1927). Animal Ecology. Macmillan Co.

Forster, J., Hirst, A.G. & Atkinson, D. (2012). Warming-induced reductions in body size are greater in aquatic than terrestrial species. *P Natl Acad Sci USA*, 109, 19310–14.

Fretwell, S.D. (1987). Food chain dynamics: the central theory of ecology? *Oikos*, 50, 291–301.

Fussmann, K.E., Schwarzmüller, F., Brose, U., Jousset, A. & Rall, B.C. (2014). Ecological stability in response to warming. *Nat Clim Chang*, 4, 206–210.

Galic, N., Sullivan, L.L., Grimm, V. & Forbes, V.E. (2018). When things don't add up: quantifying impacts of multiple stressors from individual metabolism to ecosystem processing. *Ecol Lett*, 21, 568–577.

Gallardo, B., Clavero, M., Sánchez, M.I. & Vilà, M. (2016). Global ecological impacts of invasive species in aquatic ecosystems. *Glob Chang Biol*, 22, 151–163.

Gårdmark, A., Casini, M., Huss, M., van Leeuwen, A., Hjelm, J., Persson, L., *et al.* (2015). Regime shifts in exploited marine food webs: Detecting mechanisms underlying alternative stable states using size-structured community dynamics theory. *Philos T Roy Soc B*, 370, 1–10.

Gardner, J.L., Peters, A., Kearney, M.R., Joseph, L. & Heinsohn, R. (2011). Declining body size: A third universal response to warming? *Trends Ecol Evol*, 26 (6), 285–291.

Gillooly, J.F., Charnov, E.L., West, G.B., Savage, V.M. & Brown, J.H. (2002). Effects of size and temperature on developmental time. *Nature*, 417, 70–73.

Gounand, I., Kéfi, S., Mouquet, N. & Gravel, D. (2016). Trait selection during food web assembly: the roles of interactions and temperature. *Theor Ecol*, 9, 417–429.

Herbold, B. & Moyle, P.B. (1986). Species and Vacant niches. *Am Nat*, 128, 751–760.

Holt, R.D., Grover, J. & Tilman, D. (1994). Simple Rules for Interspecific Dominance in Systems with Exploitative and Apparent Competition. *Am Nat*, 144, 741–771.

Holt, R.D. & Polis, G.A. (1997). A theoretical framework for intraguild predation. *Am Nat*, 149, 745–764.

IPBES. (2019). Global assessment report of the Intergovernmental Science-Policy Platform on Biodiversity and Ecosystem Services. E. S. Brondizio, J. Settele, S. Díaz, and H. T. Ngo (editors).

IPCC. (2022). Climate Change 2022: Impacts, Adaptation and Vulnerability. Contribution of Working Group II to the Sixth Assessment Report of the Intergovernmental Panel on Climate Change. Cambridge University Press.

Isbell, F., Gonzalez, A., Loreau, M., Cowles, J., Díaz, S., Hector, A., *et al.* (2017). Linking the influence and dependence of people on biodiversity across scales. *Nature*, 546, 65–72.

Isbell, F., Reich, P.B., Tilman, D., Hobbie, S.E., Polasky, S. & Binder, S. (2013). Nutrient enrichment, biodiversity loss, and consequent declines in ecosystem productivity. *P Natl Acad Sci USA*, 110, 11911–11916.

Janssen, A.B.G., Teurlincx, S., An, S., Janse, J.H., Paerl, H.W. & Mooij, W.M. (2014). Alternative stable states in large shallow lakes? *J Great Lakes Res*, 40, 813–826.

Johansson, J., Kristensen, N.P., Nilsson, J.Å. & Jonzén, N. (2015). The eco-evolutionary consequences of interspecific phenological asynchrony - a theoretical perspective. *Oikos*, 124, 102–112.

Kingsolver, J.G. & Huey, R.B. (2008). Size, temperature, and fitness: three rules. *Evol Ecol Res*, 10, 251–268.

Kraft, N.J.B., Adler, P.B., Godoy, O., James, E.C., Fuller, S. & Levine, J.M. (2015). Community assembly, coexistence and the environmental filtering metaphor. *Funct Ecol*, 29, 592–599.

Kratina, P., Greig, H.S., Thompson, P.L., Carvalho-Pereira, T.S.A. & Shurin, J.B. (2012). Warming modifies trophic cascades and eutrophication in experimental freshwater. *Ecology*, 93, 1421–1430.

Lavin, C.P., Gordó-Vilaseca, C., Stephenson, F., Shi, Z. & Costello, M.J. (2022). Warmer temperature decreases the maximum length of six species of marine fishes, crustacean, and squid in New Zealand. *Environ Biol Fishes*, 105, 1431–1446.

Lindmark, M., Ohlberger, J., Huss, M. & Gårdmark, A. (2019). Size-based ecological interactions drive food web responses to climate warming. *Ecol Lett*, 22, 778–786.

May, R.M. (1974). Stability and Complexity in Model Ecosystems. Princeton University Press.

McCann, K.S. (2011). Food Webs (MPB-50). Princeton University Press.

McCann, K.S. & Rooney, N. (2009). The more food webs change, the more they stay the same. *Philos T Roy Soc B*, 364, 1789–1801.

McCauley, D.J., Gellner, G., Martinez, N.D., Williams, R.J., Sandin, S.A., Micheli, F., *et al.* (2018). On the prevalence and dynamics of inverted trophic pyramids and otherwise top-heavy communities. *Ecol Lett*, 21, 439–454.

McLellan, R., Iyengar, L., Jeffries, B. & Oerlemans Natasja. (2014). *Living Planet Report 2014: Species and spaces, people and places*. WWF International.

Moyle, P.B. & Light, T. (1996). Biological invasions of fresh water: Empirical rules and assembly theory. *Biol Conserv*, 78, 149–161.

Oksanen, L., Fretwell, S.D., Arruda, J., Niemela, P. & Niemelä, P. (1981). Exploitation ecosystems in gradients of primary productivity. *Am Nat*, 118, 240–261.

Parmesan, C. & Yohe, G. (2003). A globally coherent fingerprint of climate change impacts across natural systems. *Nature*, 421, 37–42.

Persson, L., Leonardsson, K., Roos, A.M. De, Gyllenberg, M. & Christensen, B. (1998). Ontogenetic Scaling of Foraging Rates and the Dynamics of a Size-Structured Consumer-Resource Model. *Theor Popul Biol*, 293, 270–293.

Persson, L. & de Roos, A.M. (2013). Symmetry breaking in ecological systems through different energy efficiencies of juveniles and adults. *Ecology*, 94, 1487–1498.

Petchey, O.L., Beckerman, A.P., Riede, J.O. & Warren, P.H. (2008). Size, foraging, and food web structure. *P Natl Acad Sci USA*, 105, 4191–4196.

Rall, B.C., Brose, U., Hartvig, M., Vucic-pestic, O., Kalinkat, G., Schwarzmu, F., *et al.* (2012). Universal temperature and body-mass scaling of feeding rates. *Philos T Roy Soc B*, 367, 2923–2934.

Rall, B.C., Vucic-Pestic, O., Ehnes, R.B., EmmersoN, M. & Brose, U. (2010). Temperature, predator-prey interaction strength and population stability. *Glob Chang Biol*, 16, 2145–2157.

Réale, D., Garant, D., Humphries, M.M., Bergeron, P., Careau, V. & Montiglio, P.O. (2010). Personality and the emergence of the pace-of-life syndrome concept at the population level. *Philos T Roy Soc B*, 365, 4051–4063.

Reinhardt, T., Weitere, M. & Steinfartz, S. (2015). Inter-annual weather variability can drive the outcome of predator prey match in ponds. *Amphibia-Reptilia*, 36, 97–109.

Reuman, D.C., Holt, R.D. & Yvon-Durocher, G. (2014). A metabolic perspective on competition and body size reductions with warming. *J Anim Ecol*, 83, 59–69.

Reynolds, S.A. & Aldridge, D.C. (2021). Global impacts of invasive species on the tipping points of shallow lakes. *Glob Chang Biol*, 27, 6129–6138.

Rodgers, E.M. (2021). Adding climate change to the mix: Responses of aquatic ectotherms to the combined effects of eutrophication and warming. *Biol Lett*, 17, 20210442.

Rooney, N., McCann, K., Gellner, G. & Moore, J.C. (2006). Structural asymmetry and the stability of diverse food webs. *Nature*, 442, 265–269.

Rooney, N., McCann, K.S. & Moore, J.C. (2008). A landscape theory for food web architecture. *Ecol Lett*, 11, 867–881.

de Roos, A.M. (2020). Effects of life history and individual development on community dynamics: A review of counterintuitive consequences. *Ecol Res*, 35, 930–946.

de Roos, A.M. (2021). PSPManalysis: Steady-state and bifurcation analysis of physiologically structured population models. *Methods Ecol Evol*, 12, 383–390.

de Roos, A.M., Metz, J.A.J. & Persson, L. (2013). Ontogenetic symmetry and asymmetry in energetics. *J Math Biol*, 66, 889–914.

de Roos, A.M. & Persson, L. (2002). Size-dependent life-history traits promote catastrophic collapses of top predators. *P Natl Acad Sci USA*, 99, 12907–12912.

de Roos, A.M., Persson, L. & McCauley, E. (2003). The influence of size-dependent life-history traits on the structure and dynamics of populations and communities. *Ecol Lett*, 6, 473–487.

Rosenzweig, M.L. (1971). Paradox of enrichment: destabilization of exploitation ecosystems in ecological time. *Science*, 171, 385–387.

Sala, O.E., Chapin, F.S., Armesto, J.J., Berlow, E., Bloomfield, J., Dirzo, R., *et al.* (2000). Global Biodiversity Scenarios for the Year 2100. *Science*, 287, 1770–1774.

Scheffer, M., Carpenter, S., Foley, J.A., Folke, C. & Walker, B. (2001). Catastrophic shifts in ecosystems. *Nature*, 413, 591–596.

Scheffer, M., Hosper, S.H., Meijer, M.-L., Moss, B. & Jeppesen, E. (1993). Alternative equilibria in shallow lakes. *Trends Ecol Evol*, 8, 275–279.

Schindler, D. & Scheuerell, M. (2002). Habitat coupling in lake ecosystems. *Oikos*, 98, 177–189.

Schindler, D.W. (2006). Recent advances in the understanding and management of eutrophication. *Limnol Oceanogr*, 5, 356–363.

Schoener, T.W. (1989). Food webs from the small to the large. *Ecology*, 70, 1559–1589.

Seebens, H., Bacher, S., Blackburn, T.M., Capinha, C., Dawson, W., Dullinger, S., *et al.* (2021). Projecting the continental accumulation of alien species through to 2050. *Glob Chang Biol*, 27, 970–982.

Seifert, L.I., de Castro, F., Marquart, A., Gaedke, U., Weithoff, G. & Vos, M. (2014). Heated relations: Temperature-mediated shifts in consumption across trophic levels. *PLoS One*, 9 (5): e95046.

Seifert, L.I., Weithoff, G., Gaedke, U. & Vos, M. (2015). Warming-induced changes in predation, extinction and invasion in an ectotherm food web. *Oecologia*, 178, 485–496.

Sentis, A., Binzer, A. & Boukal, D.S. (2017). Temperature-size responses alter food chain persistence across environmental gradients. *Ecol Lett*, 20, 852–862.

Sentis, A., Haegeman, B. & Montoya, J.M. (2022). Stoichiometric constraints modulate temperature and nutrient effects on biomass distribution and community stability. *Oikos*, 2022: e08601.

Sentis, A., Hemptinne, J.L. & Brodeur, J. (2014). Towards a mechanistic understanding of temperature and enrichment effects on species interaction strength, omnivory and food-web structure. *Ecol Lett*, 17, 785–793.

Sentis, A., Montoya, J.M. & Lurgi, M. (2021). Warming indirectly increases invasion success in food webs. *Proc R Soc B*, 288: 20202622.

Sentis, A., Morisson, J. & Boukal, D.S. (2015). Thermal acclimation modulates the impacts of temperature and enrichment on trophic interaction strengths and population dynamics. *Glob Chang Biol*, 21, 3290–3298.

Sheridan, J.A. & Bickford, D. (2011). Shrinking body size as an ecological response to climate change. *Nat Clim Chang*, 1, 401–406.

Shurin, J.B., Clasen, J.L., Greig, H.S., Kratina, P. & Thompson, P.L. (2012). Warming shifts top-down and bottom-up control of pond food web structure and function. *Philos T Roy Soc B*, 367, 3008–3017.

Stendera, S., Adrian, R., Bonada, N., Cañedo-Argüelles, M., Hugueny, B., Januschke, K., *et al.* (2012). Drivers and stressors of freshwater biodiversity patterns across different ecosystems and scales: A review. *Hydrobiologia*.

Sunday, J.M., Bates, A.E. & Dulvy, N.K. (2012). Thermal tolerance and the global redistribution of animals. *Nat Clim Chang*, 2, 686–690.

Synodinos, A.D., Haegeman, B., Sentis, A. & Montoya, J.M. (2021). Theory of temperature-dependent consumer–resource interactions. *Ecol Lett*, 24, 1539–1555.

Tilman, D. (1985). The Resource-Ratio Hypothesis of Plant Succession. *Am Nat*, 125, 827–852.

Verberk, W.C.E.P., Atkinson, D., Hoefnagel, K.N., Hirst, A.G., Horne, C.R. & Siepel, H. (2021). Shrinking body sizes in response to warming: explanations for the temperature–size rule with special emphasis on the role of oxygen. *Biol Rev*, 96, 247–268.

Walther, G., Post, E., Convey, P., Menzel, A., Parmesank, C., Beebee, T.J.C., *et al.* (2002). Ecological response to recent climate change. *Nature*, 416, 389–395.

Wardle, D.A., Bardgett, R.D., Callaway, R.M. & Van Der Putten, W.H. (2011). Terrestrial ecosystem responses to species gains and losses. *Science*, 332, 1273–1277.

Wellborn, G.A., Skelly, D.K. & Werner, E.E. (1996). Mechanisms creating community structure across a freshwater habitat gradient. *Annu Rev Ecol Syst*, 27, 337–363.

Wollrab, S., Diehl, S. & de Roos, A.M. (2012). Simple rules describe bottom-up and top-down control in food webs with alternative energy pathways. *Ecol Lett*, 15, 935–46.

Woodward, G., Ebenman, B., Emmerson, M., Montoya, J.M., Olesen, J.M., Valido, A., *et al.* (2005). Body size in ecological networks. *Trends Ecol Evol*, 20, 402–409.

Wootton, H.F., Morrongiello, J.R., Schmitt, T. & Audzijonyte, A. (2022). Smaller adult fish size in warmer water is not explained by elevated metabolism. *Ecol Lett*, 25, 1177–1188.

Wootton, K.L. (2017). Omnivory and stability in freshwater habitats: Does theory match reality? *Freshw Biol*, 62, 821–832.

Wootton, K.L., Curtsdotter, A., Roslin, T., Bommarco, R. & Jonsson, T. (2021). Towards a modular theory of trophic interactions. *Funct Ecol*, 1–18.

Yodzis, P. & Innes, S. (1992). Body Size and Consumer-Resource Dynamics. *Am Nat*, 139, 1151–1175.

Young, H.S., McCauley, D.J., Galetti, M. & Dirzo, R. (2016). Patterns, Causes, and Consequences of Anthropocene Defaunation. *Annu Rev Ecol Evol S*, 47, 333–358.

Vander Zanden, M.J., Vadeboncoeur, Y., Avenue, O.S., Vander Zanden, M.J. & Vadeboncoeur, Y. (2002). Fishes as integrators of benthic and pelagic food webs in lakes. *Ecology*, 83, 2152–2161.

~ Chapter I ~

Body size and trophic position determine the outcomes of species invasions along temperature and productivity gradients

[Manuscript submitted to Ecology Letters]

Body size and trophic position determine the outcomes of species invasions along temperature and productivity gradients

Samuel Dijoux[1,2,*], Noémie A. Pichon[3,4], Arnaud Sentis[5], David S. Boukal[1,2]

[1.]Department of Ecosystems Biology, Faculty of Science, University of South Bohemia. Branišovská 1760, 370 05 České Budějovice, Czech Republic.
[2.]Czech Academy of Sciences, Biology Centre, Institute of Entomology, Branišovská 31, 370 05 České Budějovice, Czech Republic.
[3.]Ecology and Genetics Unit, Faculty of Science, University of Oulu, 90014 Oulu, Finland.
[4.]Swiss Federal Research Institute WSL, Zuercherstrasse 111, 8902, Birmensdorf, Switzerland.
[5.]INRAE, Aix Marseille University, UMR RECOVER, 3275 Route de Cézanne- CS 40061, 13182 Aix-en-Provence Cedex 5, France.

E-mail addresses: dijous00@prf.jcu.cz (S. Dijoux); noemie.pichon@wsl.ch (N. A. Pichon); arnaud.sentis@inrae.fr (A. Sentis); dboukal@prf.jcu.cz (D. S. Boukal).

Authors' ORCID: SD (0000-0002-8086-7696), NAP (0000-0003-2972-1912), AS (0000-0003-4617-3620), DSB (0000-0001-8181-7458).

Short running title: Species invasions and environmental gradients.

Key words: warming; eutrophication; species invasions; metabolic ecology; trophic modules; body size; predator-prey mass ratio; diversity-stability relationship.

Type of Article: Letter
Number of words in the abstract: 150
Number of words in the main text: 5000

Number of words in text box 1: 144
Number of words in text box 2: 155
Number of references: 84
Number of figures, tables and text boxes: 4 figures, 2 text boxes
* Corresponding author: Samuel Dijoux (dijous00@prf.jcu.cz)

Authorship statement: DSB, AS and SD designed the study. SD performed all numerical computations and analyses based on preliminary analyses by NAP, with additional input from AS and DSB. All authors discussed the results and their presentation. SD wrote the first draft of the manuscript and all co-authors contributed to the manuscript revision.

Data accessibility statement: All data and code required to replicate all results have been deposited in GitHub (https://github.com/Samuel-Dijoux/2022-Invasion_modules) and Zenodo (https://doi.org/10.5281/zenodo.7273775).

Abstract

Species invasions are predicted to increase in frequency with global change, but quantitative predictions of how environmental filters and species traits influence the success and consequences of invasions for local communities are lacking. Here we investigate how invaders alter the structure, diversity and stability regime of simple communities across gradients of habitat productivity, temperature, and community size structure. We examine all three-species trophic modules (apparent and exploitative competition, trophic chain and intraguild predation) with empirically derived temperature and body mass scaling of vital rates. We show that the success of an invasion and its effects on community stability and diversity are predictably determined by the effects of environmental factors on each species and the relative strengths of trophic interactions between resident and invading species. We predict that successful invaders include smaller competitors and comparatively small predators, suggesting that species invasions may facilitate the downsizing of food webs under global change.

Introduction

Human-induced global change is transforming local communities and ecosystems through five main drivers: climate change, pollution, overharvesting, land and sea use change, and invasive species (Isbell et al. 2017; IPBES 2019). Invasive species threaten biodiversity (Sala et al. 2000) and persistence of local communities worldwide (Gurevitch & Padilla 2004; Bellard et al. 2016). Shifting species ranges to higher elevations and latitudes in response to climate change (Parmesan & Yohe 2003; Sunday et al. 2012), combined with increased tourism, pet trade and commodity transport (Chan et al. 2019; McCarthy et al. 2019; Essl et al. 2020), are expected to accelerate species invasions globally over the next century (Seebens et al. 2021; Sentis et al. 2021). Species invasions can exacerbate or mitigate the pressures that ongoing environmental change exerts on local communities by altering biodiversity and community resilience to abiotic stressors (Walther et al. 2002; Wardle et al. 2011; Hong et al. 2022).

Warming and nutrient enrichment are two pervasive aspects of global change that structure local communities in aquatic (Fussmann et al. 2014; Boukal et al. 2019) and terrestrial systems (Meyer et al. 2012; Clark et al. 2017). They modulate food web dynamics (Binzer et al. 2012; Sentis et al. 2017) and can facilitate or prevent species invasions. However, a general consensus on how invaders influence community structure and persistence along temperature and habitat productivity gradients is currently lacking. In particular, the mechanisms underlying community-level responses to species invasions in future environments affected by global change remain incompletely understood (Sentis et al. 2021).

Exploring the nexus between invasibility, diversity and stability of communities (Rooney & McCann 2012; Catford et al. 2019) can help us better understand the impacts of global change on local ecosystems (Francis et al. 2014). The effects of species invasions on the diversity-stability relationship have been studied in different types of animal, animal-plant and plant interaction networks (Rooney & McCann 2012; Brose et al. 2017; Tomiolo & Ward 2018). However, previous studies considered

relatively species-rich communities with many direct and indirect effects; focusing on food web modules could allow for more mechanistic, causal insights.

One promising avenue towards a better understanding of these mechanisms is to disentangle the role of environmental filters and species traits in biological invasions (Chesson 2000; Kraft et al. 2015). Environmental filters constrain the invader per se but also structure the local community, which is a biotic filter that restricts the invader's realised niche (Kraft et al. 2015). The roles of both filters are therefore closely linked (Thompson et al. 2018a, b). This link is often neglected in studies that estimate future shifts in species distributions caused by climate based on the expected performance of invading species in new habitats (Bellard et al. 2013; Buckley & Csergo 2017; Seebens et al. 2021), but ignore the accompanying impacts of environmental change on resident communities.

The invader's realised niche is constrained by its trophic position and the topology of the local food web. Available niches may be occupied by resident species that interact with the invader directly through consumptive interactions or indirectly through competition (Dueñas et al. 2018). Classic work on species coexistence has proposed general rules for community assembly (Chesson 2000; Shea 2002). The 'R* rule' for exploitative competition states that the species with the lowest resource requirements is competitively superior (Tilman 1985). An analogous 'P* rule' for apparent competition states that the prey that can withstand the highest predation pressure will prevail (Holt et al. 1994). Both rules can also inform when species invade and how they affect resident communities in the context of global change.

Among species traits, individual body mass can be used to predict invasibility because it affects individual fitness, species interactions and energy flows (McCann & Rooney 2009; Brose et al. 2017; Dijoux & Boukal 2021). For example, larger species tend to prey on smaller species, especially in aquatic habitats (Ou et al. 2017) and warming-induced metabolic meltdown is more likely for larger consumers than smaller ones (Rall et al. 2010, 2012). Food webs may therefore be simpler in warmer habitats, with fewer species at higher trophic positions (Brose et al. 2012).

This could create niches for future invaders, which could subsequently attenuate or alter food web responses to global change through cascading effects (Reynolds & Aldridge 2021). However, little is known about how the body mass and trophic position of the invader affect community responses to invasions under climate change, and simple predictions are difficult to make. For example, previous models have shown that high consumer-resource mass ratios associated with large consumer species can either confer a higher extinction risk for top predators under warming or buffer the effects of eutrophication by dampening population fluctuations (Binzer et al. 2016; Sentis et al. 2017).

Here, we investigate in detail how consumer-resource systems respond to species invasions along temperature and habitat productivity gradients. To this end, we develop biomass-based models (Yodzis & Innes 1992) with mass- and temperature-dependent biological rates parameterised using empirically estimated relationships (Binzer et al. 2012; Fussmann et al. 2014). We simulate all possible invasions in a consumer-resource system that can lead to the four baseline three-species food web modules (apparent and exploitative competition, food chain, and intraguild predation). Our aim is to decouple the influence of the invaders and abiotic drivers. We explore (i) how temperature, nutrient levels and body mass ratios between the resident and invading species influence invasion success and (ii) how invasion-induced changes in species composition, diversity and stability of local communities vary across different food web topologies and environmental gradients.

Our main expectations are: (1) all else being equal, community responses to invasions (Box 1) follow known mechanistic processes from community ecology (Box 2); (2) based on the R* and P* rules and the higher susceptibility of larger species to metabolic meltdown at warmer temperatures, smaller invaders are more successful at warmer temperatures, especially in less productive environments, while larger invaders are more successful in more productive environments, especially at lower temperatures; and (3) invasions that result in larger and smaller consumer-resource size ratios will tend to stabilise and destabilise the community dynamics.

Methods

Community structure and dynamics

We consider a resident consumer-resource system and examine five scenarios that differ in the trophic position of the invader, including another basal resource, another consumer, a top predator, an intraguild predator feeding on both resident species, or an intraguild prey feeding on the (shared) resident resource while being consumed by the resident consumer (Fig. 1a-e). This corresponds to apparent competition (hereafter AC), exploitative competition (EC), tri-trophic chain (TC) and intraguild predation (IGP) (Tables S1–S3).

We simulate the dynamics of each module for each combination of temperature between 0°C and 40°C (step size 0.1°C) and nutrient levels (I_K) available to the basal resource species the between 0.1 $g.m^{-2}$ and 20 $g.m^{-2}$ (step size 0.1 $g.m^{-2}$), yielding 80,200 combinations of temperature and nutrient levels as in Binzer et al. (2012) and Sentis et al. (2017). We also vary the body masses of species in each module, constraining consumers to be at least as large as their resources, which is true for most predator-prey pairs (McCauley et al. 2018). For simplicity, we set the body mass of the basal resource species to 1 mg and express the other masses in relative values (Fig. 1a-e).

We denote the body mass ratio between competing resources $R_{INV}:R_{RES}$ (AC module) and the consumer:resource ratio *C:R* (TC and IGP modules) as α, the mass ratio between competing consumers $C_{INV}:C_{RES}$ (EC and IGP modules) or between predators and intermediate consumers *P:C* (TC and IGP modules) as β, and the mass ratio between resident resource and consumer $C_{RES}:R_{RES}$ (AC and EC modules) and between the top predator and resident basal resource (*P:R*; TC and IGP modules) as $\gamma = \alpha\beta$. Furthermore, we quantify the asymmetry in size ratios between adjacent trophic levels with a ratio parameter $\delta = \beta/\alpha$ (Table S4). We consider module-specific sets of mass ratios to reflect the different trophic positions of the invader: 4 or 15 consumer-resource body mass ratios for the resident system, and 16 or 25 combinations of species mass ratios (i.e., at least all pairwise combinations of α and β = 1, 2, 5 and 10, Text S1) in each module

(Tables S5–S7). All numerical simulations were run in the packages 'deSolve' and 'rootSolve' in the R software (Soetaert & Herman 2009; Soetaert et al. 2010).

Analyses of community structure and stability before and after invasion

We distinguish six mechanisms of invasion-induced change in the community based on the observed changes in local composition and diversity (hereafter *invasion outcomes*, Box 1). The invasion-induced change in diversity $\Delta D = N_{INV} - N_{RES}$ is calculated as the difference between the number of species in the invaded and resident community N_{INV} and N_{RES} present after 5000 years (end of simulation) under the same environmental conditions and species masses.

To assess how invaders affect the stability of the resident system, we first calculate the Jacobian matrix at the equilibrium with the species present after 5000 years (Eqs 10–13, Table S8) and use its dominant eigenvalue to determine the stability of the resulting community. We distinguish three stability regimes for the invaded community (hereafter S_{INV}) and the resident system (hereafter S_{RES}): stable equilibrium (*E*), population oscillations (*O*), and a collapsed system with no remaining species (*N*) (Binzer et al. 2012; Sentis et al. 2017), to which we arbitrarily assign values $v(E) = 2$, $v(O) = 1$ and $v(N) = 0$. We then compare the stability regimes between the resident system and the invaded community under the same environmental conditions and species mass ratios. Nine outcomes (hereafter *regime states*, $S_{RES} \rightarrow S_{INV}$) define all possible changes in stability caused by species invasion. Similar to ΔD, we calculate the invasion-induced change in stability as $\Delta S = v(S_{INV}) - v(S_{RES})$. Positive, zero and negative values of ΔS correspond to stabilizing (*O*→*E*, *N*→*O* and *N*→*E*), neutral (*O*→*O*, *E*→*E* and *N*→*N*) and destabilising (*O*→*N*, *E*→*O*, *E*→*N*) effects of the invader on the local consumer-resource system, respectively.

To assess how the body mass of the invader affects the community responses across food web modules and abiotic conditions, we calculate the percentage of each invasion outcome (Box 1) and regime state for a

given set of body mass ratios across all 80,200 combinations of temperature (0–40ºC) and nutrient levels (0.1–20 $g.m^{-2}$) for each combination of body masses in each food web module (Tables S4–S7), and average these percentages across all combinations of body masses considered for each module.

Results

Community response to invasion: the role of environmental conditions and food web topology

Temperature, nutrient levels and size structure of the resident community influence its composition, stability (Text S2 and Fig. S1) and response to invasion. We first focus on responses for fixed body mass ratios $\alpha = \beta = 10$ describing invasions by a 10-fold larger resource species in the AC module (Fig. 1a), a 10-fold smaller consumer species in the EC module (Fig. 1b), a large top predator in the TC module (Fig. 1c), and a medium-sized intraguild prey (Fig. 1d) or a large intraguild predator (Fig. 1e) in the IGP module.

The impact of an invader on the resident community varies with temperature, nutrient levels and the invader's trophic position (Fig. 1f-p). The community resists invasion in the following cases: (1) the invading consumer or predator suffers from metabolic meltdown at combinations of relatively high temperatures and low nutrient levels (Fig. 1g-1j, blue area top left), (2) the invading resource (AC module) or consumer (IGP module) is competitively inferior to resident resource or intraguild predator, respectively, at a wide range of intermediate temperatures and nutrient levels (Fig. 1f and 1i, blue area away from top left and bottom right) and (3) the consumer-resource system collapses due to the paradox of enrichment at combinations of relatively low temperatures and high nutrient levels (Fig. 1f-1j, blue area bottom right).

Successful invasion and occupancy of a vacant niche occur at combinations of relatively high temperatures and low nutrient levels that are above the extinction limit (caused by metabolic meltdown) of the local consumer or

predator, but also below the extinction limit of the invader for invading larger resource species (AC module), smaller consumers (EC module) and intraguild prey (IGP module; Fig. 1f, 1g and 1i, yellow areas). Invading intraguild predator occupies a vacant niche when the intraguild prey goes extinct due to the paradox of enrichment at sufficiently low temperatures and high nutrient levels (Fig. 1j, yellow area).

Furthermore, a larger resource outcompetes and substitutes the resident resource in the AC module under environmental conditions just below the extinction limit of the resident consumer (Fig. 1f, green area), because a larger resource provides more energy to the consumer due to lower consumer: resource body mass ratio. An invading smaller consumer (EC module) and intraguild predator (IGP module) substitute the competitively inferior resident consumer over a much wider range of intermediate temperatures and nutrient levels; in the latter case, the environmental conditions must be sufficiently below the extinction threshold of the invading predator (Fig. 1g and 1j, green area).

Only invading top predator (TC module) can integrate into the community across a broad range of environmental conditions (Fig. 1h, light brown area). Intraguild prey integrates into the community when environmental conditions are just below the metabolic meltdown threshold of the resident intraguild predator, making the latter a poor competitor for the shared prey (Fig. 1i, light brown area). Intraguild predator integrates into the community when conditions are just below its own extinction threshold (Fig. 1j, light brown area; note that the extinction threshold is higher than in Fig. 1i due to the additional intraguild prey).

Vulnerability to invasion occurs for a smaller consumer in the EC module at low temperatures and sufficiently high nutrient levels (Fig. 1g, black area), where the resulting lower consumer-resource mass ratio triggers population oscillations. Finally, at sufficiently low temperatures and high nutrient levels, an invading top predator (TC module) rescues the resident resource by dampening population oscillations during its temporary presence in the system, so that only the top predator and resident consumer die out (Fig. 1h, ochre area).

These module-specific outcomes of invasions are reflected in different effects on community stability. Invading basal resource (AC module), intraguild prey and intraguild predator (IGP module) does not alter system stability except the invading intraguild predator, which can stabilise the dynamics over a narrow range of combinations of nutrient levels and (low to moderately high) temperatures (Fig. 1l, 1o and 1p). Successful invasion at low temperatures and high nutrient levels in the EC module always destabilises the community towards cycles or complete collapse due to the paradox of enrichment (Fig. 1m). Finally, successfully invading top predator may or may not change system stability depending on temperature and nutrient levels (TC module, Fig. 1n).

Community response to invasion: the role of species body mass ratios

We examine the role of body mass ratios in community response to invasion from two perspectives: competition in the AC, EC and IGP_C module and predation in the TC and IGP_P module. To this end, we investigate the role of body mass ratios α and β between competitors and the role of size structure asymmetry between multiple trophic levels given by δ. For brevity, we summarise here only the general patterns of invasion outcomes (Fig. 2) and effects on community regime state (Fig. 3); Text S3 and Table S9 provide further details.

Resistance to invasion and species substitution dominate the results for the three modules with invading competitors (Fig. 2a-c, S2ab and S3a-c), with predominantly neutral effects on the community regime ($\Delta S = 0$; Fig. S2cd, dotted lines in Figs. 3a-c and S3f-j). Invasion-induced increase in stability is less frequent but occurs in all modules except EC (Figs. 2b and S3g). Integration of the invader and rescue of the resident species are rare and limited to TC and IGP modules (Figs. 2a-c and S2ab). Invasion-induced vulnerability occurs only for smaller ($\beta < 1$) or, very rarely, much larger ($\beta \gg 1$) invading consumers in the EC module (Fig. 2b) and promotes system instability (Figs. 2b and S3g).

The predominant outcomes in the AC, EC and IGP_C modules, i.e. resistance to invasion or substitution of the resident competitor, correspond to predictions based on the P* and R* rules (Box 2) and depend strongly on the resident: invader body size ratio (Fig. 2a-c, Text S4). In the AC module, a smaller competitor can sustain a higher equilibrium predator biomass and exclude a larger competitor (P* rule, Figs. 2a, S4a-l and S5a-l). In the EC module, a smaller consumer has lower resource requirements at equilibrium and therefore excludes a larger competitor (R* rule, Figs. 2b, S4s-x and S5s-x). Invading smaller resource in the AC module can stabilise the dynamics and prevent collapse ($\Delta S > 0$ for $\alpha < 1$; Figs. 3a and S3f), while invasion of a smaller consumer in the EC module can destabilise the dynamics, leading to population cycles or collapse ($\Delta S < 0$ for $\beta < 1$; Figs. 3b and S3g). In the IGP module, a smaller intraguild prey is competitively superior to the intraguild predator (Fig. S6g-l) but cannot withstand its predation pressure (Figs. 2c and S6m-o). Intraguild prey therefore collapses immediately after its introduction (Fig. S6m-o) or is displaced by an invading intraguild predator (Fig. S6a-f) as soon as the biomass of the latter becomes too high, with a stabilising effect similar to that in the AC module (for $\beta > 1$; Fig. 3c).

Community responses to an invading top predator in the TC and IGP modules vary predictably with the size-structure asymmetry between trophic levels characterised by δ (Figs. 2de and 3de). Successful invasion of the top predator in the TC module requires the presence of an intermediate consumer, which is more common with large α (Fig. S1) and thus smaller δ values. That is, an invading top predator is more likely to integrate or to rescue a resident species than to fail if it is more similar in size to the resident consumer (for $\delta < 1$, Fig. 2d). In this way, the top predator triggers oscillations more frequently, but prevents community collapse through the rescue effect (Fig. 3d). Changes in community composition and stability decrease when the resident consumer and the resource become more similar in size ($\delta > 1$ in Figs. 2d and 3d). In this case, the invasion of a comparatively large top predator usually fails and the resident system collapses due to the paradox of enrichment driven by the resident consumer-resource interaction (cf. Fig. S1b). On the other hand, the intraguild predator in the IGP module feeds on two prey

populations, which explains the independence of community resistance from δ (Fig. 2e). Given the influence of the intraguild prey-resource mass ratio on the dynamics of the resident system (Fig. S3), species substitution occurs more frequently the more similar the size of the intraguild predator and intraguild prey ($\delta < 1$), while niche occupancy occurs more often the more similar the size of the intraguild prey and shared resource ($\delta > 1$, Fig. 2e). Invading intraguild predator stabilises the resident community and prevents its collapse more often as it gets more dissimilar in size to the intraguild prey ($\delta > 1$; Fig. 3e).

Invasion outcomes and the diversity-stability relationship

The effects of invasion on community stability and diversity observed in our simulations depend on the outcome of the invasion. Invasion-induced destabilisation occurs primarily under vulnerability, where it almost always leads to community collapse (regime states $E \rightarrow N$ and $O \rightarrow N$; Figs. 4 and S8, Tables S9–S11). More than half of the invasions leading to integration and some leading to substitutions also trigger a loss of stability, with invasion-induced cycles replacing equilibrium ($E \rightarrow O$). We do not observe invasion-induced destabilisation under resistance, occupancy and rescue mechanisms. An invasion-triggered increase in stability, which would prevent a complete collapse of the resident community and is characteristic of the rescue ($N \rightarrow E$), occurs less frequently under occupancy ($N \rightarrow E$ and $N \rightarrow O$) and integration ($N \rightarrow O$). An invasion-triggered increase in stability associated with a shift from oscillations to stable equilibria ($O \rightarrow E$) is rare and occurs only under substitution and vulnerability (Fig. S1a).

As a result, we find that invasion-induced changes in diversity and stability are interrelated, but one cannot be predicted from the other alone (Fig. 4b). Diversity loss ($\Delta D < 0$) is almost always associated with invasion-induced loss of stability ($\Delta S < 0$). No net change in diversity ($\Delta D = 0$) is mostly associated with no change in stability as expected, but loss of stability (invasion-induced cycles in EC) or increased stability (dampen cycles induced by invasion through species substitution in IGP_P) also occur as a result of invasion. Interestingly, invasions leading to increased diversity

($\Delta D > 0$) have the most evenly distributed effects on stability. About one third of the simulations each lead to reduced, increased or unchanged stability across species mass ratios, food web topologies and environmental conditions (Fig. 4b).

Discussion

Our study summarises how simple communities respond to the combination of three major drivers of global change: warming, eutrophication and species invasions (IPBES 2019). While these drivers have received considerable attention separately (Bellard et al. 2013; Binzer et al. 2016; Gallien & Carboni 2017), their combined impacts on local communities remain poorly understood despite some recent advances (Latombe et al. 2021; Sentis et al. 2021). We focused on two ubiquitous interactions through which invaders affect resident communities—predation and competition (Gallardo et al. 2016; Dueñas et al. 2018)—to understand how invasion outcomes relate to changes in community composition, diversity and stability (Tilman 1999). We showed that the outcomes depend predictably on the interplay between environmental conditions and differences in body mass and trophic position between the invader and its local competitor or predator/prey (Table S12). This allowed us to (i) identify combinations of environmental conditions, invader traits and community size structure that characterise communities prone to successful invasions, and (ii) describe the community-level consequences of such invasions.

What drives successful invasions and when do they occur?

Environmental and biotic filters underpin invasion success in local communities (Mitchell et al. 2006; Blackburn et al. 2011; Gray et al. 2015). Species living in warm, nutrient-poor environments such as tropical and subtropical seas (Sunday 2020; Trisos et al. 2020) may be at risk of metabolic meltdown (Pörtner & Farrell 2008), while species living in relatively cold, nutrient-rich environments such as shallow lakes at higher

latitudes (Janssen et al. 2014; Glibert 2017) are vulnerable to unstable dynamics and community collapse (Oksanen et al. 1981). Previous models have shown that (1) "intermediate" environmental conditions that balance the opposing effects of warming and eutrophication can prevent biodiversity loss and maintain food web structure and that (2) larger consumer-resource body mass ratios mitigate the destabilising effect of eutrophication but tend to increase the vulnerability of top predators to warming (Binzer et al. 2016; Sentis et al. 2017). Our results extend these findings in the context of species invasions. That is, large species cannot invade warm, nutrient-limited habitats because of the risk of metabolic meltdown (Pörtner & Farrell 2008), while nutrient enrichment in colder habitats limits invasions by smaller species due to the paradox of enrichment and community collapse (Oksanen *et al.* 1981).

Size structure of the local community plays an additional filtering role in invasions (Gray et al. 2015). We observed that invasion success was mainly determined by size differences between resident and invading competitors, while asymmetries in size structure between adjacent trophic levels determined the fate of invading predators. This can be explained by the limiting similarity hypothesis, which states that the coexistence of species sharing the same (trophic) niche requires similar traits (MacArthur & Levins 1967), while this requirement does not hold for invaders in different trophic positions. Apart from competition for resources, we did not consider self-limiting mechanisms that would lead to stronger intraspecific than interspecific competition in our models and favour species coexistence (Holt et al. 1994). In our case, the application of the R* and P* rules (Box 2; Tilman 1985; Holt et al. 1994) can explain why only smaller competitors could successfully invade. We also considered a homogeneous environment, which tends to amplify the impact of invasive species on resident communities through high levels of interspecific competition, leading to limited coexistence due to frequent species replacement or strong resistance to the invader (Melbourne et al. 2007). This is in contrast to heterogeneous environments, where competing species with different traits can coexist through niche partitioning (Ricklefs 1977).

Our results also extend previous theory by showing that successful invasions in the IGP module depend on asymmetric competition between the intraguild predator and prey (Wootton 2017). Intraguild predators have a double advantage over pure competitors (as in the EC module) or specialist predators (as in the TC module): they depend less on a particular food source and can suppress intraguild prey through high predation pressure, even if the latter is a better competitor for the shared resource (Wootton 2017). These results are corroborated by experiments on intraguild predation between poeciliid fishes along a productivity gradient (Schröder et al. 2009), where the larger *Poecilia reticulata* most often successfully invaded the system and drove the smaller *Heterandria formosa* to extinction. Here we found that intraguild prey and predator can only coexist when environmental conditions are close to the metabolic meltdown threshold of the latter species, i.e. when high temperatures are combined with nutrient limitation.

Comparing results between modules, we found that intraguild prey (regardless of body size, IGP module), larger consumer (EC module) and larger resource (AC module) species were the least likely to successfully invade. This contrasts with the frequent successful invasions of intraguild predators (IGP module). Overall, we predict that successful invasions should involve comparatively smaller species, i.e. smaller competitors at lower trophic levels and predators that are not much larger than their prey. Invaders with other traits may need specific environmental conditions to be successful: for example, larger competitors at lower trophic levels and intraguild prey may only invade relatively warm and nutrient-poor environments that are not suitable for their predators.

When and how do invasions change the diversity and stability of resident communities?

Overall, our results were consistent with the classic diversity-stability hypothesis which states that more diverse ecosystems are more resilient to disturbance (Elton 1927; Tilman & Downing 1994; Rooney & McCann 2012). However, we also observed results that deviated from this

relationship: invaders could either stabilise communities by increasing local diversity, or they could disrupt initial community stability (e.g. by integrating an invading predator that destabilises the local community) and cause species extinctions. Invaders affected the diversity and stability of resident communities even when their presence was only temporary. These contrasting findings highlight the ambivalent role of invasions as both contributors to and threats to local biodiversity (e.g., Henriksson et al. 2016; Tomiolo & Ward 2018).

The effect of invasion on the diversity-stability relationship depended on the outcome of the invasion in our models. Successful invasions led to variable, outcome-dependent changes in system stability. Our results suggest that one-to-one species substitutions in simple communities rarely alter system stability, while invasions that lead to increased diversity can both destabilise (outcome type: integration) and stabilise (occupancy and, to a lesser, extent integration) community dynamics. We have found that these potential changes in stability occur primarily in relatively cold, nutrient-rich environments in communities that are vulnerable to population fluctuations caused by eutrophication. These communities are sensitive to changes in vital rates, which determine the population dynamics and interactions of their constituent species (Binzer et al. 2012; Fussmann et al. 2014). For example, a long-term study of the plankton community in Lake Washington found that community stability was lowest during a period of increased nutrient loading following a successful invasion by a subsequently dominant cyanobacterium (Francis et al. 2014).

Surprisingly, our study revealed that failed invasions can still affect the diversity and stability of local communities in cold, nutrient-rich habitats prone to the paradox of enrichment. Diversity could decrease due to increased population cycles after failed invasions of smaller consumers (EC module). Diversity could also increase due to rescue by invading top predators (TC module) if their temporary presence dampened consumer-resource cycles and rescued the basal resource, but not the consumer, from the collapse caused by enrichment. Such feedbacks from transient top predators on resident species might also arise from cascading effects of an invading top predator on lower trophic levels in more complex food webs

(Woodward & Hildrew 2002; Gallardo et al. 2016; Reynolds & Aldridge 2021). However, adequate evidence of the rescue effect would require long-term data, ideally from experiments with controlled introductions and subsequent removal of the invading species (Bell et al. 2003).

Conclusion and perspectives

Warming and eutrophication are expected to alter the dynamics and simplify the structure of larger food webs (Brose et al. 2012), facilitating species invasions and increasing their impact on invaded systems (Sentis et al. 2021). We have shown how body size and trophic position determine the fate of species invasions and that species invasions can mitigate or amplify the negative effects of environmental stressors on local communities. Our predictions showed that smaller species are particularly likely to invade communities in warmer, nutrient-limited environments, while communities facing cold temperatures and nutrient enrichment are vulnerable to invasions by larger predators. Invaders can also fill vacant niches when resident species disappear. For example, the predicted poleward shift of smaller zooplankton species may benefit warming Arctic habitats (Evans et al. 2020). Invading predators may also buffer local communities against eutrophic effects at lower temperatures (as in Hughes et al. (2013)). Therefore, invasive species may not always need to be eradicated or controlled (Simberloff 2009; Glen et al. 2013), especially if the associated costs are too high. On the other hand, our findings support active management and eradication of invaders with negative impacts on local communities, including those that destabilise local communities such as small consumers in cold, nutrient-rich habitats (Robertson et al. 2020). Overall, we predict that species invasions may contribute to the downsizing of food webs (Young et al. 2016), as successful invaders will include smaller competitors and comparatively small predators.

Acknowledgements: This research was supported by the Grant Agency of the Czech Republic (Grant no. 21-29169S). NAP was supported by the University of Oulu and the Academy of Finland Profi4 Grant 318930 Arctic Interactions (ArcI). AS was supported by the ANR project EcoTeBo (ANR-19-CE02-0001-01) from the French National Research Agency (ANR). Computational resources were supplied by the project "e-Infrastruktura CZ" (e-INFRA CZ ID:90140) supported by the Ministry of Education, Youth and Sports of the Czech Republic. The authors have no conflict of interest to declare.

References

Bell, T., Neill, W.E. & Schluter, D. (2003). The effect of temporal scale on the outcome of trophic cascade experiments. *Oecologia*, 134, 578–586.

Bellard, C., Cassey, P. & Blackburn, T.M. (2016). Alien species as a driver of recent extinctions. *Biol Lett*, 12, 24–27.

Bellard, C., Thuiller, W., Leroy, B., Genovesi, P., Bakkenes, M. & Courchamp, F. (2013). Will climate change promote future invasions? *Glob Chang Biol*, 19, 3740–3748.

Binzer, A., Guill, C., Brose, U. & Rall, B.C. (2012). The dynamics of food chains under climate change and nutrient enrichment. *Philos T R Soc B*, 367, 2935–2944.

Binzer, A., Guill, C., Rall, B.C. & Brose, U. (2016). Interactive effects of warming, eutrophication and size structure: Impacts on biodiversity and food-web structure. *Glob Chang Biol*, 22, 220–227.

Blackburn, T.M., Pyšek, P., Bacher, S., Carlton, J.T., Duncan, R.P., Jarošík, V., *et al.* (2011). A proposed unified framework for biological invasions. *Trends Ecol Evol*, 26, 333–339.

Bøhn, T., Amundsen, P.A. & Sparrow, A. (2008). Competitive exclusion after invasion? *Biol Invasions*, 10, 359–368.

Boukal, D.S., Bideault, A., Carreira, B.M. & Sentis, A. (2019). Species interactions under climate change: connecting kinetic effects of temperature on individuals to community dynamics. *Curr Opin*

Insect Sci, 35, 88–95.

Brose, U., Blanchard, J.L., Eklöf, A., Galiana, N., Hartvig, M., R. Hirt, M., *et al.* (2017). Predicting the consequences of species loss using size-structured biodiversity approaches. *Biol Rev*, 92, 684–697.

Brose, U., Dunne, J.A., Montoya, J.M., Petchey, O.L., Schneider, F.D. & Jacob, U. (2012). Climate change in size-structured ecosystems. *Philos T Roy Soc B*, 367, 2903–2912.

Brown, J.H. & Kodric-Brown, A. (1977). Turnover Rates in Insular Biogeography : Effect of Immigration on Extinction. *Ecology*, 58, 445–449.

Buckley, Y.M. & Csergo, A.M. (2017). Predicting invasion winners and losers under climate change. *P Natl Acad Sci USA*, 114, 4040–4041.

Byers, J.E. & Noonburg, E.G. (2003). Scale dependent effects of biotic resistance to biological invasion. *Ecology*, 84, 1428–1433.

Catford, J.A., Smith, A.L., Wragg, P.D., Clark, A.T., Kosmala, M., Cavender-Bares, J., *et al.* (2019). Traits linked with species invasiveness and community invasibility vary with time, stage and indicator of invasion in a long-term grassland experiment. *Ecol Lett*, 22, 593–604.

Chan, F.T., Stanislawczyk, K., Sneekes, A.C., Dvoretsky, A., Gollasch, S., Minchin, D., *et al.* (2019). Climate change opens new frontiers for marine species in the Arctic: Current trends and future invasion risks. *Glob Chang Biol*, 25, 25–38.

Chesson, P. (2000). Mechanisms of Maintenance of Species Diversity. *Annu Rev Ecol Syst*, 31, 343–366.

Clark, C.M., Bell, M.D., Boyd, J.W., Compton, J.E., Davidson, E.A., Davis, C., *et al.* (2017). Nitrogen-induced terrestrial eutrophication: Cascading effects and impacts on ecosystem services. *Ecosphere*, 8 (7): e01877.

Dijoux, S. & Boukal, D.S. (2021). Community structure and collapses in multichannel food webs: Role of consumer body sizes and mesohabitat productivities. *Ecol Lett*, 24, 1607–1618.

Downing, A.S., van Nes, E.H., Mooij, W.M. & Scheffer, M. (2012). The Resilience and Resistance of an Ecosystem to a Collapse of

Diversity. *PLoS One*, 7, 1–7.

Dueñas, M.A., Ruffhead, H.J., Wakefield, N.H., Roberts, P.D., Hemming, D.J. & Diaz-Soltero, H. (2018). The role played by invasive species in interactions with endangered and threatened species in the United States: a systematic review. *Biodivers. Conserv.*, 27, 3171–3183.

Elton, C.S. (1927). Animal Ecology. Macmillan Co.

Essl, F., Lenzner, B., Bacher, S., Bailey, S., Capinha, C., Daehler, C., *et al.* (2020). Drivers of future alien species impacts: An expert-based assessment. *Glob Chang Biol*, 26, 4880–4893.

Francis, T.B., Wolkovich, E.M., Scheuerell, M.D., Katz, S.L., Holmes, E.E. & Hampton, S.E. (2014). Shifting regimes and changing interactions in the Lake Washington, U.S.A., plankton community from 1962-1994. *PLoS One*, 9 (10): e110363.

Fussmann, K.E., Schwarzmüller, F., Brose, U., Jousset, A. & Rall, B.C. (2014). Ecological stability in response to warming. *Nat Clim Chang*, 4, 206–210.

Gallardo, B., Clavero, M., Sánchez, M.I. & Vilà, M. (2016). Global ecological impacts of invasive species in aquatic ecosystems. *Glob Chang Biol*, 22, 151–163.

Gallien, L. & Carboni, M. (2017). The community ecology of invasive species: where are we and what's next? *Ecography*, 40, 335–352.

Glen, A.S., Atkinson, R., Campbell, K.J., Hagen, E., Holmes, N.D., Keitt, B.S., *et al.* (2013). Eradicating multiple invasive species on inhabited islands: The next big step in island restoration? *Biol Invasions*, 15, 2589–2603.

Glibert, P.M. (2017). Eutrophication, harmful algae and biodiversity — Challenging paradigms in a world of complex nutrient changes. *Mar Pollut Bull*, 124, 591–606.

Gray, S.M., Dykhuizen, D.E. & Padilla, D.K. (2015). The effects of species properties and community context on establishment success. *Oikos*, 124, 355–363.

Gurevitch, J. & Padilla, D. (2004). Are invasive species a major cause of extinctions? *Trends Ecol Evol*, 19, 470–474.

Henriksson, A., Wardle, D.A., Trygg, J., Diehl, S. & Englund, G. (2016). Strong invaders are strong defenders - implications for the resistance of invaded communities. *Ecol Lett*, 19, 487–494.

Herbold, B. & Moyle, P.B. (1986). Species and Vacant niches. *Am Nat*, 128, 751–760.

Holt, R.D., Grover, J. & Tilman, D. (1994). Simple Rules for Interspecific Dominance in Systems with Exploitative and Apparent Competition. *Am Nat*, 144, 741–771.

Holt, R.D. & Polis, G.A. (1997). A theoretical framework for intraguild predation. *Am Nat*, 149, 745–764.

Hong, P., Schmid, B., De Laender, F., Eisenhauer, N., Zhang, X., Chen, H., *et al.* (2022). Biodiversity promotes ecosystem functioning despite environmental change. *Ecol Lett*, 25, 555–569.

Hughes, B.B., Eby, R., Van Dyke, E., Tinker, M.T., Marks, C.I., Johnson, K.S., *et al.* (2013). Recovery of a top predator mediates negative eutrophic effects on seagrass. *P Natl Acad Sci USA*, 110, 15313–15318.

IPBES. (2019). Global assessment report of the Intergovernmental Science-Policy Platform on Biodiversity and Ecosystem Services. E. S. Brondizio, J. Settele, S. Díaz, and H. T. Ngo (editors)

Isbell, F., Gonzalez, A., Loreau, M., Cowles, J., Díaz, S., Hector, A., *et al.* (2017). Linking the influence and dependence of people on biodiversity across scales. *Nature*, 546, 65–72.

Janssen, A.B.G., Teurlincx, S., An, S., Janse, J.H., Paerl, H.W. & Mooij, W.M. (2014). Alternative stable states in large shallow lakes? *J Great Lakes Res*, 40, 813–826.

Kraft, N.J.B., Adler, P.B., Godoy, O., James, E.C., Fuller, S. & Levine, J.M. (2015). Community assembly, coexistence and the environmental filtering metaphor. *Funct Ecol*, 29, 592–599.

Latombe, G., Richardson, D.M., McGeoch, M.A., Altwegg, R., Catford, J.A., Chase, J.M., *et al.* (2021). Mechanistic reconciliation of community and invasion ecology. *Ecosphere*, 12.

MacArthur, R.H. & Levins, R. (1967). The limiting similarity, convergence, and divergence of coexisting species. *Am Nat*, 101,

377.

Macdougall, A.S., McCann, K.S., Gellner, G. & Turkington, R. (2013). Diversity loss with persistent human disturbance increases vulnerability to ecosystem collapse. *Nature*, 494, 86–89.

McCann, K.S. & Rooney, N. (2009). The more food webs change, the more they stay the same. *Philos T Roy Soc B*, 364, 1789–1801.

McCarthy, A.H., Peck, L.S., Hughes, K.A. & Aldridge, D.C. (2019). Antarctica: The final frontier for marine biological invasions. *Glob Chang Biol*, 25, 2221–2241.

McCauley, D.J., Gellner, G., Martinez, N.D., Williams, R.J., Sandin, S.A., Micheli, F., *et al.* (2018). On the prevalence and dynamics of inverted trophic pyramids and otherwise top-heavy communities. *Ecol Lett*, 21, 439–454.

Melbourne, B.A., Cornell, H. V., Davies, K.F., Dugaw, C.J., Elmendorf, S., Freestone, A.L., *et al.* (2007). Invasion in a heterogeneous world: Resistance, coexistence or hostile takeover? *Ecol Lett*, 10, 77–94.

Meyer, K.M., Vos, M., Mooij, W.M., Hol, W.H.G., Termorshuizen, A.J. & van der Putten, W.H. (2012). Testing the Paradox of Enrichment along a Land Use Gradient in a Multitrophic Aboveground and Belowground Community. *PLoS One*, 7, 1–9.

Mitchell, C.E., Agrawal, A.A., Bever, J.D., Gilbert, G.S., Hufbauer, R.A., Klironomos, J.N., *et al.* (2006). Biotic interactions and plant invasions. *Ecol Lett*, 9, 726–740.

Moyle, P.B. & Light, T. (1996). Biological invasions of fresh water: Empirical rules and assembly theory. *Biol Conserv*, 78, 149–161.

Oksanen, L., Fretwell, S.D., Arruda, J., Niemela, P. & Niemelä, P. (1981). Exploitation ecosystems in gradients of primary productivity. *Am Nat*, 118, 240–261.

Ou, C., Montaña, C.G. & Winemiller, K.O. (2017). Body size-trophic position relationships among fishes of the lower Mekong basin. *Roy Soc Open Sci*, 4.

Parmesan, C. & Yohe, G. (2003). A globally coherent fingerprint of climate change impacts across natural systems. *Nature*, 421, 37–42.

Pörtner, H.O. & Farrell, A.P. (2008). Ecology: Physiology and climate

change. *Science*, 322, 690–692.

Rall, B.C., Brose, U., Hartvig, M., Vucic-pestic, O., Kalinkat, G., Schwarzmu, F., *et al.* (2012). Universal temperature and body-mass scaling of feeding rates. *Philos T Roy Soc B*, 367, 2923–2934.

Rall, B.C., Vucic-Pestic, O., Ehnes, R.B., EmmersoN, M. & Brose, U. (2010). Temperature, predator-prey interaction strength and population stability. *Glob Chang Biol*, 16, 2145–2157.

Reynolds, S.A. & Aldridge, D.C. (2021). Global impacts of invasive species on the tipping points of shallow lakes. *Glob Chang Biol*, 27, 6129–6138.

Ricklefs, R.E. (1977). Environmental Heterogeneity and Plant Species Diversity: A Hypothesis. *Am Nat*, 111, 376–381.

Robertson, P.A., Mill, A., Novoa, A., Jeschke, J.M., Essl, F., Gallardo, B., *et al.* (2020). A proposed unified framework to describe the management of biological invasions. *Biol Invasions*, 22, 2633–2645.

Rooney, N. & McCann, K.S. (2012). Integrating food web diversity, structure and stability. *Trends Ecol Evol*, 27, 40–45.

Sala, O.E.O.E., Chapin III, F.S., Armesto, J.J., Berlow, E., Bloomfield, J., Dirzo, R., *et al.* (2000). Global biodiversity scenarios for the Year 2100. *Science*, 287, 1770–1774.

Schröder, A., Nilsson, K.A., Persson, L., Van Kooten, T. & Reichstein, B. (2009). Invasion success depends on invader body size in a size-structured mixed predation-competition community. *J Anim Ecol*, 78, 1152–1162.

Seebens, H., Bacher, S., Blackburn, T.M., Capinha, C., Dawson, W., Dullinger, S., *et al.* (2021). Projecting the continental accumulation of alien species through to 2050. *Glob Chang Biol*, 27, 970–982.

Sentis, A., Binzer, A. & Boukal, D.S. (2017). Temperature-size responses alter food chain persistence across environmental gradients. *Ecol Lett*, 20, 852–862.

Sentis, A., Montoya, J.M. & Lurgi, M. (2021). Warming indirectly increases invasion success in food webs. *Proc R Soc B*, 288.

Shea, K. (2002). Community ecology theory as a framework for biological invasions. *Trends Ecol Evol*, 17, 170–176.

Simberloff, D. (2009). We can eliminate invasions or live with them. Successful management projects. *Biol Invasions*, 11, 149–157.

Soetaert, K. & Herman, P.M.J. (2009). *A Practical Guide to Ecological Modelling. using R as a simulation platform.* Springer.

Soetaert, K., Petzoldt, T. & Setzer, R.W. (2010). Solving Differential Equations in R : Package deSolve. *J Stat Softw*, 33.

Sunday, J.M. (2020). The pace of biodiversity change in a warming climate. *Nature*, 580, 460–461.

Sunday, J.M., Bates, A.E. & Dulvy, N.K. (2012). Thermal tolerance and the global redistribution of animals. *Nat Clim Chang*, 2, 686–690.

Thompson, P.L., MacLennan, M.M. & Vinebrooke, R.D. (2018a). An improved null model for assessing the net effects of multiple stressors on communities. *Glob Chang Biol*, 24, 517–525.

Thompson, P.L., MacLennan, M.M. & Vinebrooke, R.D. (2018b). Species interactions cause non-additive effects of multiple environmental stressors on communities. *Ecosphere*, 9 (11): e02518.

Tilman, D. (1985). The Resource-Ratio Hypothesis of Plant Succession. *Am Nat*, 125, 827–852.

Tilman, D. (1999). The ecological consequences of changes in biodiversity: A search for general principles. *Ecology*, 80, 1455–1474.

Tilman, D. & Downing, J.A. (1994). Biodiversity and stability in grasslands. *Nature*, 367, 363–365.

Tomiolo, S. & Ward, D. (2018). Species migrations and range shifts: A synthesis of causes and consequences. *Perspect Plant Ecol*, 33, 62–77.

Trisos, C.H., Merow, C. & Pigot, A.L. (2020). The projected timing of abrupt ecological disruption from climate change. *Nature*, 580, 496–501.

Walther, G., Post, E., Convey, P., Menzel, A., Parmesank, C., Beebee, T.J.C., *et al.* (2002). Ecological response to recent climate cnahge. *Nature*, 416, 389–395.

Wardle, D.A., Bardgett, R.D., Callaway, R.M. & Van Der Putten, W.H.

(2011). Terrestrial ecosystem responses to species gains and losses. *Science*, 332, 1273–1277.

Woodward, G. & Hildrew, A.G. (2002). Differential vulnerability of prey to an invading top predator: Integrating field surveys and laboratory experiments. *Ecol Entomol*, 27, 732–744.

Wootton, K.L. (2017). Omnivory and stability in freshwater habitats: Does theory match reality? *Freshw Biol*, 62, 821–832.

Yodzis, P. & Innes, S. (1992). Body Size and Consumer-Resource Dynamics. *Am Nat*, 139, 1151–1175.

Young, H.S., McCauley, D.J., Galetti, M. & Dirzo, R. (2016). Patterns, Causes, and Consequences of Anthropocene Defaunation. *Annu Rev Ecol Evol S*, 47, 333–358.

Legends

Fig. 1. Community responses to species invasion along environmental gradients for each food web module. (a-e) Trophic position of the invader (blue circle) relative to the resident species (green circles) under apparent competition (AC, panels a, f and l), exploitative competition (EC, panels b, g and m), trophic chain (TC, panels c, h and n), and intraguild predation (IGP) with invading consumer (IGP_C, panels d, i and o) and with invading predator (IGP_P, panels e, j and p). Invasion outcomes (panels f-j) as in Box 1 summarize community changes with gain in diversity ($\Delta D > 0$), no net change ($\Delta D = 0$) or loss in diversity ($\Delta D < 0$) after invasion. Regime states $S_{RES}.S_{INV}$ (panels l-p) summarize all possible combinations of the system qualitative state prior to (S_{RES}) and after (S_{INV}) invasion leading to a gain of stability (stabilizing, $\Delta S > 0$), no net change (neutral, $\Delta S = 0$) or loss of stability (destabilizing, $\Delta S < 0$) after invasion. Regime state abbreviations: N = no species present, O = population oscillations with at least two species present, E = 1 to 3 species in stable equilibrium. Species body mass ratios fixed at $\alpha = \beta = 10$.

Fig. 2. Module-specific effects of species body mass ratios on the averaged proportions of invasion outcomes that drive local diversity change. Body mass ratio given for (a-c) invader and its resident competitor (d, e) and adjacent trophic levels. Food web modules: (a) AC = apparent competition, (b) EC = exploitative competition, (c) IGP = intraguild predation with invading intraguild prey ($\beta \leq 1$) and invading intraguild predator ($\beta \geq 1$), (d) TC = trophic chain and (e) IGP_P = intraguild predation with invading intraguild predator. Species: *R* = basal resource, *C* = consumer, *P* = predator. Symbols denote gain of diversity (squares), no net change (circles) or diversity loss (triangles) following invasions. Colours as in Fig. 1f-j.

Fig. 3. Module-specific effects of species body mass ratios on the averaged proportions of regime states following invasion. Body mass ratio between (a-c) invader and its resident competitor, and (d, e) between adjacent trophic levels. Food web modules and species as in Fig. 1. Regime state abbreviations: N = no species present, O = population oscillations with at least two species present, E = 1 to 3 species in stable equilibrium. Lines = neutral (dotted lines) and non-neutral (solid lines): influence of invader on local stability regime; symbols = gain of stability (squares), neutral change (circle) and loss of stability (triangles) following invasions. Colours identical to Fig. 1l-p.

Fig. 4. Differences in stability change (Δ*S*) between (a) invasion outcomes and (b) biodiversity change (Δ*D*) following successful species invasions. Values = cumulative proportions of regime states shown in Fig. S1. Biodiversity change in (b) illustrates the cumulative proportions observed across invasion outcomes in (a) broken by their effect on diversity, i.e. $\Delta D > 0$ for integration, occupancy and rescue, $\Delta D = 0$ for substitution and $\Delta D < 0$ for vulnerability. Change in stability: $\Delta S < 0$, loss of stability; $\Delta S = 0$, no change; $\Delta S > 0$, increase in stability. Note that resistance to invasion (with $\Delta S = 0$ and $\Delta D = 0$) is excluded in both panels.

Box

Box 1: Invasion outcomes driving local diversity change.

Integration: Invader integrates and coexists with resident species (Moyle & Light 1996), leading to increased diversity.

Occupancy: Invader occupies a niche vacated by a species lost from the resident community prior to the invasion event (Herbold & Moyle 1986), leading to increased diversity.

Rescue: Invader fails to persist in the system but facilitates the persistence of a resident species that would otherwise go extinct (Brown & Kodric-Brown 1977), leading to increased diversity.

Substitution: Invader replaces its resident competitor (Bøhn et al. 2008), leaving the diversity unchanged.

Resistance: Invader disappears without affecting the resident community. This includes both environmental and biotic resistance to invasion (Moyle & Light 1996) and leaves the diversity unchanged.

Vulnerability: Invading species permanently or temporarily destabilizes the resident system and triggers diversity loss through extinctions (Downing et al. 2012; Macdougall et al. 2013).

Box 2: Principles of species coexistence and exclusion in trophic modules

P* rule (apparent competition): The basal (or prey) species capable of sustaining the highest predation pressure dominates the competition and can indirectly exclude its competitor due to higher predation mortality (Holt et al. 1994).

R* rule (exploitative competition): Consumer species with the lowest resource requirements is competitively superior (Tilman 1985). This can lead to the exclusion of the inferior competitor or its presence at a lower biomass density.

Extinction cascade (trophic chain): A specialist predator cannot persist without its prey. Any species loss within a chain leads to a cascading collapse of all species at higher trophic levels in that chain.

Omnivory (intraguild predation): Coexistence in the IGP module relies on two principles, i.e., intraguild prey must be competitively superior to the intraguild predator (R* rule) and must be resilient to predation-induced mortality to avoid its own exclusion (Holt & Polis 1997; Wootton 2017).

Figures

Fig. 1

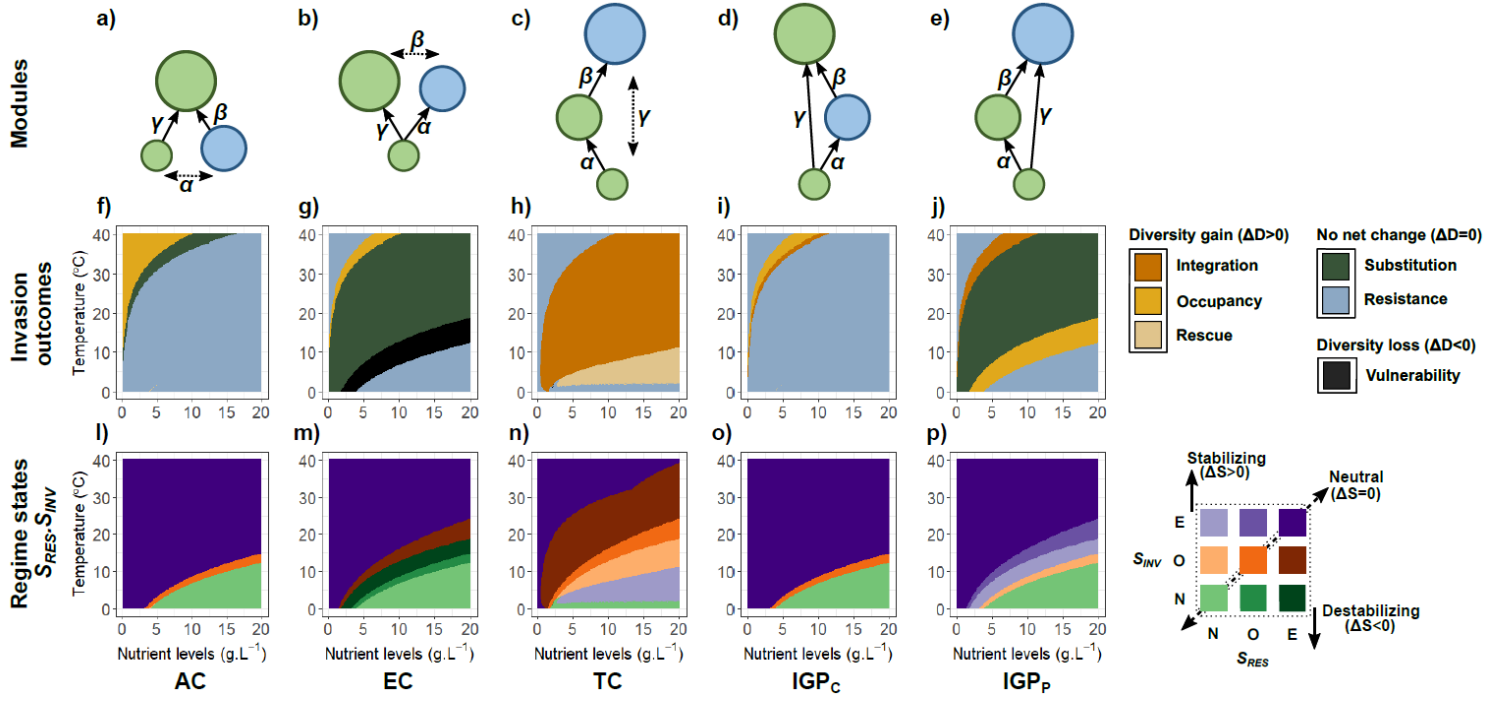

Fig. 2

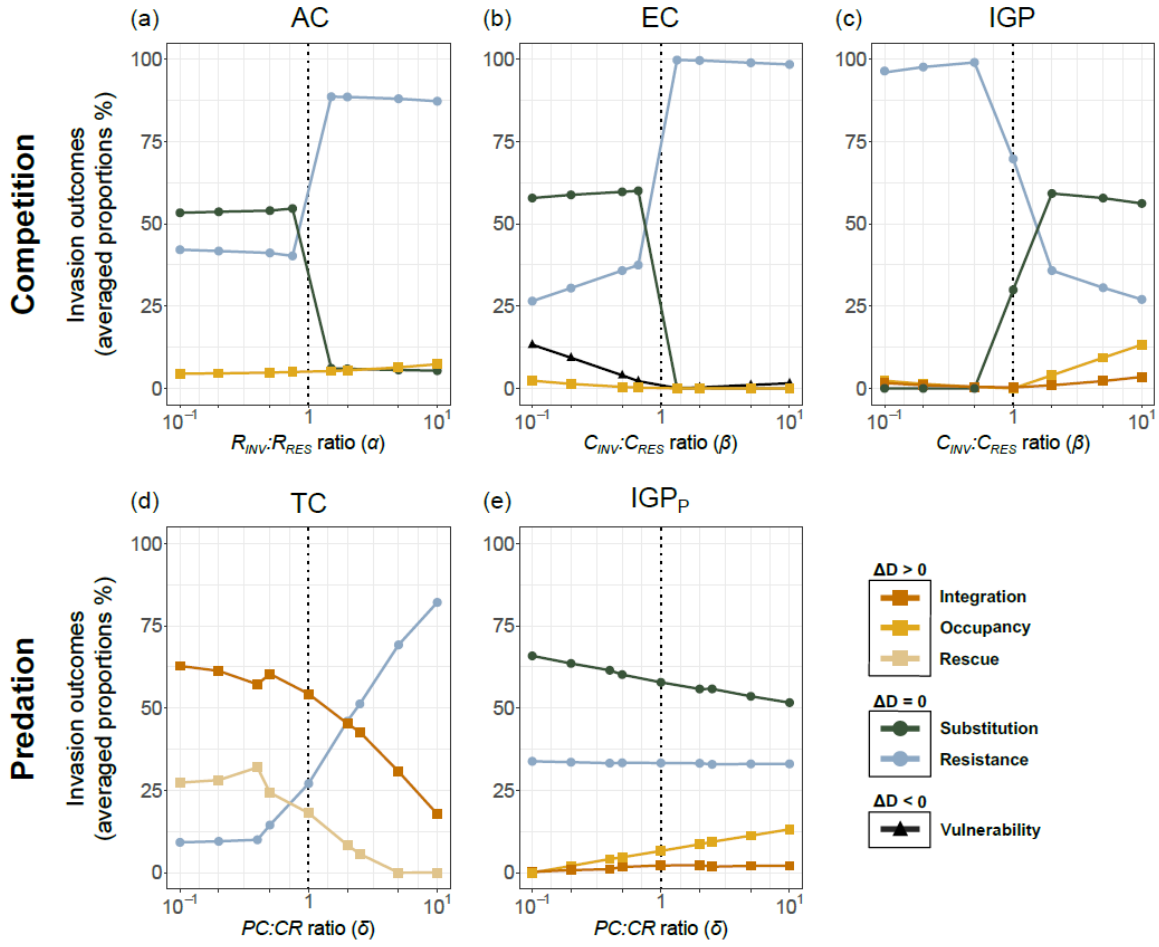
Competition
Predation
Invasion outcomes (averaged proportions %)
(a) AC
(b) EC
(c) IGP
(d) TC
(e) IGP$_P$
R_{INV}:R_{RES} ratio (α)
C_{INV}:C_{RES} ratio (β)
C_{INV}:C_{RES} ratio (β)
PC:CR ratio (δ)
PC:CR ratio (δ)
ΔD > 0
Integration
Occupancy
Rescue
ΔD = 0
Substitution
Resistance
ΔD < 0
Vulnerability

Fig. 3

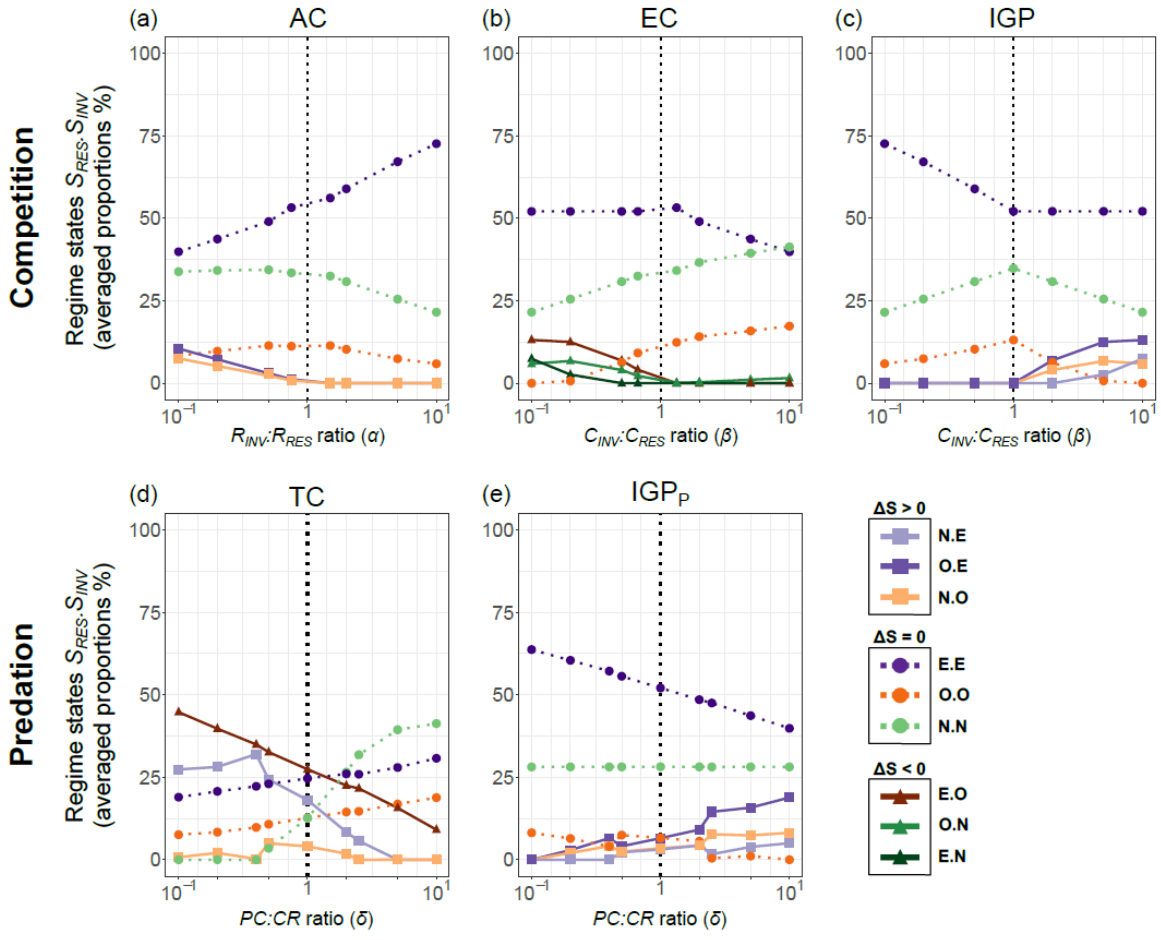
Competition
Predation
Regime states $S_{RES}.S_{INV}$ (averaged proportions %)
(a) AC
(b) EC
(c) IGP
(d) TC
(e) IGP_P
$R_{INV}:R_{RES}$ ratio (α)
$C_{INV}:C_{RES}$ ratio (β)
$PC:CR$ ratio (δ)
ΔS > 0
N.E
O.E
N.O
ΔS = 0
E.E
O.O
N.N
ΔS < 0
E.O
O.N
E.N

Fig. 4

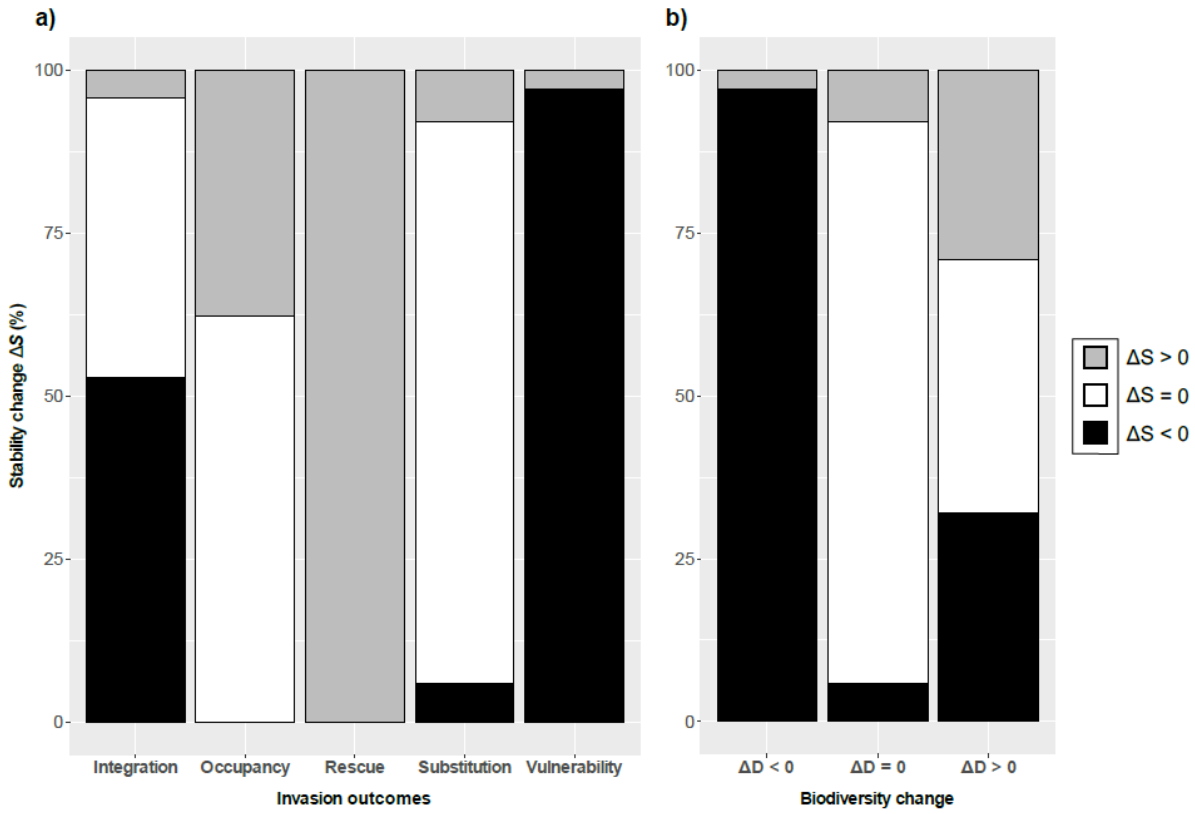
a)
b)
100
75
50
25
0
Stability change ΔS (%)
Integration
Occupancy
Rescue
Substitution
Vulnerability
Invasion outcomes
ΔD < 0
ΔD = 0
ΔD > 0
Biodiversity change
ΔS > 0
ΔS = 0
ΔS < 0

Supplementary information for

Body size and trophic position determine the outcomes of species invasions along temperature and productivity gradients

[Submitted to Ecology Letters]

Samuel Dijoux[1,2,*], Noémie A. Pichon[3,4], Arnaud Sentis[5], David S. Boukal[1,2]

[1.]Department of Ecosystems Biology, Faculty of Science, University of South Bohemia. Branišovská 1760, 370 05 České Budějovice, Czech Republic.
[2.]Czech Academy of Sciences, Biology Centre, Institute of Entomology, Branišovská 31, 370 05 České Budějovice, Czech Republic.
[3.]Ecology and Genetics Unit, Faculty of Science, University of Oulu, 90014 Oulu, Finland.
[4.] Swiss Federal Research Institute WSL, Zuercherstrasse 111, 8902, Birmensdorf, Switzerland.
[5.]INRAE, Aix Marseille University, UMR RECOVER, 3275 Route de Cézanne- CS 40061, 13182 Aix-en-Provence Cedex 5, France.
E-mail addresses: dijoux.samuel@gmail.com (S. Dijoux); noemie.pichon@wsl.ch (N. A. Pichon); arnaud.sentis@inrae.fr (A. Sentis); dboukal@prf.jcu.cz (D. S. Boukal).

This supplementary material contains the following texts, tables and figures:

Text S1. Model specifications.
Text S2. Role of environmental conditions and size structure in the dynamics of the resident consumer-resource system.
Text S3. Additional details on the neutral effects of species invasions on regime stability.
Text S4. Additional details on the observed outcomes of invasions in competitive modules (AC, EC and IGP) along the gradients of species body mass ratios.
Table S1. Models of the resident system and invaded communities.
Table S2. Overview of model parameters.
Table S3. Values of the intercept, slope and activation energy for the body mass and temperature dependence of biological rates used in the model.
Table S4. Species body mass ratio notation in the resident and invaded communities.
Table S5. Species body mass ratios used in the TC and IGP modules.
Table S6. Species body mass ratios used in the AC module.
Table S7. Species body mass ratios used in the EC module.
Table S8. Steady states and biomass densities of individual species at equilibria.
Table S9. Synthesis of invasion outcomes and regime states across community size structure gradients.
Table S10. Average percentages of invasion outcomes and changes in local diversity ΔD due to invasion across species mass ratios in each module.
Table S11. Average percentages of regime states $S_{RES} \rightarrow S_{INV}$ and changes in local stability regime ΔS due to invasion across species mass ratios in each module.
Table S12. Summary of invasion outcomes, their impact on community diversity and stability, and the traits and environmental conditions under which they occur.
Figure S1. Dependence of the qualitative behaviour of the consumer-resource system on environmental conditions and consumer-resource body mass ratio.

Figure S2. Percentage of observed invasion outcomes and regime states across all size ratios and environmental gradients across modules and within each module.
Figure S3. Effect of species body mass ratios on biodiversity change (ΔD) and stability change (ΔS) following species invasion.
Figure S4. Invasion outcomes and regime states along environmental gradients for varying size ratio between competing species in AC and EC modules.
Figure S5. Drivers of species coexistence and exclusion along environmental gradients for varying size ratio between competing species in AC and EC modules.
Figure S6. Drivers of species coexistence and exclusion in IGP module along environmental gradients and varying size ratio between invading and resident species.
Figure S7. Effect of species body mass ratios on community responses to invasion of top predator (TC module) and intraguild predator (IGP module).
Figure S8. Differences between invasion outcomes in stability change following species invasion.
Figure S9. Examples of population biomasses at equilibrium or limit cycle along temperature gradient in invaded communities for varying species body mass ratios γ and fixed nutrient levels.
Figure S10. Examples of population biomasses at equilibrium or limit cycle along gradient of nutrient levels in invaded communities for varying species body mass ratios γ and fixed temperature.

References used in the Supplementary information

Binzer, A., Guill, C., Brose, U. & Rall, B.C. (2012). The dynamics of food chains under climate change and nutrient enrichment. *Philos T Roy Soc B*, 367, 2935–2944.

Binzer, A., Guill, C., Rall, B.C. & Brose, U. (2016). Interactive effects of warming, eutrophication and size structure: Impacts on biodiversity and food-web structure. *Glob Chang Biol*, 22, 220–227.

Brose, U., Jonsson, T., Berlow, E.L., Warren, P., Banasek-Richter, C., Lix Bersier, L.-F., *et al.* (2006). Consumer-resource body size relationships in natural food webs. *Ecology*, 87, 2411–2417.

Brown, J.H., Gillooly, J.F., Allen, A.P., Savage, V.M. & West, G.B. (2004). Toward a Metabolic Theory of Ecology. *Ecology*, 85, 1771–1789.

Ehnes, R.B., Rall, B.C. & Brose, U. (2011). Phylogenetic grouping, curvature and metabolic scaling in terrestrial invertebrates. *Ecol Lett*, 14, 993–1000.

Forster, J., Hirst, A.G. & Atkinson, D. (2012). Warming-induced reductions in body size are greater in aquatic than terrestrial species. *P Natl Acad Sci USA*, 109, 19310–14.

Meehan, T.D. (2006). Energy use and animal abundance in litter and soil communities. *Ecology*, 87, 1650–1658.

Mylius, S.D., Klumpers, K., De Roos, A.M. & Persson, L. (2001). Impact of intraguild predation and stage structure on simple communities along a productivity gradient. *Am Nat*, 158, 259–276.

Rall, B.C., Brose, U., Hartvig, M., Vucic-pestic, O., Kalinkat, G., Schwarzmu, F., *et al.* (2012). Universal temperature and body-mass scaling of feeding rates. *Philos T Roy Soc B*, 367, 2923–2934.

Savage, V.M., Gillooly, J.F., Brown, J.H., West, G.B. & Charnov, E.L. (2004). Effects of body size and temperature on population growth. *Am Nat*, 163, 429–441.

Sentis, A., Binzer, A. & Boukal, D.S. (2017). Temperature-size responses alter food chain persistence across environmental gradients. *Ecol Lett*, 20, 852–862.

Yodzis, P. & Innes, S. (1992). Body Size and Consumer-Resource Dynamics. *Am Nat*, 139, 1151–1175.

Text S1. Model specifications

Density dependence and temperature and mass scaling of biological rates

We do not explicitly model intra- or interspecific competition between individuals occupying the same trophic level in our models, but assume a density-dependent feeding rate f_{ji} of consumers j feeding on resource R_i (Table S1; Eqs 1–5) and following a type II functional response

$$f_{ji} = \left(\frac{a_{ji}R_i}{1+a_{ji}h_{ji}R_i}\right) \text{ (Eq. 6)}$$

with attack rate a_{ji} ($m^2.s^{-1}$) and handling time h_{ji} (s).

Furthermore, we assume that all biological rates Φ_i of species i, i.e. the maximum growth rate and carrying capacity of basal resource and the metabolic rate of the consumer, scale with its body mass M_i (g) and environmental temperature T (K) as

$$\Phi_i(M_i, T) = e^{\mathrm{I}_\Phi} M_i^{\mathrm{S}_\Phi} e^{\mathrm{E}_\Phi \frac{(\mathrm{T}_0 - T)}{kT\mathrm{T}_0}}, \text{ (Eq. 7)}$$

where Φ is r, K or χ; I_Φ is a parameter-specific intercept calculated for M_i = 1 g and T = 20°C (= 293.15 K), S_Φ is the mass scaling exponent, E_Φ is the activation energy (eV), k is the Boltzmann's constant (k = $8.62.10^{-5}$ $eV.K^{-1}$) and T_0 is the normalisation temperature fixed at 20°C (Brown et al., 2004). Functional response parameters a_{ji} and h_{ji} scale with the body masses of consumer M_j and its prey M_i and environmental temperature T analogous to Eq. 7. Furthermore, we assume that both functional response parameters follow a concave-down relationship to predator-prey body mass ratio and that handling time follows a concave-up relationship with temperature (Rall et al. 2012):

$$a_{ji} = a_{ji}(\mathrm{M}_j, \mathrm{M}_i, T) = e^{\mathrm{I}_{\mathrm{a}_0}} M_j^{\mathrm{S}_{\mathrm{j}_{\mathrm{a}_0}}} M_i^{\mathrm{S}_{\mathrm{i}_{\mathrm{a}_0}}} e^{\mathrm{E}_{\mathrm{a}_0} \frac{(\mathrm{T}_0 - T)}{kT\mathrm{T}_0}} e^{\mathrm{I}_{\mathrm{a_m}} + \mathrm{S}_{1_{\mathrm{a_m}}} \ln\left(M_j/M_i\right) + \mathrm{S}_{2_{\mathrm{a_m}}} \left(\ln\left(M_j/M_i\right)\right)^2} \text{ (Eq. 8)}$$

$$h_{ji} = h_{ji}(\mathrm{M}_j, \mathrm{M}_i, T) = e^{\mathrm{I}_{\mathrm{h}_0}} M_j^{\mathrm{S}_{\mathrm{j}_{\mathrm{h}_0}}} M_i^{\mathrm{S}_{\mathrm{i}_{\mathrm{h}_0}}} e^{\mathrm{E}_{\mathrm{h}_0} \frac{(\mathrm{T}_0 - T)}{kT\mathrm{T}_0}} * e^{\mathrm{I}_{\mathrm{h_m}} + \mathrm{S}_{1_{\mathrm{h_m}}} \ln\left(M_j/M_i\right) + \mathrm{S}_{2_{\mathrm{h_m}}} \left(\ln\left(M_j/M_i\right)\right)^2} e^{\mathrm{I}_{\mathrm{h_T}} + \mathrm{S}_{1_{\mathrm{h_T}}} \mathrm{T} + \mathrm{S}_{2_{\mathrm{h_T}}} T^2} \text{ (Eq. 9)}$$

The values for the parameter-specific intercepts I_Φ, slopes S_Φ and activation energies E_Φ used in all equations are summarized in Table S3.

Population dynamics

We start the simulations of the resident system and the invaded community near the consumer-resource equilibrium and simulate the invasion by adding a low population density of the invader. We simulate the changes in species biomass densities within each module described by Eqs 1–9 for 5000 years, which allows the system to reach an attractor (a stable equilibrium or a limit cycle around an unstable equilibrium, Figs. S9 and S10) for each combination of environmental conditions and body mass ratios (Tables S5–S7; 10,025,000 combinations in total). The initial biomass density of each resident species is set to 1.02 times its equilibrium value (Eqs. 11, Table S8). We set the initial biomass density of an invading species to 10^{-6} g.m^{-2} and use 10^{-12} g.m^{-2} as the extinction threshold for each species as in (Sentis et al. 2017).

We did not find a reasonable closed-form formula for the three-species equilibrium and therefore could not calculate the Jacobian matrix in the IGP module. To determine the regime state of the three-species system in the IGP module, we examined the population biomass in the last 10 years of each simulation to determine whether the population was cycling or in a stable equilibrium.

We set the resident consumer-resource body mass ratios to α (notation relevant for the TC and IGP$_P$ predation modules) or γ (notation relevant for the AC, EC and IGP$_C$ competitive modules) = 1, 2, 5 and 10 as in (Sentis et al. 2017) to cover a wide range of species mass ratios observed between interacting species in natural systems (Brose et al. 2006; Forster et al. 2012). The combinations of 4 × 4 = 16 body mass ratios for the two consumer-resource pairs with two resident species and one resident and one invading species (Table S5) were used in all four trophic modules. In the competitive modules, we added body mass ratios α or β = 0.1, 0.2, 0.5, 0.75 and 1.5, reflecting the baseline values and characterising smaller or slightly larger competitors to further investigate their invasion success. We excluded combinations of α and β yielding resident consumer-resource

mass ratios $\gamma = \alpha\beta < 1$, resulting in nine additional combinations of body mass ratios in the competitive modules (Tables S6 and S7).

Text S2. Role of environmental conditions and size structure in the dynamics of the resident consumer-resource system

We summarise here the effects of temperature, nutrient levels and consumer-resource body mass ratio on the resident consumer-resource system prior to invasion; see also (Binzer et al., 2012, 2016; Sentis et al., 2017). The system can reach a stable equilibrium point with 0–2 species present or a stable consumer-resource cycle (Fig. S1). While the combination of high temperature and limited nutrient input leads to the metabolic meltdown of the consumer, increasing nutrient supply at lower temperatures leads to the paradox of enrichment, i.e. population oscillations that can lead to a collapse of the consumer-resource system (Fig. S1a). Larger consumer-resource body mass ratios have a stabilizing effect and prevent the collapse, although larger consumers also become more susceptible to metabolic meltdown as a result. This is shown by the changing proportions of each system regime along the gradient of the consumer-resource size ratio (equilibrium *E*, from 40% to 81%; oscillations *O*, from 19% to 4%; collapse *N*, from 4% to 9%; Fig. S1b).

Text S3. Additional details on the neutral effects of species invasions on regime stability

We summarise here the regime states $S_{RES} \rightarrow S_{INV}$ observed in our analyses that resulted in neutral changes in community stability ($\Delta S = 0$) following species invasion. Overall, community resistance to invasion is the dominant outcome across all invader characteristics (trophic position and size) and environmental conditions in our analyses (Fig. S2a). Resistance is followed by species substitution, integration, and niche occupancy, while rescue and vulnerability are the least common (Fig. S2a). The predominance of resistance to invasion contributes to the fact that community stability usually does not change after the invasion ($\Delta S = 0$,

including the $E \rightarrow E$, $N \rightarrow N$ and $O \rightarrow O$ regime states). That is, species invasion does not change community stability in 86.6% of all simulations ($E \rightarrow E$ ~ 50.5%, $N \rightarrow N$ ~ 27.4% and $O \rightarrow O$ ~ 8.7%; Fig. S2a).

Community size structure and abiotic conditions jointly drive the (lack of) change in regime state. Overall, proportions of environmental conditions for which the regime state remains the same after invasion decline as the invading species becomes much smaller than the resident competitor (Fig. S3a-c). That is, the invasion of an increasingly smaller basal resource species in the AC module ($\alpha < 1$, Figs. 3a and S3a) leads to a decreasing proportion of unchanged equilibria ($E \rightarrow E$, from ~ 53% for α = 0.75 to ~ 40% for α = 0.1) and stable cycles ($O \rightarrow O$, from ~ 11% for α = 0.75 to ~ 8% for α = 0.1), and a nearly constant proportion of collapsed states ($N \rightarrow N$ ~ 33% over all values of $\alpha < 1$). The invasion of an increasingly smaller consumer species in the EC module ($\beta < 1$, Figs. 3b and S3b) leads to decreasing proportions of unchanged collapsed states ($N \rightarrow N$, from ~ 32% for α = 0.75 to ~ 21% for α = 0.1) and unchanged stable cycles ($O \rightarrow O$ ~ 9% for α = 0.75 to 0% for α = 0.1), while the proportion of unchanged equilibria remains constant ($E \rightarrow E$ ~ 52%). Similarly, the invasion of an increasingly larger intraguild predator in the IGP module ($\beta > 1$, Figs. 3c and S3c) mainly leads to decreasing proportions of unchanged collapsed states ($N \rightarrow N$, from ~ 31% for β = 2 to ~ 22% for β = 10) and the disappearance of unchanged stable cycles ($O \rightarrow O$, from ~ 6% to 0%), while the proportion of unchanged equilibria remains constant ($E \rightarrow E$ ~ 52%).

Finally, the changes in the proportions of unchanged regime states differ across the size structure gradient between the TC and IGP_P modules. In the TC module, the proportions of unchanged regime states increase as the top predator and intermediate consumer become similar in size: $E \rightarrow E$ increases from ~ 19% to ~ 31%, $O \rightarrow O$ from ~ 8% to ~ 19%, and $N \rightarrow N$ from 0% to ~ 41% when δ increases from 0.1 to 10 (Figs. 3d and S3d). In the IGP_P module, the trend is opposite as the proportions of unchanged equilibria and stable cycles decrease ($E \rightarrow E$: from ~ 64 to ~ 40%, $O \rightarrow O$: from ~ 8% to 0%), while collapsed states remain constant ($N \rightarrow N$ ~ 28%) when δ increases from 0.1 to 10 (Figs. 3e and S3e).

Text S4. Additional details on invasion outcomes in competitive modules (AC, EC and IGP) along gradients of species body mass ratios.

AC module can be invaded by a smaller basal species ($\alpha < 1$) at intermediate nutrient levels and temperatures, while a larger invader can replace the competitor only if it leads to higher feeding rates by the predator, which hereby avoids metabolic meltdown (Figs. 2f, S4d-f and S5d-f). Consequently, species substitution is more common than resistance for smaller invading competitors (substitution ~ 55% and resistance ~ 42% of all simulations for each $\alpha < 1$), while resistance dominates for larger invading competitors (substitution ~ 5%, resistance ~ 88% of all simulations for each $\alpha < 1$; Fig. 3a). Similar patterns of size ratio-dependent results occur in the EC module (Fig. 3b), although the system resists smaller invading competitors less often, while larger consumers invade very rarely (resistance: ~ 26–37% of all simulations for each $\beta < 1$ and 98–100% for each $\beta > 1$). Invasion of smaller consumers also increases the propensity to collapse (vulnerability: ~ 0–13% of all simulations for each $\beta < 1$). Occupation of a vacant niche by the invader is rare and almost independent of the size ratio between the competing species (occupancy: ~ 4–7% of all simulations for each size ratio in the AC module and 0–2% in the EC module).

The role of species body mass ratio in the IGP module cannot be completely separated from the role of trophic position, as we assumed that the prey is smaller than the predator (Fig. 3c). Invasions of a smaller consumer C_{INV} that becomes the intraguild prey almost always fail (resistance: ~ 96–99% of all simulations for each $\beta < 1$), while larger consumers that become the intraguild predator mainly replace the local consumer (substitution: ~ 56–59% of all simulations for each $\beta > 1$). Thus, resistance to invasion by a larger consumer drops to 27% of all simulations for each $\beta > 1$ as larger consumers can also occupy niches left vacant by an extinct consumer (up to 13% for each $\beta > 1$) or integrate into the system and coexist with resident IG prey (up to 3% for each $\beta > 1$).

Table S1: Models of the resident consumer-resource system and invaded communities. The respective rates of change $\dot{R}$, $\dot{C}$ and $\dot{P}$ of basal resource, consumer and top predator biomass densities R, C and P (g.m^{-2}) in each model depend on carrying capacity K_R (g.m^{-2}) and maximum growth rate r_R (s^{-1}) of the resource, rates of biomass loss of the (intermediate) consumer and top predator χ_C and χ_P (s^{-1}), their feeding rates (see Eq. 6 in Text S1) and feeding efficiency ϵ that denotes the fraction of ingested biomass converted into consumer biomass (unitless, set to 0.85 as in (Yodzis & Innes, 1992). Indices i = 1 and 2 in Eqs 2 and 3 denote species with the same trophic position.

Resident system		
Consumer-resource (CR)	$\dot{R} = r_R R\left(1 - \frac{R}{K_R}\right) - f_{CR} C$ $\dot{C} = C(\varepsilon f_{CR} - \chi_C)$	**Eq. 1**
Invaded communities		
Apparent competition (AC)	$\dot{R}_i = r_{R_i} R_i \left(1 - \frac{R_i}{K_{R_i}}\right) - f_{CR_i} C$ $\dot{C} = C\left(\sum_{i=1}^{2} \varepsilon f_{CR_i} - \chi_C\right)$	**Eq. 2**
Exploitative competition (EC)	$\dot{R} = r_R R\left(1 - \frac{R}{K_R}\right) - \sum_{i=1}^{2} f_{C_i R}\ C_i$ $\dot{C}_i = C_i\left(\varepsilon f_{C_i R} - \chi_{C_i}\right)$	**Eq. 3**
Tri-trophic chain (TC)	$\dot{R} = r_R R\left(1 - \frac{R}{K_R}\right) - f_{CR}\ C$ $\dot{C} = C(\varepsilon f_{CR} - \chi_C) - f_{PC}\ P$ $\dot{P} = P(\varepsilon f_{PC} - \chi_P)$	**Eq. 4**
Intraguild predation (IGP)	$\dot{R} = r_R R\left(1 - \frac{R}{K_{R_r}}\right) - (f_{CR}\ C + f_{PR}\ P)$ $\dot{C} = C(\varepsilon f_{CR} - \chi_C) - f_{PC}\ P$ $\dot{P} = P(\varepsilon f_{PC} + \varepsilon f_{PR} - \chi_P)$	**Eq. 5**

Table S2: Overview of model parameters. See Table S3 for the values and meaning of I_ϕ, S_ϕ and E_ϕ.

Parameter	Value	Unit	Description
r_R	-	day^{-1}	Intrinsic growth rate of resource *R*
K_R	varied	$g.L^{-1}$	Carrying capacity of resource *R*
ε	0.85	-	Biomass conversion efficiency
χ_j	-	day^{-1}	Metabolic loss rate of species *j*
h_{ji}	-	s	Handling time of predator *j* feeding on prey *i*
a_{ji}	-	$g.m^{-2}$	Attack rate of predator *j* feeding on prey *i*
E_ϕ	Table S2	$eV.K^{-1}$	Activation energy for biological parameter ϕ
I_ϕ	Table S2	-	Intercept for biological parameter ϕ
S_ϕ	Table S2	-	Scaling coefficient for biological parameter ϕ
T	varied	K	Temperature
T_0	293.15	K	Normalization temperature (20°C)
k	8.617×10^{-5}	$eV.K^{-1}$	Boltzmann constant

Table S3: Values of the intercept I_ϕ, slope S_ϕ and activation energy E_ϕ for the body mass and temperature dependence of biological rates used in the model, i.e. of the maximum growth rate r (s^{-1}) (Savage et al. 2004) and carrying capacity K ($g.m^{-2}$) (Meehan 2006) of the basal resource and the metabolic rate χ (s^{-1}) (Ehnes et al. 2011), maximum consumption rate $h_{0_{ji}}$ (s^{-1}), and half-saturation density $a_{0_{ji}}$ ($g.m^{-2}$) (Rall et al. 2012) and mass- and temperature-dependent attack rate and handling time of predator j feeding on prey i. Symbols S_1 and S_2 respectively refer to the linear and quadratic term of the mass slope.

Parameter	r	K	χ	$a_{0_{ji}}$	$h_{0_{ji}}$	$a_{m_{ji}}$	$h_{m_{ji}}$	$h_{T_{ji}}$
I_ϕ	-15.68	0–15	-16.54	-13.1	9.66	-1.81	1.92	0.5
S_ϕ	-0.25	0.28	-0.31	S_j = -0.8 S_i = 0.25	S_j = 0.47 S_i = -0.45	S_1 = 0.39 S_2 = -0.017	S_1 = -0.48 S_2 = 0.0256	S_1 = -0.055 S_2 = 0.0013
E_ϕ	-0.84	0.71	0.69	-0.38	0.26	-	-	-

Table S4: Species body mass ratio notation in the resident and invaded communities. Solid arrows = trophic interactions and body mass ratios between resident (green circles; subscript *RES*) and invading species (blue circles; subscript *INV*); dashed double-headed arrows = indirect interactions between species. Thin arrows = trophic interactions between resident species; thick arrows = trophic interactions involving the invader. Note that $\gamma = \alpha\beta$ and $\delta = \beta/\alpha$ ('-' = parameter not relevant). Body mass ratios α and γ in the CR module denote the same property; four values of α are used in the predation modules and 15 values of γ are used in the competitive modules (Text S1).

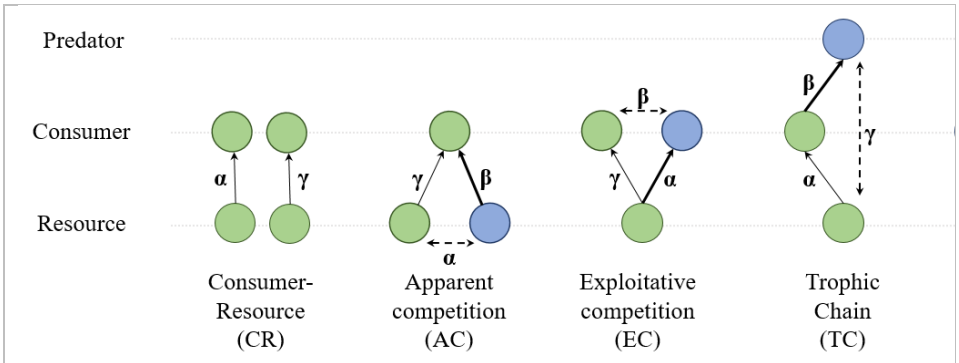

Ratio	CR	AC	EC	TC	IGP_C	IGP_P
α	$C_{RES}:R_{RES}$	$R_{INV}:R_{RES}$	$C_{INV}:R_{RES}$	$C_{RES}:R_{RES}$	$C_{INV}:R_{RES}$	$C_{RES}:R_{RES}$
β	-	$C_{RES}:R_{INV}$	$C_{RES}:C_{INV}$	$P_{INV}:C_{RES}$	$P_{RES}:C_{INV}$	$P_{INV}:C_{RES}$
γ	$C_{RES}:R_{RES}$	$C_{RES}:R_{RES}$	$C_{RES}:R_{RES}$	$P_{INV}:R_{RES}$	$P_{RES}:R_{RES}$	$P_{INV}:R_{RES}$
δ	-	-	-	$\frac{P_{INV}:C_{RES}}{C_{RES}:R_{RES}}$	$\frac{P_{RES}:C_{INV}}{C_{INV}:R_{RES}}$	$\frac{P_{INV}:C_{RES}}{C_{RES}:R_{RES}}$

Table S5: Species body mass ratios used in the TC and IGP modules. Values given as P:C:R with R = 1. Note that $\gamma = \alpha\beta = P$:R.

Ratio		***β***			
		1	2	5	10
α	1	1:1:1	2:1:1	5:1:1	10:1:1
	2	2:2:1	4:2:1	10:2:1	20:2:1
	5	5:5:1	10:5:1	25:5:1	50:5:1
	10	10:10:1	20:10:1	50:10:1	100:10:1

Table S6: Species body mass ratios used in the AC module. Values given as C_{RES}:R_{INV}:R_{RES} with R_{RES} = 1. Values of $\alpha < 1$ and $\alpha > 1$ respectively denote the invasion of a smaller and larger resource species. '-' = consumers smaller than resources (C_{RES}:$R_{RES} < 1$) were not considered.

Ratio		***β***			
		1	2	5	10
α	0.1	-	-	-	1:0.1:1
	0.2	-	-	1:0.2:1	2:0.2:1
	0.5	-	1:0.5:1	2.5:0.5:1	5:0.5:1
	0.75	-	1.5:0.75:1	3.75:0.75:1	7.5:0.75:1
	1	1:1:1	2:1:1	5:1:1	10:1:1
	1.5	1.5:1.5:1	3:1.5:1	7.5:1.5:1	15:1.5:1
	2	2:2:1	4:2:1	10:2:1	20:2:1
	5	5:5:1	10:5:1	25:5:1	50:5:1
	10	10:10:1	20:10:1	50:10:1	100:10:1

Table S7: Species body mass ratios used in the EC module. Values given as C_{RES}:C_{INV}:R_{RES} with R_{RES} = 1. Values of $\beta < 1$ and $\beta > 1$ respectively denote the invasion of a larger and smaller consumer species. '-' = consumers smaller than resources (C_{RES}:$R_{RES} < 1$ or C_{INV}:$R_{RES} < 1$) were not considered.

Ratio		***β***								
		0.1	0.2	0.5	0.75	1	1.5	2	5	10
α	1	-	-	-	-	1:1:1	1.5:1:1	2:1:1	5:1:1	10:1:1
	2	-	-	1:2:1	1.5:2:1	2:2:1	3:2:1	4:2:1	10:2:1	20:2:1
	5	-	1:5:1	2.5:5:1	3.75:5:1	5:5:1	7.5:5:1	10:5:1	25:5:1	50:5:1
	10	1:10:1	2:10:1	5:10:1	7.5:10:10	10:10:1	15:10:1	20:10:1	50:10:1	100:10:1

Table S8: Steady states and biomass densities of individual species at equilibria. Note that coexistence of all three species in the AC and EC modules is not possible.

Steady state	Composition	Equilibrium biomass densities	Equations
Trivial equilibrium	No species present	$R^* = C^* = P^* = 0$	
Basal resource present	R_{RES} R_{INV} $R_{RES} + R_{INV}$ (AC)	$R^* = K_R$ $C^* = P^* = 0$	Eq. 10
Consumer-resource (CR)	$C_{RES} + R_{RES}$ $C_{RES} + R_{INV}$ (AC) $C_{INV} + R_{RES}$ (EC, IGP_C) $P_{RES} + R_{RES}$ (IGP_C) $P_{INV} + R_{RES}$ (IGP_P)	$R^* = \frac{\chi_C}{a_{CR}(\epsilon - \chi_C h_{CR})}$ $C^* = \frac{r_R}{K_R\, a_{CR}\, (1 + (a_{CR} h_{CR}\, R^*)(K_R - R^*)}$ $P^* = 0$	Eqs. 11

Three species present (TC)	P_{INV} + C_{RES} +R_{RES}	$R^* = \frac{\left(r_R(K_R\, a_{CR}\, h_{CR} - 1) + \sqrt{\Delta}\right)}{2 r_R a_{CR} h_{CR}}$ $C^* = \frac{\chi_P}{a_{PC}(\epsilon - \chi_P h_{PC})}$ $P^* = \frac{(1 + a_{PC} h_{PC} C^*)(a_{CR} R^* (\epsilon - \chi_C h_{CR}) - \chi_C)}{a_{PC}(1 + a_{CR} h_{CR} R^*)}$, where $\Delta = (K_R r_R a_{CR} h_{CR} - r_R)^2 + 4\left(K_R r_R a_{CR} h_{CR}\left(r_R - \frac{a_{CR}\chi_P}{\epsilon - h_{PC}\chi_P}\right)\right)$	Eqs. 12
Three species present (IGP)	P_{INV} + C_{RES} + R_{RES} P_{RES} + C_{INV} + R_{RES}	We did not find a meaningful closed-form formula for the three-species equilibrium and used numerical continuation techniques (see Text S1) to find the equilibrium values for each combination of temperature, nutrient levels and species body masses see e.g., (Mylius et al. 2001) for a slightly different IGP model.	-

Table S9: Synthesis of invasion outcomes and regime states across community size structure gradients (illustrated in Figs 3-4)**.** Values in parentheses give the range of the percentage of outcomes pooled across all environmental conditions for each size structure. Neutral effect corresponds to $\Delta S = 0$ and can include regime states $E \rightarrow E$, $O \rightarrow O$, and $N \rightarrow N$.

Interaction	Body mass ratio	Module	Invasion outcomes	Regime states $S_{RES} \rightarrow S_{INV}$
competition	Smaller invader ($\alpha < 1$ or $\beta < 1$)	AC	Substitution (~ 53–55%) Resistance (~ 40–42%) Occupancy (~ 5%)	Mostly neutral effects, sometimes stabilizing ($O \rightarrow E$: 1–11%) or preventing collapse ($N \rightarrow O$: 1–8%)
		EC	Substitution (~58–60%) Resistance (~27–38%) Vulnerability (~ 2–13%) Occupancy (~ 0–2%)	Mostly neutral effects, sometimes inducing cycles ($E \rightarrow O$: 4–13%) or promoting collapse ($E \rightarrow N$: 0–7%, $O \rightarrow N$: 2–7%)
		IGP_C	Resistance (~ 96–99%) Occupancy (~ 0–2%) Integration (~ 0–2%)	Only neutral effects
	Larger invader ($\alpha > 1$ or $\beta > 1$)	AC	Resistance (~ 87–89%) Occupancy (~5–7%) Substitution (~5–6%)	Only neutral effects
		EC	Resistance (~ 98–99.8%) Vulnerability (~ 0–2%)	Mostly neutral effects, rarely promotes collapse ($O \rightarrow N$: 0–2%)
		IGP_P	Substitution (~ 56–59%) Resistance (~ 37–36%) Occupancy (~ 4–13%)	Mostly neutral effects, sometimes stabilising and preventing collapse

			Integration (~ 1–4%)	(*O*→*E*: 7–13%, *N*→*E*: 0–7%, *N*→*O*: 4–7%)
direct trophic link	Invading predator and resident consumer more similar in size ($\delta < 1$)	TC	Integration (~ 60–63%) Rescue (~ 24–32%) Resistance (~ 9–15%)	Inducing cycles (*E*.*O*: 33–45%) or stabilising and preventing collapse (*N*→*E*: 27–32%, *N*→*O*: 0–5%, and *O*→*E*: 0–1%)
		IGP_P	Substitution (~ 60–66%) Resistance (~ 33%) Integration (~ 0–2%)	Mostly neutral effect (89–100%), sometimes stabilising (*O*→*E*: 0–7%) or preventing collapse (*N*→*O*: 0–4%)
	Resident consumer and resource more similar in size ($\delta > 1$)	TC	Resistance (~ 50–82%) Integration (~ 18–40%) Occupancy (~ 0–5%)	Mostly neutral effect (67–91%), sometimes inducing cycles (*E*→*O*: 9–22%) or preventing collapse (*N*→*E*: 0–8%)
		IGP_P	Substitution (~ 52–56%) Resistance (~ 33%) Occupancy (~ 9–13%) Integration (~ 2%)	Mostly neutral effects, sometimes stabilising and preventing collapse (*O*→*E*: 9–19%, *N*→*O*: 4–8%, *N*→*E*: 2–5%)

Table S10: Average percentages of invasion outcomes and changes in local diversity Δ*D* due to invasion across species mass ratios in each module (illustrated in Figs. 3, S3a-e, S5a-f, S5m-r, S6a-f and S9a-d). BMR = body mass ratio, given by the 'Ratio' column (see Fig. 2). Change in diversity: $\Delta D < 0$, diversity loss; $\Delta D = 0$, no net change of diversity; $\Delta D > 0$, increased diversity.

Note: this table is kept as a separate file (not included in the thesis) available in Zenodo and GitHub repositories (https://doi.org/10.5281/zenodo.7273775) and can be provided by the author upon request.

Table S11: Average percentages of regime states $S_{RES} \rightarrow S_{INV}$ and changes in local stability regime Δ*S* due to invasion across species mass ratios in each module (illustrated in Figs. 4, S3f-j). BMR = body mass ratio, given by the 'Ratio' column (see Fig. 2). Regime state abbreviations: *N* = no species present, *O* = population oscillations with 2–3 species present, *E* = 1–3 species in stable equilibrium. Invader effect: $\Delta S < 0$, destabilizing; $\Delta S = 0$, neutral; $\Delta S < 0$, stabilizing.

Note: this table is kept as a separate file (not included in the thesis) available in Zenodo and GitHub repositories (https://doi.org/10.5281/zenodo.7273775) and can be provided by the author upon request.

Table S12. Summary of invasion outcomes, their impact on community diversity and stability, and the traits and environmental conditions under which they occur. Changes in diversity (Δ*D*) and community stability (Δ*S*) following invasion depend on the invader traits (body size and trophic position) and environmental conditions. Qualitative changes in diversity and regime states: '+' = increased diversity (Δ*D*) or stabilizing (Δ*S*), '0' = no effect (Δ*D* or Δ*S*), '-' = diversity loss (Δ*D*) or destabilizing (Δ*S*); uncommon effects in parentheses. See Box 1 for the definitions of invasion outcomes, Methods for the definitions of Δ*D* and Δ*S*, and Figs. S1–S9 for their illustrations. Resistance to invasion (see Results for details) is excluded.

Invasion success/failure	**Invasion outcomes**	**Community impact**		**Invader traits (module)**	**Environmental conditions**
		Δ*D*	**Δ*S***		
success	**Substitution**	0	(-)/0/(+)	Small consumer (EC) or basal resource (AC)	Warm, nutrient-rich habitat
				Large basal resource (AC)	Warm, nutrient-limited habitat
				Large omnivorous predator (IGP_P)	Warm, nutrient-rich habitat
	Integration	+	-/0/(+)	Large predator (TC, IGP_P)	Warm, nutrient-rich habitat
				Intraguild prey (IGP_C)	
	Occupancy	+	0/+	Basal resource (AC)	Warm, nutrient-limited habitat (absence of consumer)
				Small consumer (EC) or intraguild prey (IGP_C)	Warm, nutrient-limited habitat
				Intraguild predator (IGP_P)	Cold, nutrient-rich habitat
failure	**Rescue**	+	+	Large specialist predator (TC)	Cold, nutrient-rich habitat
	Vulnerability	-	-/(+)	Small consumer (EC)	Cold, nutrient-rich habitat
				Large specialist predator (TC)	Cold, nutrient-limited habitat

Fig. S1. Dependence of the qualitative behaviour of the consumer-resource system on (a) environmental conditions and (b) consumer-resource body mass ratio. (a) Regime states along gradients of temperature and nutrient levels for consumer-resource mass ratio C_{RES}:R_{RES} = 100. (b) Proportion of each regime state in local community S_{RES} (colour coded as in panel a) across all environmental conditions for the given consumer-resource body mass ratio. *E* = equilibrium, *O* = stable oscillations, *N* = community collapse; proportion of equilibrium state sums the proportions of resource-only (*R*, dashed line) and two-species equilibria (*C*-*R*, dotted line).

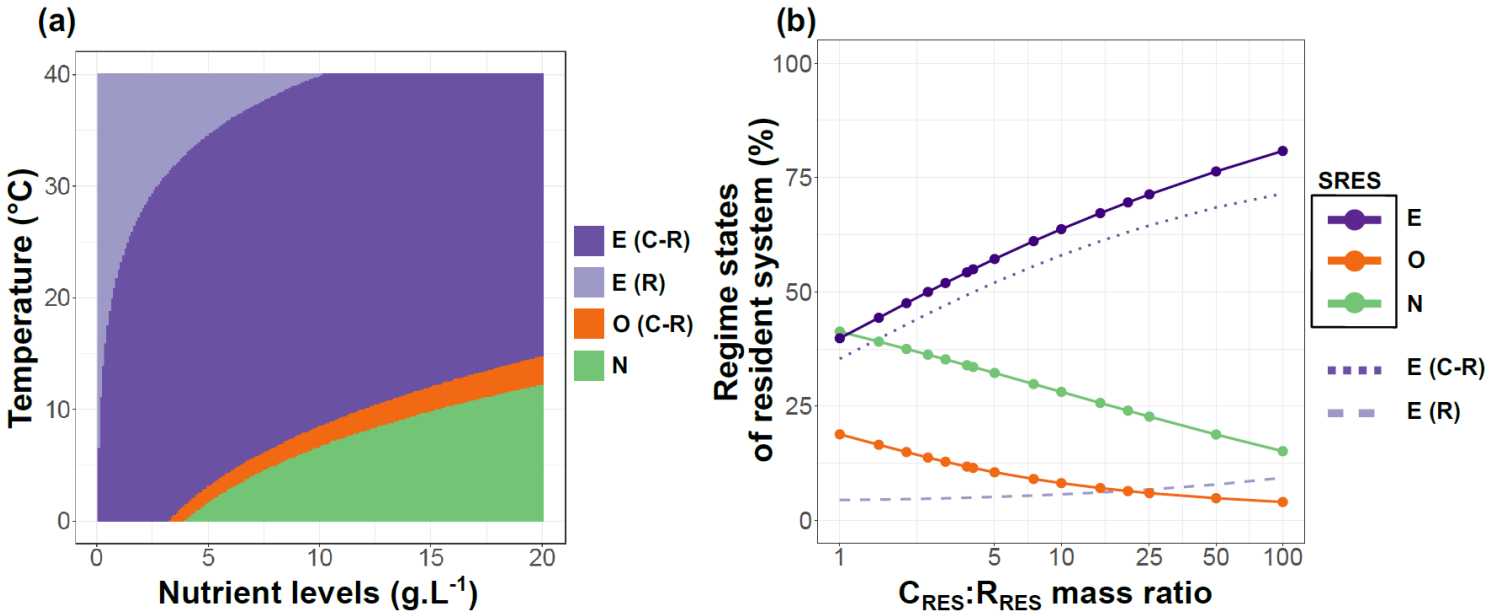

Fig. S2. Percentage of observed invasion outcomes (a-b) and regime states (c-d) across all size ratios and environmental gradients across modules (a-c) and within each module (b-d). Colours as in Fig. 1.

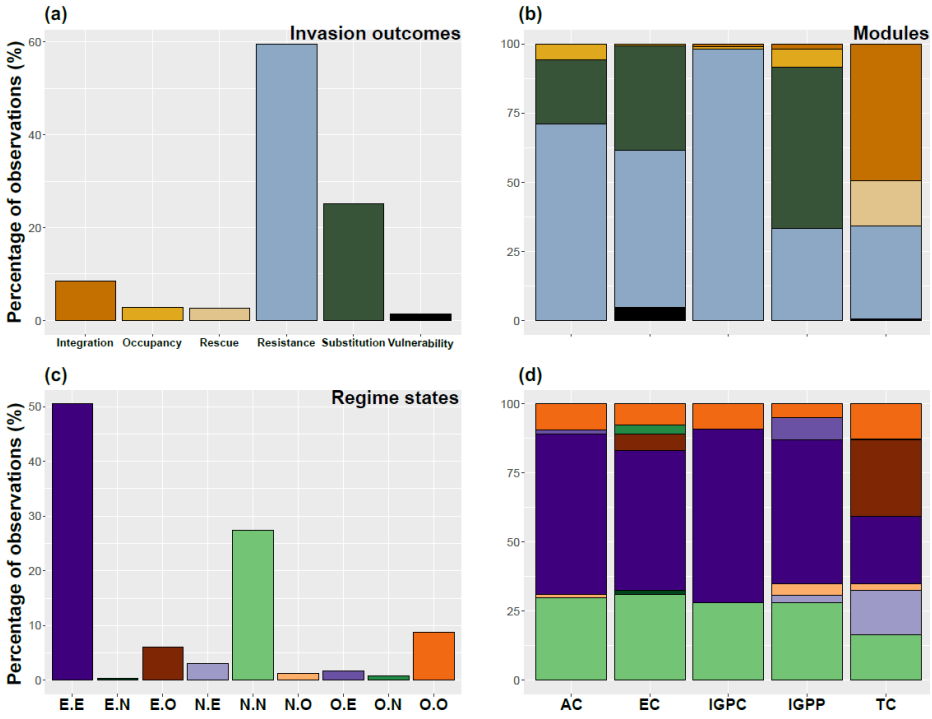

Fig. S3. Effect of species body mass ratios on biodiversity change (Δ*D*, a-e) and stability change (Δ*S*, f-j) following species invasion. Body mass ratio given for (a-c, f-h) invading species and its resident competitor, and (d-e, i-j) adjacent trophic levels. Food web modules: (a, f) AC = apparent competition, (b, g) EC = exploitative competition, (c, h) IGP = intraguild predation with invading IG prey (IGP_C, $\beta \leq 1$) and invading predator (IGP_P, $\beta \geq 1$), (d, i) TC = trophic chain and (e, j) IGP_P = intraguild predation with invading IG predator. Species: *R* = basal resource, *C* = consumer, *P* = predator. Changes following invasions represent cumulative proportions of observed invasion outcomes and stability regimes, and denote either a positive ($\Delta > 0$, dashed lines and square symbols), neutral ($\Delta = 0$, dotted lines and circle symbols) or negative effects ($\Delta < 0$, solid lines and triangle symbols) of invading species across all combinations of temperature and nutrient levels.

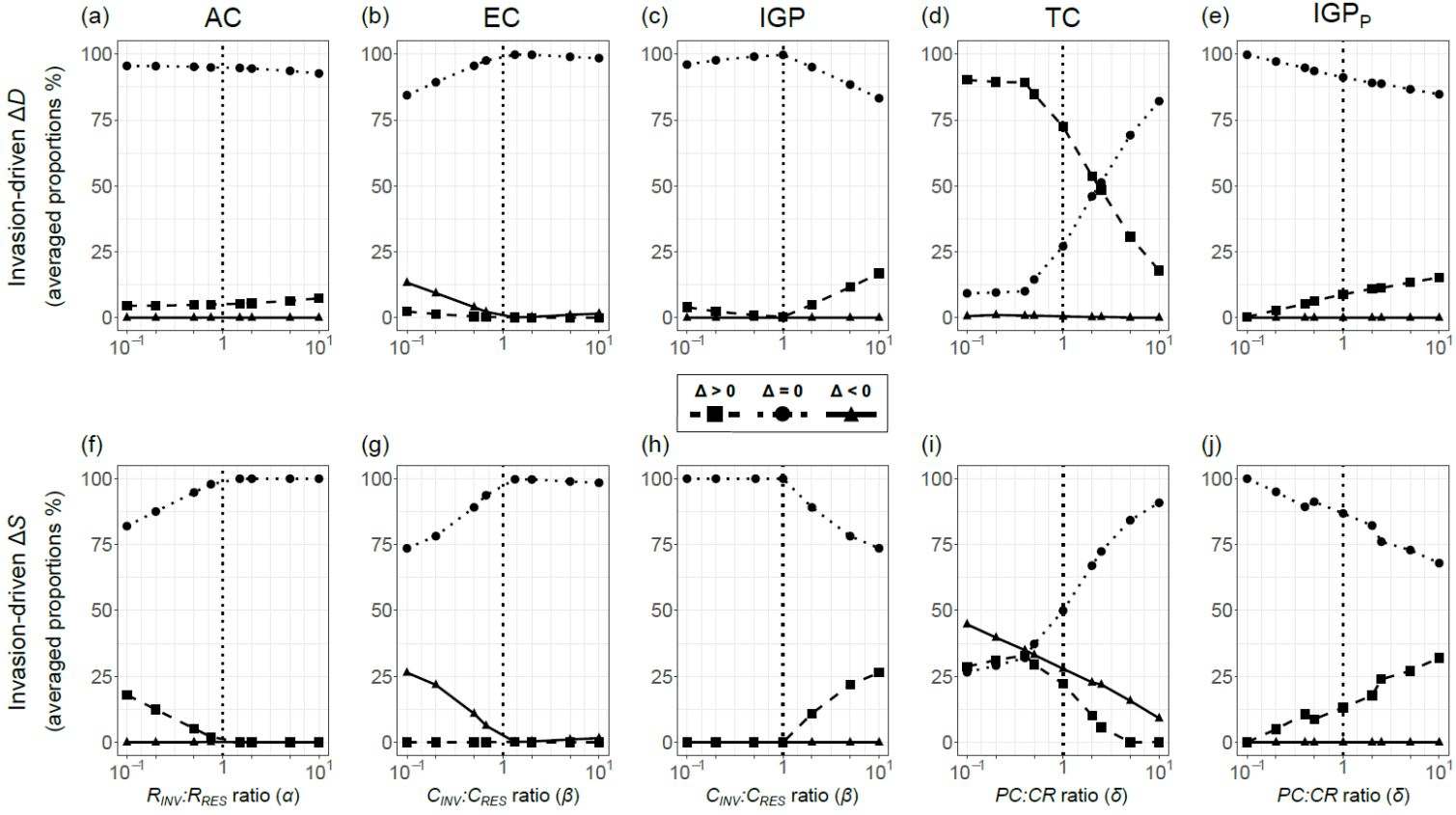
(a) AC
(b) EC
(c) IGP
(d) TC
(e) IGP$_P$
Invasion-driven ΔD (averaged proportions %)
Δ > 0
Δ = 0
Δ < 0
(f)
(g)
(h)
(i)
(j)
Invasion-driven ΔS (averaged proportions %)
R_{INV}:R_{RES} ratio (α)
C_{INV}:C_{RES} ratio (β)
C_{INV}:C_{RES} ratio (β)
PC:CR ratio (δ)
PC:CR ratio (δ)

Fig. S4. Invasion outcomes and regime states along environmental gradients for varying size ratios between competing species in the AC and EC modules. (a-l) AC = apparent competition, (m-x) EC = exploitative competition. Invasion outcomes (as in Box 1, a-f (AC) and m-r (EC)) and regimes states $S_{RES} \rightarrow S_{INV}$ (g-l and s-x). Body mass ratio between competing species ($BMR_{INV:RES}$) denotes the invasions of smaller ($BMR_{INV:RES} < 1$) or larger ($BMR_{INV:RES} > 1$) species. State abbreviations: N = no species present, C = population cycles with at least two species present, E = 1–3 species in stable equilibrium. Species body mass ratios fixed at $\beta = 10$ (AC) and $\alpha = 10$ (EC). Legends and colours as in Fig. 2.

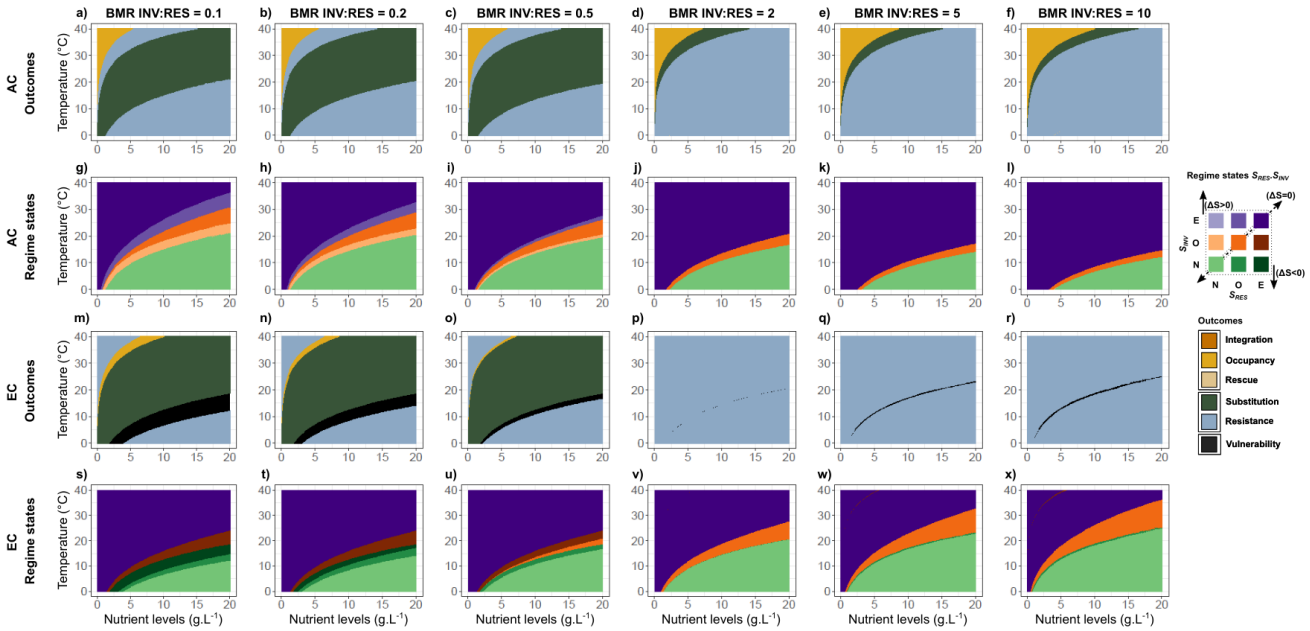

Fig. S5. Drivers of species coexistence and exclusion along environmental gradients for varying size ratios between competing species in AC and EC modules. Data restricted to combinations with both resident consumer and resource present before invasion. (a-l) AC module, (m-x) EC module. Invasion outcomes as in Box 1 (panels a-f and m-r) and their corresponding drivers defined by the P^* rule (g-l) or R^* rule (s-x). $BMR_{INV:RES}$ as in Fig. S4. $P_{INV}{}^*$ and $P_{RES}{}^*$ respectively denote equilibrium predator biomass when feeding on the invading resource or on the resident resource; $R_{INV}{}^*$ and $R_{RES}{}^*$ respectively denote equilibrium basal resource biomass when fed upon by the invading or resident consumer. Colour coding of invasion outcomes in panels a-f and m-r as in Fig. 2. Panels g-l and s-x illustrate the competitive advantage (orange) or disadvantage (purple) of the invading species over the resident competitor; no colour = absence of both resident and invading species. Species body mass ratios fixed at $\beta = 10$ (AC module) and $\alpha = 10$ (EC module).

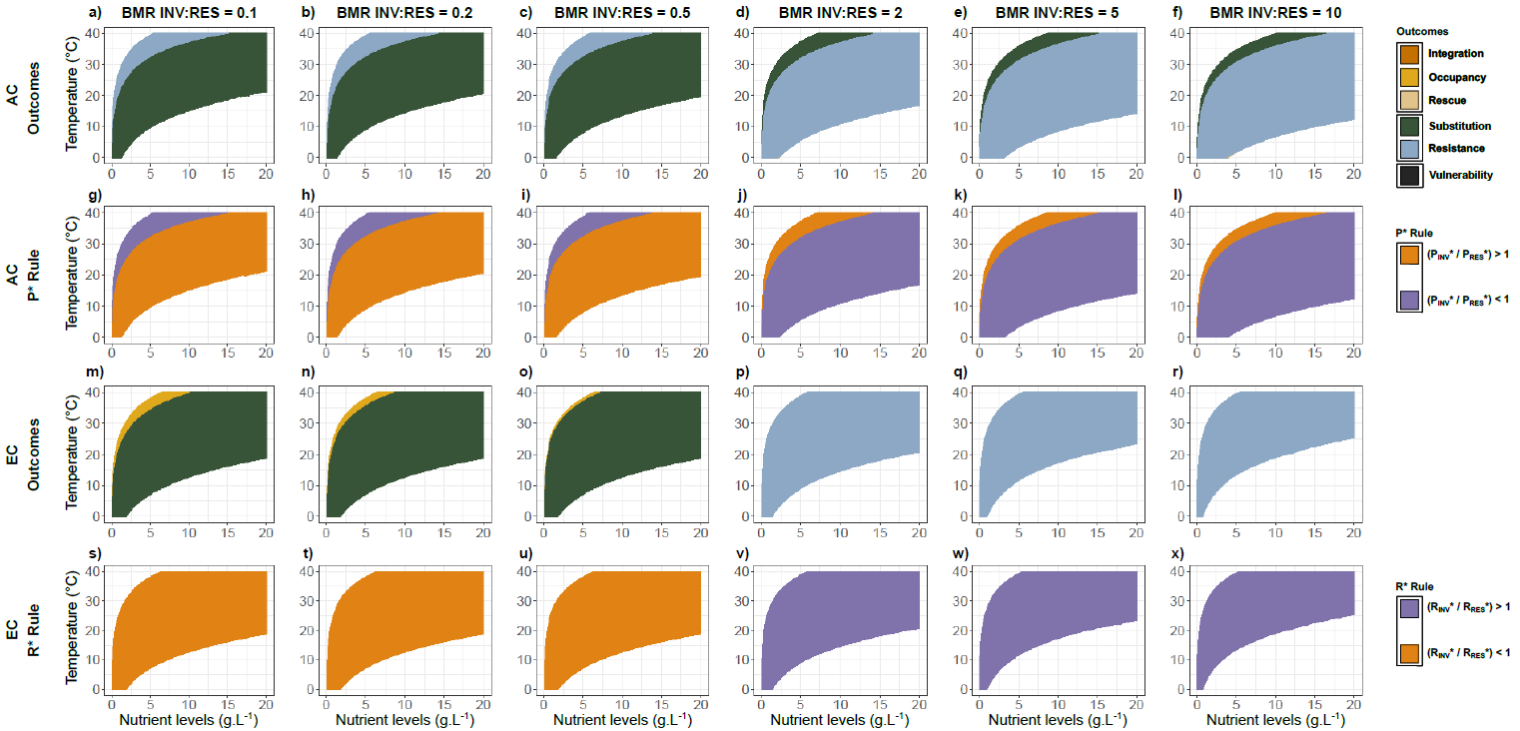
a) BMR INV:RES = 0.1
b) BMR INV:RES = 0.2
c) BMR INV:RES = 0.5
d) BMR INV:RES = 2
e) BMR INV:RES = 5
f) BMR INV:RES = 10
AC Outcomes
AC P* Rule
EC Outcomes
EC R* Rule
Temperature (°C)
Nutrient levels (g.L-1)
Outcomes
Integration
Occupancy
Rescue
Substitution
Resistance
Vulnerability
P* Rule
(PINV* / PRES*) > 1
(PINV* / PRES*) < 1
R* Rule
(RINV* / RRES*) > 1
(RINV* / RRES*) < 1

Fig. S6. Drivers of species coexistence and exclusion in IGP module along environmental gradients for different size ratios between invading and resident species. Invasion outcomes as in Box 1 (a-f), corresponding driver defined by the R* rule (g-l), and initial biomass density growth rate of intraguild prey at the beginning of the transient analyses (m-r) are illustrated along environmental gradients. Invasions involve intraguild prey for size ratios C_{INV}:C_{RES} < 1 (three leftmost columns) and intraguild predator for C_{INV}:C_{RES} > 1 (three rightmost columns). Colour coding of invasion outcomes in panels a-f as in Fig. 2. Panels g-l illustrate the competitive advantage (orange) or disadvantage (purple) of the invading species over the resident competitor; no colour = absence of both resident and invading species.

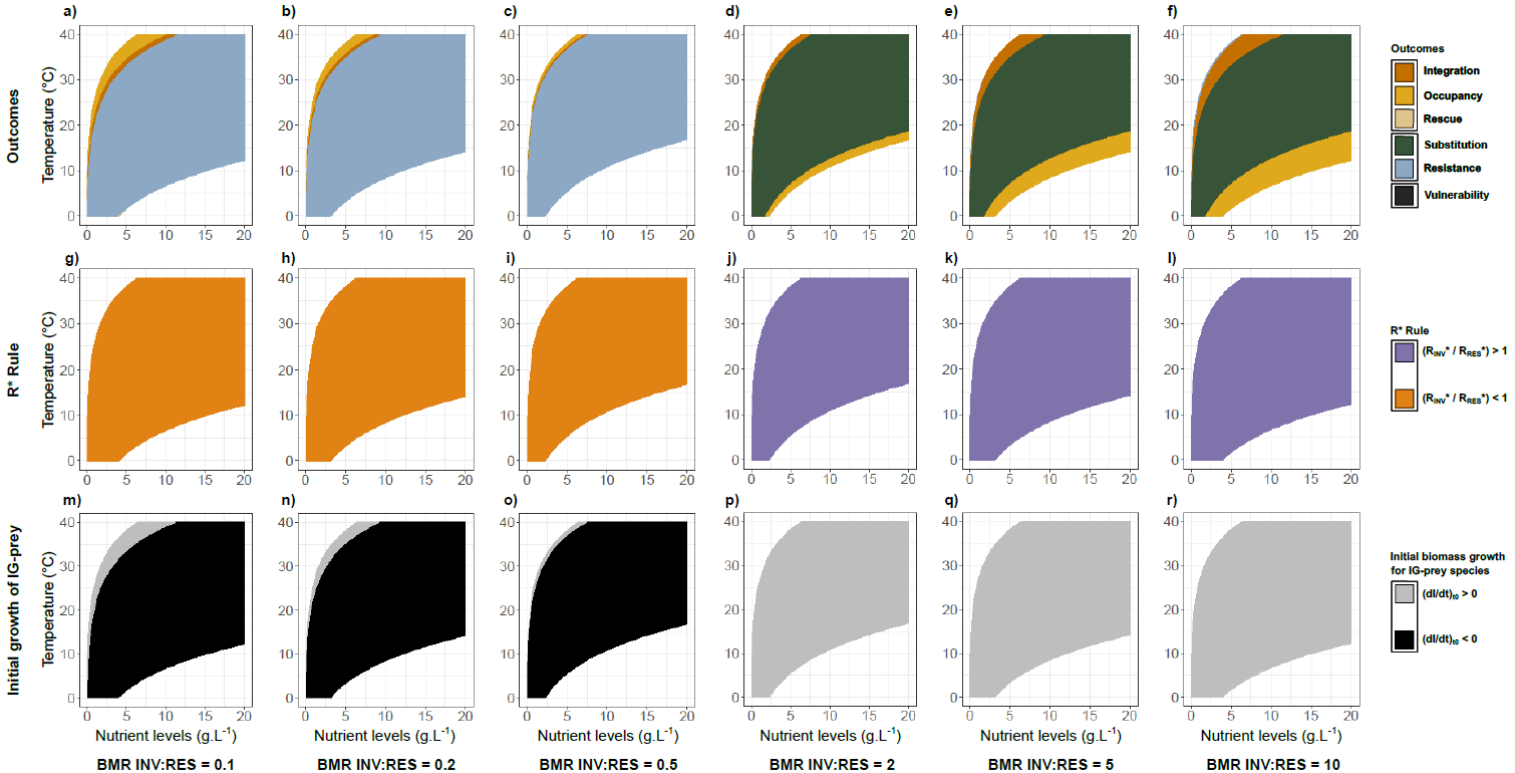
a)
b)
c)
d)
e)
f)
g)
h)
i)
j)
k)
l)
m)
n)
o)
p)
q)
r)
Outcomes
R* Rule
Initial growth of IG-prey
Temperature (°C)
Nutrient levels (g.L-1)
BMR INV:RES = 0.1
BMR INV:RES = 0.2
BMR INV:RES = 0.5
BMR INV:RES = 2
BMR INV:RES = 5
BMR INV:RES = 10
Outcomes
Integration
Occupancy
Rescue
Substitution
Resistance
Vulnerability
R* Rule
(RINV* / RRES*) > 1
(RINV* / RRES*) < 1
Initial biomass growth for IG-prey species
(dI/dt)IG > 0
(dI/dt)IG < 0

Fig. S7. Effect of species body mass ratios on community responses to invasion of top predator (TC module) and intraguild predator (IGP module). Body mass ratio between invading top predator and resident consumer (β: panels a, c, e, g), or with resident basal species ($\gamma = \alpha\beta$: panels b, d, f, h). Food web modules: (a, b, e, f) TC = trophic chain, (c, d, g, h) IGP_P = intraguild predation with invading IG predator. Species: *R* = basal resource, *C* = consumer, *P* = predator. Colours as in Fig. 1. Symbols denote the influences of invading species on community responses, i.e. squares = positive ($\Delta > 0$), circles = neutral ($\Delta = 0$), triangles = negative ($\Delta < 0$) effects. Note that the absence of influence on local stability regime due to invasions are in dotted line for more readability.

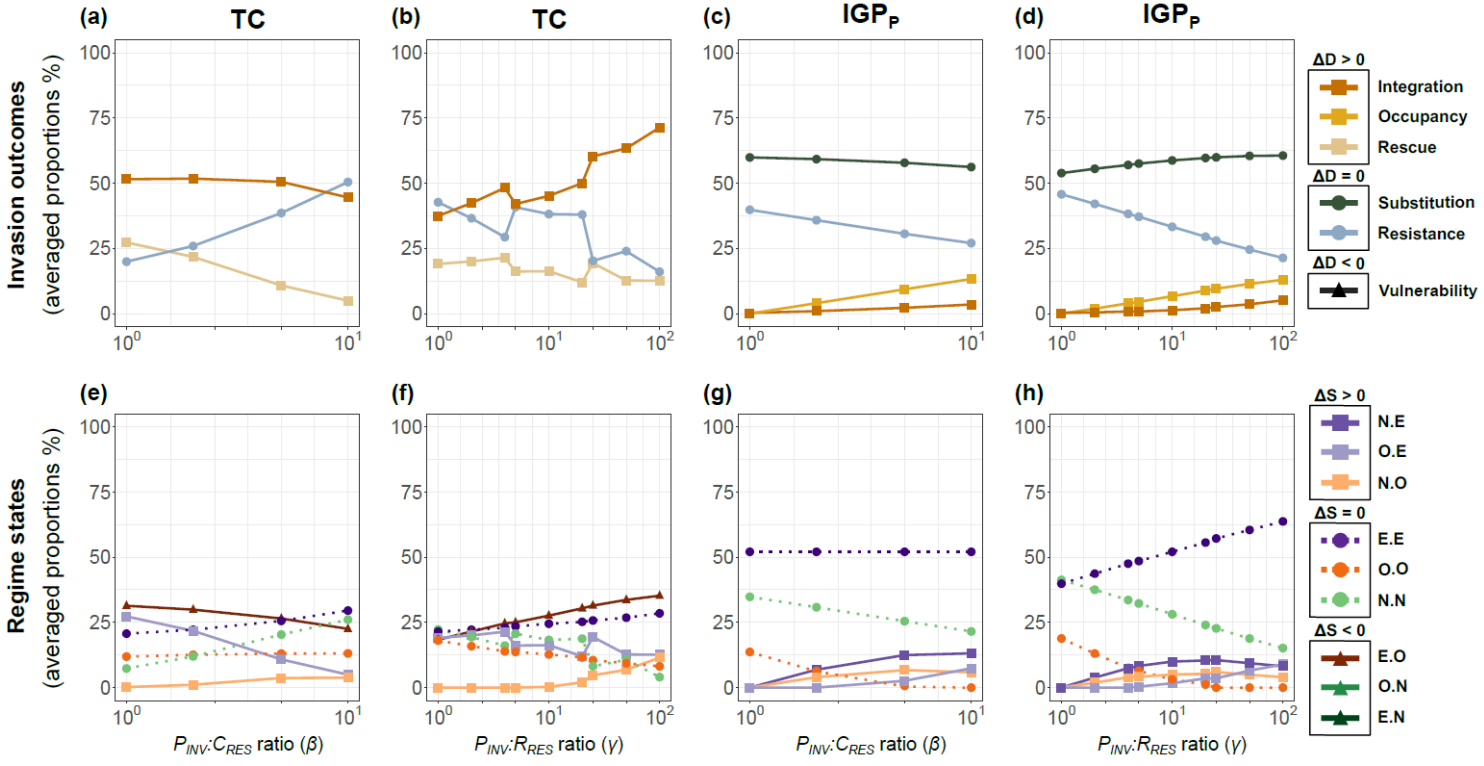
(a) TC
(b) TC
(c) IGP$_P$
(d) IGP$_P$
Invasion outcomes
(averaged proportions %)
Regime states
(averaged proportions %)
ΔD > 0
Integration
Occupancy
Rescue
ΔD = 0
Substitution
Resistance
ΔD < 0
Vulnerability
ΔS > 0
N.E
O.E
N.O
ΔS = 0
E.E
O.O
N.N
ΔS < 0
E.O
O.N
E.N
P_{INV}:C_{RES} ratio (β)
P_{INV}:R_{RES} ratio (γ)

Fig. S8. Differences between invasion outcomes in stability change (Δ*S*) following species invasion. Data are pooled across all modules, size ratios and abiotic conditions. The distribution of regimes states observed across invasion outcomes illustrates the propensity of a given outcome to destabilize, have no effect or stabilize the community structure. See Fig. 4 for the cumulative percentages corresponding to changes in stability. State abbreviations: N = no species present, O = population oscillations with at least two species present, E = 1–3 species in stable equilibrium. Colours as in Fig. 2l-p.

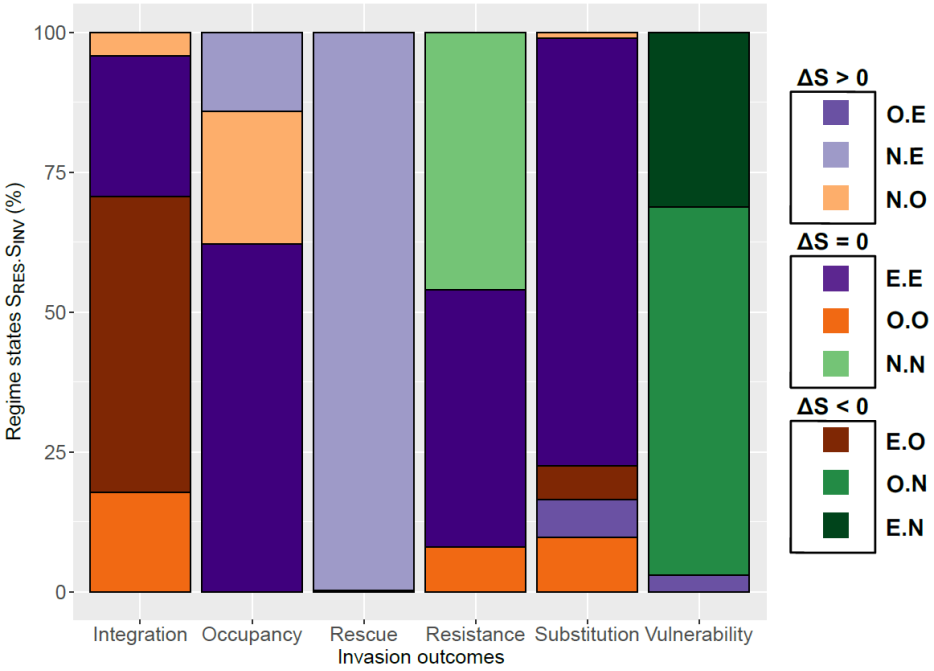

Fig. S9. Example of population biomass densities (g.m^{-2}) at equilibrium or limit cycle along the temperature gradient in invaded communities for varying species body mass ratios γ and fixed nutrient levels (5 g.m^{-2}). Trophic modules: AC = apparent competition, EC = exploitative competition, TC = trophic chain, IGP_C = IGP module with invading IG prey, and IGP_P = IGP module with invading IG predator. Species: *P* = predator, *C* = consumer, *R* = basal resource. Different colours code size ratios between top predator and basal resource $\gamma = \alpha\beta$. Values of γ = 1, 4, 25 and 100 correspond respectively to $\alpha = \beta = 1$, $\alpha = \beta = 2$, $\alpha = \beta = 5$ and $\alpha = \beta = 10$ in Tables S5–S7. Limit cycles are illustrated by their minima and maxima (except some truncated values for top predator and γ = 25 and 100 in TC module). Overlapping equilibria for multiple values of γ, especially at zero densities, are illustrated by the largest value of γ for which they occur.

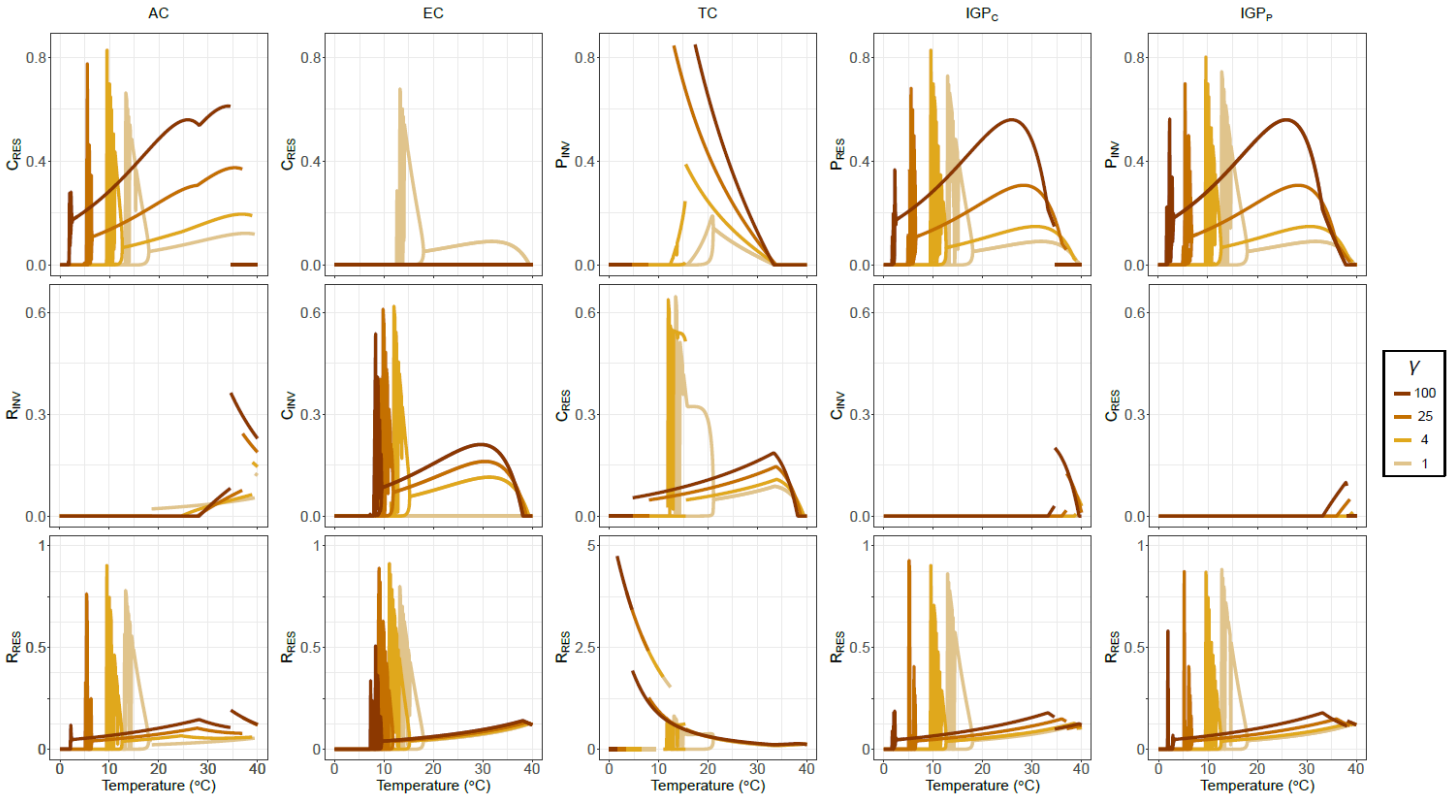
AC
EC
TC
IGP$_C$
IGP$_P$
C_{RES}
P_{INV}
R_{INV}
C_{INV}
R_{RES}
Temperature (°C)
γ
100
25
4
1

Fig. S10. Example of population biomass (g.m^{-2}) at equilibrium or limit cycle along the gradient of nutrient levels in invaded communities for varying species body mass ratios γ and fixed temperature (10°C). Legend and colour coding as in Fig. S9.

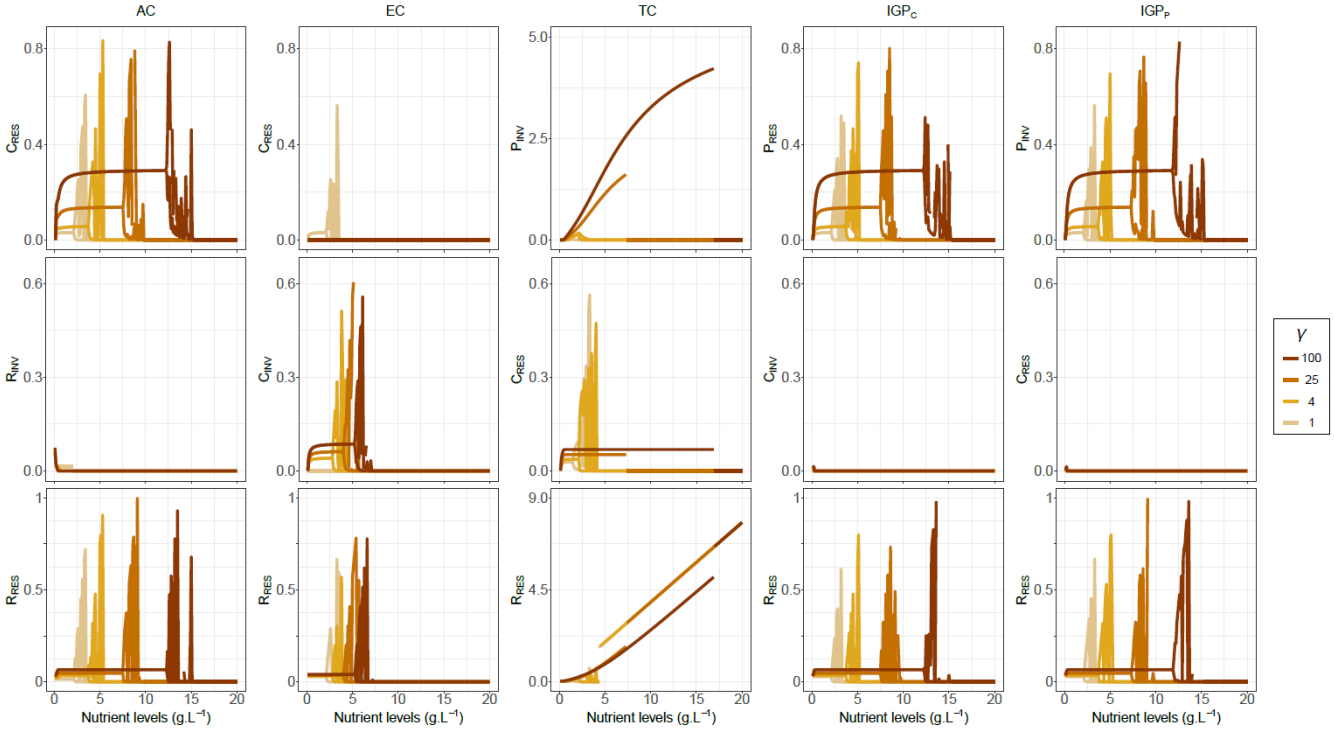

Chapter I

~ Chapter II ~

Community structure and collapses in multichannel food webs: Role of consumer body sizes and mesohabitat productivities

[Ecology Letters (2021), 24: 1607-1618]

Received: 3 December 2020 | Revised: 19 January 2021 | Accepted: 12 April 2021

DOI: 10.1111/ele.13772

ECOLOGY LETTERS cnrs WILEY

LETTER

Community structure and collapses in multichannel food webs: Role of consumer body sizes and mesohabitat productivities

Samuel Dijoux[1,2] | **David S. Boukal**[1,2]

[1]Department of Ecosystem Biology, Faculty of Science, University of South Bohemia, České Budějovice, Czech Republic

[2]Czech Academy of Sciences, Biology Centre, Institute of Entomology, České Budějovice, Czech Republic

Correspondence
Samuel Dijoux, Department of Ecosystem Biology, Faculty of Science, University of South Bohemia, Branišovská 1760, 370 05 České Budějovice, Czech Republic.
Email: dijoux.samuel@gmail.com

Funding information
Grantová Agentura České Republiky, Grant/Award Number: project nr. 14-29857S

Editor: Peter Thrall

Abstract

Multichannel food webs are shaped by the ability of apex predators to link asymmetric energy flows in mesohabitats differing in productivity and community traits. While body size is a fundamental trait underlying life histories and demography, its implications for structuring multichannel food webs are unexplored. To fill this gap, we develop a model that links population responses to predation, and resource availability to community-level patterns, using a tri-trophic food web model with two populations of intermediate consumers and a size-selective top predator. We show that asymmetries in mesohabitat productivities and consumer body sizes drive food web structure, merging previously separate theory on apparent competition and emergent Allee effects (i.e. abrupt population collapses) of top predators. Our results yield theoretical support for empirically observed stability of asymmetric multichannel food webs and discover three novel types of emergent Allee effects involving intermediate consumers, multiple populations or multiple alternative stable states.

KEYWORDS
alternative stable states, Apparent competition, emergent Allee effects, limiting similarity, size-dependent predation

INTRODUCTION

Non-random distribution of trophic links underlies the persistence and stability of food webs (Otto et al., 2007; Rooney et al., 2006). Most food webs rely on the linkage of alternative asymmetric energy sources by predators at higher trophic levels (Barnes et al., 2018; McCann & Rooney, 2009; Rooney et al., 2008). Asymmetric energy flows strengthen the resilience of food webs (Rooney et al., 2006; Wolkovich et al., 2014), for example, by reducing population fluctuations and subsequent extinction cascades due to the paradox of enrichment (Dolson et al., 2009; Otto et al., 2007). Asymmetric energy flows often arise in freshwater ecosystems when mobile generalist predators link different mesohabitats, such as the littoral, pelagic and benthic habitats in lentic systems (Dolson et al., 2009; Marklund et al., 2018; Schindler & Scheuerell, 2002) or downstream and upstream areas in lotic systems (Lapointe et al., 2010; Rosenblatt & Heithaus, 2011). Energy in these mesohabitats often comes from different sources, and the flows differ in turnover and production rates (Rooney & McCann, 2012). In lentic systems, energy flow driven by photosynthesis in the more productive 'green' pelagic mesohabitat is usually faster than the flow driven by decomposers that depend on detritus and dissolved organic carbon in the 'brown' benthic mesohabitat (Zou et al., 2016).

Asymmetries in regulatory processes within multichannel food webs can influence the coexistence of competing species at intermediate trophic levels. Such asymmetries can arise in bottom-up regulatory processes from differences in basal productivity rate and prey biomass (Chesson & Kuang, 2008; DeCesare et al., 2010) or in top-down processes stemming from differences in the feeding behaviour of the top predator (Marklund et al., 2019; Post et al., 2000) and hence asymmetric predation

pressure (Rooney et al., 2006; Wolkovich et al., 2014). In particular, linkage by top predators may influence communities in different mesohabitats in a way that either permits their coexistence or makes the least resilient community vulnerable to extinctions as suggested by earlier work on apparent competition in simple food web modules (Chase, 1999; Holt et al., 1994).

Asymmetric energy flows in multichannel food webs relate to the limiting similarity hypothesis (MacArthur & Levins, 1967), which posits that increasing niche overlap of co-occurring species diminishes their ability to coexist (Abrams & Rueffler, 2009; Meszéna et al., 2006). For example, species competing for a common resource and sharing the same predator can only coexist if they differ sufficiently in morphological or physiological traits, niche overlap and environmental requirements (Leibold, 1996, 1998). Other studies, however, highlighted possible coexistence of similar species due to asymmetric predation pressure (Holt et al., 1994) or due to varying fitness caused by variable phenotypes (Godoy et al., 2018; McPeek, 2019) or variable body sizes.

Food webs can also undergo abrupt ecological regime shifts when they exceed their ecological stability boundaries, leading to a switch between alternative stable states (May, 1977; Scheffer et al., 2001). These shifts occur in response to external perturbations such as eutrophication in freshwater (Folke et al., 2004; Scheffer & van Nes, 2007) and marine habitats (Möllmann & Diekmann, 2012; Muthukrishnan et al., 2016) or arise from positively reinforcing feedbacks to population dynamics such as Allee effects (Beisner et al., 2003; Oliver et al., 2015; de Roos & Persson, 2002). Various mechanisms can generate alternative stable states in food webs (reviewed in Schröder et al., 2005 and Gårdmark et al., 2015). For example, prey size refugia can lead to alternative stable states at intermediate nutrient levels in a food web consisting of two consumers sharing the same resource and predator (Chase, 1999, 2003). However, the propensity of multichannel food webs to ecological regime shifts has not yet been addressed.

Body size and resource productivity are ubiquitous drivers of community structure (Persson et al., 2014). Different community size spectra also characterize the fast- and slow-energy channels in aquatic food webs (Mehner et al., 2018): pelagic habitats are dominated by small-bodied phytoplankton and zooplankton, while benthic habitats host mainly larger-bodied macroinvertebrates (McCann & Rooney, 2009). The combined asymmetries in consumer body sizes and energy partition across mesohabitats may stabilize multichannel food webs (Rooney & McCann, 2012) or promote population collapses (de Roos & Persson, 2002) and alternative stable states (Chase, 2003), but we lack quantitative theory to resolve these interacting roles of consumer body size and resource productivity in the structuring of multichannel food webs.

To fill these gaps, we modelled the effect of varying body sizes and mesohabitat productivities on multichannel food webs. We focused on a case in which a top predator integrates two tri-trophic chains (as in Post et al., 2000) with size-structured populations of intermediate consumers that differ in body size using a modified tri-trophic chain model by de Roos and Persson (2002). This food chain model exhibits an emergent Allee effect due to predation-induced competitive release in the prey (Gårdmark et al., 2015) and the possibility of sudden predator collapse. Integrating two such food chains in different mesohabitats with a shared top predator opens the possibility for additional, qualitatively different community structures and steady-state transitions. We thus examined how differences in productivity and consumer body sizes affect consumer life histories, the structure of each food chain, apparent competition between the intermediate consumers and the persistence of the top predator. We were particularly interested in the combinations of consumer body sizes and habitat productivities that (1) enabled coexistence of the intermediate consumers when linked by the top predator and (2) lead to alternative stable states and possible collapses of top predator or intermediate consumer populations.

METHODS

Food web structure

Our minimal multichannel, tri-trophic food web includes seven possible communities differing in the presence of the intermediate consumers and the top predator (Communities 0–6 in Figure 1). For convenience, we refer to the mesohabitats as pelagic ($i = 1$) and benthic ($i = 2$), each with its own basal resource R_i and intermediate consumer species C_i, and apex predator P integrating both habitats. We begin by outlining expected transitions between these communities. Increasing productivity in each mesohabitat should lead to lengthening of the food chain and successful establishment of the consumer followed by the top predator (Fretwell, 1987; Oksanen et al., 1981) (community state transitions $0 \rightarrow 1 \rightarrow 4$ and $0 \rightarrow 3 \rightarrow 6$ in Figure 1). Benthic and pelagic consumers coexist in the absence of the top predator if each mesohabitat is sufficiently productive (Community 2). Successful invasion of the top predator in this community (transition $2 \rightarrow 5$) may subsequently affect consumer coexistence and lead to the exclusion of the less resilient consumer due to apparent competition (transition $5 \rightarrow 4$ or $5 \rightarrow 6$ in Figure 1). Possible alternative stable states involving two or more of these communities are described in Results.

Population structure and dynamics

In our model, the top predator P with a fixed body size feeds indiscriminately on the size-structured populations

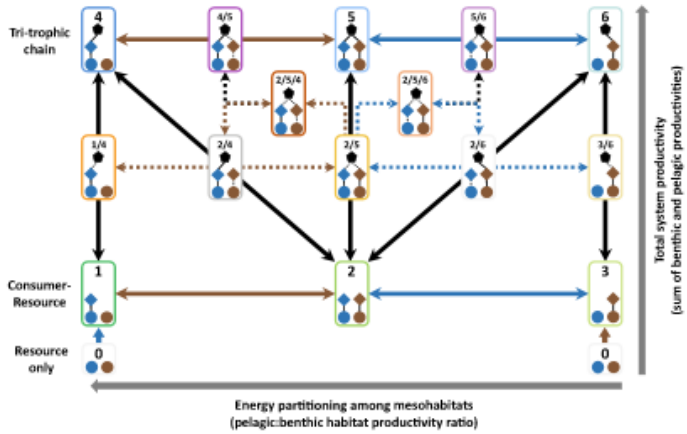

FIGURE 1 Classification of all possible scenarios of community assembly in the multichannel food web. Populations and trophic links: top predator (pentagons), consumers (diamonds) and resources (circles) linked by stable (solid lines) or bistable (dotted lines) trophic links; pelagic species in blue, benthic species in brown. Transitions between possible community states (numbered rectangles) correspond to the invasion/extinction threshold of one consumer (blue or brown arrows), or top predator (black arrows). Dotted arrows = transitions between communities with two to three alternative stable states (multiple numbers separated by slashes). Grey arrows illustrate gradients of energy partitioning among mesohabitats and total system productivity

of intermediate consumers C_1 and C_2, while each consumer population feeds on its own basal resource that follows a semi-chemostat dynamics with carrying capacity K_i and flow-through rate ρ_i (i = 1, 2). We keep the same model structure and parameter values used in de Roos and Persson (2002) as a baseline scenario for the benthic food chain R_2–C_2–P and modify them for the pelagic food chain R_1–C_1–P (see Text S1 and Tables S1–S4 for details). We also assume that the pelagic resource R_1 has a faster turnover rate than the benthic resource R_2 (Fortier et al., 1994) and set $\rho_1 = 2\,\rho_2$.

Individual consumers are born at length $l_{b,i}$, mature at length $l_{j,i}$ and can grow to the maximum length $l_{m,i}$ under unlimited resources (i = 1, 2). For simplicity, we assume that both consumers differ by a given size ratio β in all three traits ($\frac{l_{b,1}}{l_{b,2}} = \frac{l_{j,1}}{l_{j,2}} = \frac{l_{m,1}}{l_{m,2}} = \beta$; pelagic consumers are larger than benthic ones if $\beta > 1$ and smaller if $\beta < 1$) and that all processes regulating their populations are qualitatively identical, that is, any differences arise only through their difference in body size and resource availability. We use the same dynamic energy budget model as in de Roos and Persson (2002) for both consumer populations (Text S1). The individuals are characterised by size- and resource-dependent feeding rates, growth rates and fecundities and size- and predator-dependent mortality rates. Individuals of both consumers follow a von Bertalanffy growth curve with resource-dependent growth rate and asymptotic size. This is because their ingestion rate of the respective basal resource follows a Type II functional response and scales with length^2, while the maintenance rate scales with length^3 (Text S1, Table S3). They produce offspring after maturation at a *per capita* rate proportional to the ingestion rate. Individuals of both consumers die with the same size-independent background mortality rate and are further vulnerable to predation until reaching a vulnerability size threshold l_v that is independent of β. This vulnerability window provides a qualitatively correct description, for example, for many fish population (Andersen & Beyer, 2006).

The top predators feed indiscriminately on vulnerable individuals from both consumer populations when present, following a Holling Type II functional response. Predator biomass increases by converting ingested prey biomass and declines exponentially in the absence of consumers (see Text S1 and Tables S1–S4 for a full model description). In sum, both tri-trophic food chains in our model have identical properties except the mesohabitat productivity and the ratio of consumer body sizes, although the model could be easily modified to further explore the consequences of, for example, consumer-specific functional response parameters or different size scaling of the vital rates.

We focus on three key properties that can affect the community structure and transitions including the emergent Allee effects: consumer size ratio β and the productivity in each mesohabitat, which we attribute to the resource carrying capacities K_1 and K_2. We first quantify the impact of consumer body size and habitat productivity on its ontogeny including predation risk, population growth rate and birth rate with and without predation. We then examine the effects of consumer body size and habitat productivity on the structure of each food chain and the whole food web to understand how asymmetries in consumer body size and mesohabitat productivity influence the apparent competition between intermediate consumers and the community structure (Figure 1). We

solve Eqs. (S7)–(S11) numerically using the R package *PSPManalysis* version 3.1.2 (de Roos, 2021) to track the system equilibria and detect thresholds associated with successful establishment or collapse of intermediate consumers and the top predator.

RESULTS

Effects of body size, habitat productivity and predation on consumer life history

Body size has a strong effect on nearly all aspects of the intermediate consumer life history (Figure 2). Larger consumers take longer time to reach their asymptotic size but benefit from an earlier escape from predation, while very small consumers stay vulnerable to predation even as adults (Figure 2a). In the absence of predation, larger consumers have faster population-level growth rates (Figure 2b) but lower birth rates than smaller consumers (Figure 2c). As a result, the critical resource density required to sustain the consumer population in the absence of predation is almost independent of the consumer relative body size, although it is slightly higher in smaller consumers (black line in Figure 2d).

Size-dependent predation releases the survivors from intraspecific competition and leads to higher birth rates relative to the non-predated population if some juvenile consumers are invulnerable to predation ($\beta > 0.245$, size at maturation $l_j > 27$ mm; red vs. black lines in Figure 2c). Increased mortality of the vulnerable juveniles also increases the critical resource density, especially for

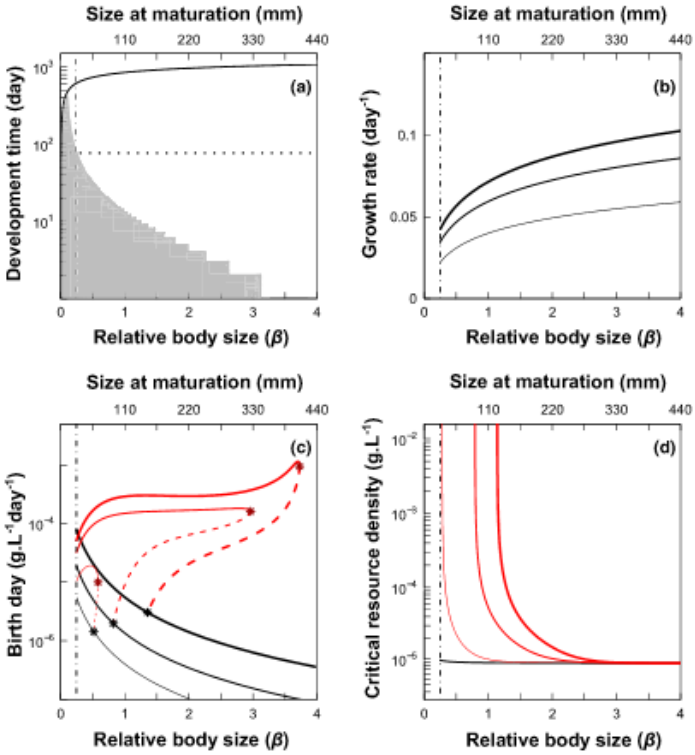

FIGURE 2 Influence of consumer relative body size β on key life history characteristics (a), population growth rate (b), birth rate (c) and critical resource density (d). (a) Grey area: consumers vulnerable to predation (daily resolution); black dotted line = maturation time; black solid line = time to reach maximum size, defined as age when individual growth rate declines below 0.01 mm day^{-1}; resource level R fixed at ca. 3×10^{-4} g L^{-1}. (b and c) Population-level rates without predation (black lines) and with predation (red lines, c); resource carrying capacity fixed at $K = 3 \times 10^{-5}$ (thin lines), 8×10^{-5} (medium lines) and 3×10^{-4} g L^{-1} (thick lines). (d) Critical resource density without predation (black line) and under additional mortality of vulnerable juveniles ($\mu_p = 0.1$, 0.5 and 0.9; thin, medium and thick red lines). Other parameters as in Table S1. Community structure in panel C: solid lines = stable equilibria dashed lines = unstable equilibria of the tri-trophic chain; black points = predator invasion thresholds, red points = predator persistence thresholds; dash-dotted line = adult predation vulnerability threshold

smaller consumers, and can drive small consumers extinct (red lines in Figure 2d) when the increased resource-dependent growth and birth rates (Figure 2b and c) cannot compensate for the increased mortality even at very high productivity levels. In what follows, we constrain our analyses to sufficiently large consumers with invulnerable adults ($l_j \geq l_v$ =27 mm, i.e. $\beta \geq 0.245$).

Tri-trophic chain: Role of intermediate consumer body size and mesohabitat productivity

For a wide range of consumer body sizes, the food chain lengthens as the habitat productivity increases and exhibits an emergent Allee effect in the top predator with two alternative stable states at intermediate habitat productivity levels (community state 1/4; Figure 3a). That is, a relatively high habitat productivity is required for the top predator population to establish, but established top predators can sustain lower habitat productivity as they modify the stage structure of the consumer population (de Roos & Persson, 2002; also Figure 4a for β = 1.2, i.e. l_j =132 mm). The food chain collapses abruptly to a stable consumer–resource equilibrium when the habitat productivity decreases below the top predator persistence level (Figure 4a). The productivity threshold required for consumer establishment is essentially independent of consumer body size (compare Figure 2d), but those associated with top predator establishment and collapse are highly sensitive to consumer body size: top predators feeding on consumers characterised by larger body sizes require more resources to survive because the consumers are born larger and outgrow the predation size window earlier (Figure 3a, compare Figure 2a). The predator cannot survive when all consumers become invulnerable (β > ca. 3.8, l_b >27 mm; Figure 3a).

Multichannel food web: Role of asymmetries in intermediate consumer size and mesohabitat productivities

Coexistence and exclusion of apparent competitors are determined by their relative ability to sustain predation pressure, mediated by the mesohabitat-specific critical resource density (Figure 2d). Here, we analyse the effects of varying mesohabitat productivities and consumer body size on the structure of the multichannel food web, with emphasis on the coexistence of both intermediate consumers. We found surprisingly complex patterns of consumer body size ratios and habitat productivities required for their coexistence with the top predator. We first outline the range of habitat productivity levels that maintain both benthic and pelagic consumers of a given size ratio in the food web and subsequently provide more detailed results on body size differences that enable consumer coexistence and top predator persistence at given productivity levels in one of the mesohabitats (community state 5 and states 2/5, 4/5, 5/6, 2/4/5 and 2/5/6 that include state 5 as one of the alternatives; see Figure 1).

For a given consumer body size ratio β, the food web structure is driven by the pelagic–benthic habitat productivity ratio (expressed as the relative contribution of the pelagic habitat $K_1/(K_2 + K_1)$; abbreviated as PB ratio) and the total amount of resources required to sustain the top predator population. This amount is determined by the sum of resource carrying capacities $K_1 + K_2$ (hereafter 'total carrying capacity', abbreviated as TCC), irrespective of the PB ratio when both consumers are of similar size as in Figure 3b, or depends on both the PB ratio and TCC when the pelagic and benthic consumers differ substantially in size (see below). Resource carrying capacity in the given habitat determines the invasion

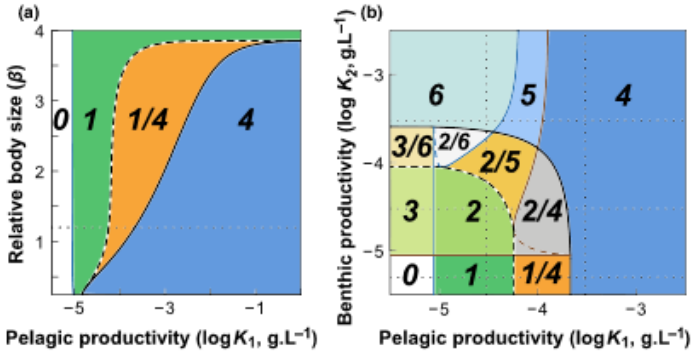

FIGURE 3 Changes in community structure of the tri-trophic food chain (a) and the multichannel food web (b) along gradients of mesohabitat productivity and consumer body size. Community structures, numbered as in Figure 1: resource-only equilibrium (0, white), consumer–resource equilibria (green, 1–3), four-species equilibria (blue, 4 and 6), and coexistence of all five species (blue, 5). Solid lines: invasion thresholds of pelagic (C_1, blue) and benthic (C_2, brown) consumers and the top predator (black). Dashed lines: invasion thresholds of pelagic (blue) and benthic (brown) consumers in an unstable equilibrium with top predator and extinction threshold of top predator with one or both consumers present (black). Parameters: (A) $K_2 = 5 \times 10^{-6}$ g L^{-1}, (b) β = 1.2, other values as in Table S1. Dotted lines: (a), β and K_2 values used in Figure 4; (b), K_1 and K_2 values used in Figure 5

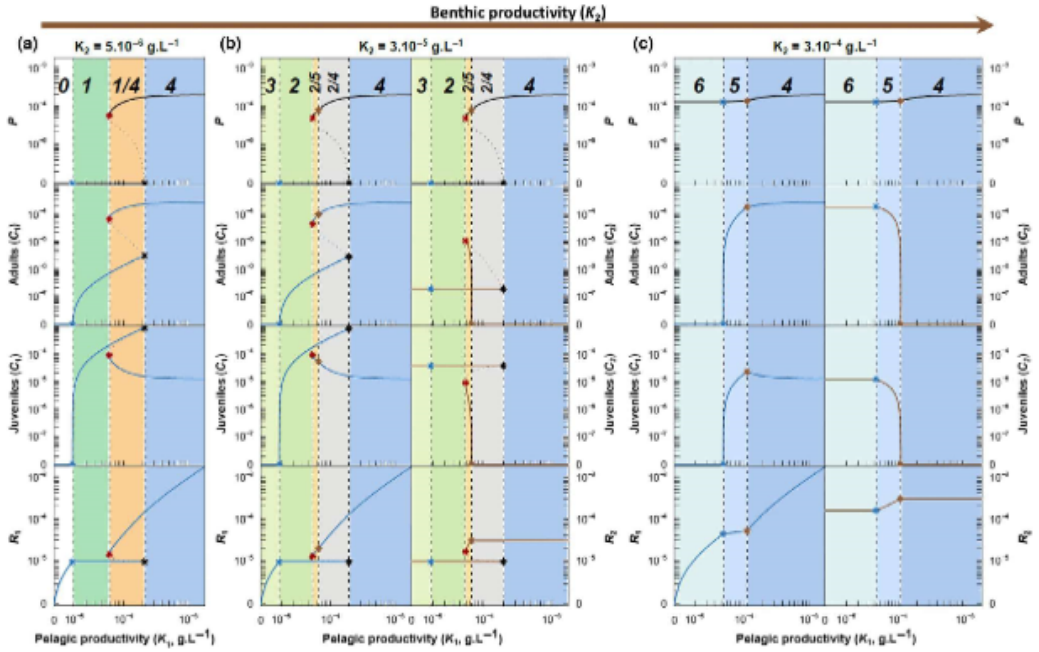

FIGURE 4 Emergent Allee effects in tri-trophic chain (a) and multichannel food web (b) and community transition between consumer coexistence and exclusion (c) along the pelagic productivity gradient. Parameter values: $\beta = 1.2$; $K_2 = 5 \times 10^{-6}$ (a), 3×10^{-5} (b) and 3×10^{-4} g L^{-1} (c), that is, benthic resource productivity increasing from (a) to (c). Other parameters as in Table S1. Solid lines: stable equilibria; dotted lines: unstable equilibria. Threshold productivity values marked by vertical dotted lines: invasions of pelagic (blue points) and benthic (brown points) consumer, top predator invasion (black points), top predator collapse (red points). Top predator panel duplicated in (b) and (c) to enable comparison within each mesohabitat. Community structures numbered as in Figure 1. Axes scaling: x axis transformed as $\log_{10}(x + 10^{-5})$; y axis transformed as $\log_{10}(y + 10^{-8})$ for juvenile and adult consumers and as $\log_{10}(y + 10^{-6})$ for resources and top predator

threshold of each intermediate consumer (Figures 2d and 5), while the total amount of resources required to sustain the top predator population determines its invasion and collapse thresholds (Figure S1). Competitive exclusion and coexistence of the two intermediate consumers when linked by the top predator are driven mainly by the PB ratio (Figure 3b and S3).

Consumer coexistence along the habitat productivity gradients is promoted by larger body size differences. That is, the coexistence of all five species is constrained to a narrow range of PB ratios and sufficiently high TCC values for same-sized intermediate consumers ($\beta \approx 1$; community states 5 and 2/5 in Figure 5 and S3d). When one of the consumers is substantially larger ($\beta << 1$ or $\beta >> 1$) and hence competitively superior (see above), all five species can coexist only if its habitat is moderately productive. High productivity in that habitat leads to competitive exclusion of the smaller consumer because the top predator population supported by the larger consumer imposes additional mortality that cannot be mitigated by increased resource productivity (Figure 2d), while lower productivity cannot support the larger consumer. On the other hand, coexistence is almost independent of the productivity in the smaller consumer's habitat as long as it can support the top predator (ca. $K_1 > 1.5 \times 10^{-4}$ to 4×10^{-4} g L^{-1} in Figure S3a–c and $K_2 > 9 \times 10^{-5}$ g L^{-1} in Figure S3e–i).

Unequal consumer body sizes also underpin asymmetric roles of habitat productivities in the fate of the top predator. TCC values required for top predator persistence are nearly independent of the PB ratio for most consumer body size ratios β and increase with PB only when the pelagic consumers are much larger ($\beta = 3$ in Figure S1a). TCC thresholds associated with predator invasion are more sensitive to β and PB ratios: they decline with the PB ratio when $\beta \leq 1$ and increase otherwise (Figure S1b). This asymmetric role of the pelagic and benthic habitat productivities is caused by the habitat-specific consumer vulnerability to predation driven by the size differences, as both consumers are equivalent in terms of contribution to the critical prey biomass required by the top predator (Figure S2). That is, a more productive pelagic habitat is required to sustain the top predator as β increases and the pelagic prey becomes less vulnerable (Figure S1a).

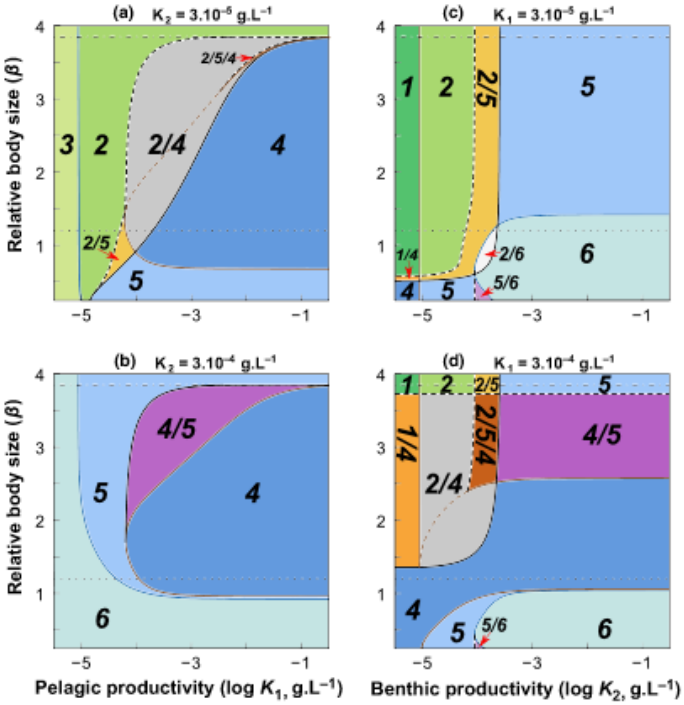

FIGURE 5 Dependence of community structure of the multichannel system on resource productivity and consumer relative body size β. Resource carrying capacity always fixed in one habitat: $K_2 = 3 \times 10^{-5}$ (a) and 3×10^{-4} g L^{-1} (b); $K_1 = 3 \times 10^{-5}$ (c) and 3×10^{-4} g L^{-1} (d). Other parameters as in Table S1. Community structures numbered as in Figure 1; coexistence of all five species denoted by '5'. Line type and colour as in Figure 3. Dotted lines ($\beta = 1.2$): results shown in Figure 3b. Dash-dotted lines ($\beta = 3.8$): predation vulnerability limit of the pelagic consumer

At low benthic productivities K_2, all five species therefore coexist if pelagic consumers are sufficiently small and pelagic productivity sufficiently high (community state 5; ca. $\beta < 0.66$, i.e. l_j <73 mm for $K_1 > 10^{-4}$ g L^{-1} in Figure 5a). Surprisingly, coexistence is also possible if the pelagic consumers are larger and pelagic productivity intermediate (community state 2/5; up to $\beta = 1.5$, i.e. l_j =165 mm for K_1 between ca. 10^{-5} and 10^{-4} g L^{-1} in Figures 3b and 5a; see also Figure 4b and S4a–d). Coexistence at high benthic productivity K_2 requires sufficiently large pelagic consumers (ca. $\beta > 0.9$, i.e. l_j >100 mm in Figure 5b) in a moderately productive pelagic mesohabitat; the range of pelagic productivity leading to possible coexistence increases with β (community states 5, 4/5 and 2/4/5; Figure 5b and S4G-I; see also Figure 4c). Intermediate benthic productivities K_2 combine the outcomes for low and high K_2, that is, all five species can coexist when sufficiently high pelagic productivity supports small pelagic consumers or when large pelagic consumers are constrained by intermediate pelagic productivity (community states 5, 2/5, 4/5 and 2/4/5; Figure S4e and f).

We observe similar patterns for fixed pelagic productivities K_1: coexistence is possible if benthic consumers are substantially larger and occupy a less productive habitat or if they are substantially smaller and live in a more productive habitat than the benthic consumers (community states 5, 2/5, 4/5, 5/6, 2/4/5 and 2/5/6; Figure 5c and d and S5). Coexistence is less likely, that is, occurs for a smaller range of β and K_2, as the pelagic productivity becomes very low (Figure S5a) or very high (Figure 5d and S5g–i). At intermediate values of pelagic productivity, even similarly sized benthic and pelagic consumers may however coexist within a range of intermediate benthic productivity (community state 2/5 in Figure 5c and states 5 and 2/5 in Figure S5b–f).

Emergent Allee effects and alternative stable states in the multichannel food web

We identified nine possible alternative stable state configurations in the food web and classify them into four groups. First, they include the 'classical' *emergent Allee*

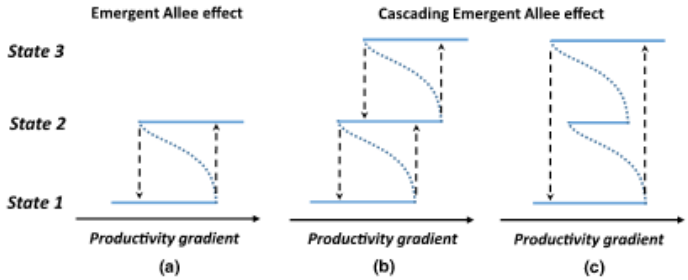

FIGURE 6 Diagram of (a) emergent Allee effect and (b and c) cascading emergent Allee effects along a productivity gradient. Dashed arrows = sudden community transitions between alternative system states; stable states (solid blue lines) separated by unstable equilibria (dotted lines). In cascading emergent Allee effect, sudden community transitions follow in succession (b; e.g. community state 2/5/6 in Figures S3b and S5b) or in a single event (c; community state 2/5/4 in Figure S4c and d). Note that stable state 2 cannot be reached by gradual changes in (c)

effect in the top predator associated with its sudden collapse (de Roos & Persson, 2002; Figure 6a) when one or both consumer populations are present (community states 1/4, 3/6 and 2/5 in Figures 1 and 5). Second, an *emergent Allee effect in an intermediate consumer* represents the collapse of a competitively inferior consumer population due to apparent competition when all other species are present (community states 4/5 and 5/6 in Figure 1). Third, an *emergent two-species Allee effect* is associated with the invasion of the competitively inferior consumer species upon the sudden collapse of the top predator or its disappearance after the top predator establishes in the trophic food chain (community states 2/4 and 2/6 in Figure 1). Finally, the community can have *three* alternative stable states: presence of the top predator with one or both consumer populations or both consumer populations without the top predator (community states 2/5/4 and 2/5/6 in Figure 1). This outcome combines the emergent Allee effects in the top predator and in an intermediate consumer; we call it a *cascading emergent Allee effect* characterised by consecutive (Figure 6b) or nested (Figure 6c) population collapses of the top predator and one or both consumers. While the consecutive collapses enable the food web structure pass through all three alternative stable states through gradual change of the environmental conditions alone, the nested collapses make one of the stable states unreachable by gradual change.

We observed emergent Allee effects across a wide range of habitat productivities (Figure 3 and S3) and consumer size ratios (Figure 5 and S4–S5). Emergent Allee effects in the top predator and the two-species Allee effects (community states 1/4, 2/4, 2/5, 2/6 and 3/6) occurred at all consumer size ratios β but were restricted to intermediate TCC levels; the exact TCC range varied with the PB ratio when β deviated strongly from unity (Figure 5 and S3). Emergent Allee effects in intermediate consumers (community states 4/5 and 5/6) occurred only when β deviated strongly from unity and TCC levels were high enough for the top predator to persist (Figure 5b and S3–S5). Cascading emergent Allee effects (community states 2/5/4 and 2/5/6) appeared mainly for sufficiently dissimilar consumer body size ratios and intermediate TCC levels (Figure 5a and d, S3b, S3E–I, S4e–g and S5b and S5e–i). They almost always included consecutive population collapses (Figures S6b and S7a and c) and very rarely the nested collapse (community states 2/4 and 2/5/4 in Figure S4c and d). Finally, emergent Allee effects in our simulations predominately affected communities in which the top predator gained a feeding link to the pelagic or both consumers (community states 1/4, 2/4, 2/5 and 2/4/5) or in which apparent competition drove benthic consumers extinct (4/5; Figure 5b and d). This was likely caused by the constant size of benthic consumers in our analyses (see Text S2 for details).

DISCUSSION

Variation in predator–prey body size ratios underpins the structure and stability of food webs (Brose et al., 2006; Petchey et al., 2008). Furthermore, individual growth in size plays an important role in predator–prey interactions as large prey often become invulnerable to predation (Andersen & Beyer, 2006; de Roos & Persson, 2002). However, the importance of varying body sizes in multichannel food webs that arise in many aquatic and terrestrial ecosystems has not been explored. Here, we provided theoretical support for the key role of asymmetric body sizes and resource productivities in the empirically observed stability of multichannel food webs (Rooney et al., 2006). We also showed that alternative stable states in these food webs can go beyond the emergent Allee effect in the top predator (de Roos & Persson, 2002) and mutual exclusion via apparent competition (Chase, 1999; Holt et al., 1994) as we discovered three new types of emergent Allee effects affecting intermediate consumers or multiple populations or involving multiple alternative stable states. Our results emphasise

the need to jointly consider the strength of bottom-up regulatory processes, individual ontogeny and size-dependent interactions to improve our understanding of the responses of multichannel food webs to environmental change.

Multichannel food webs and apparent competition

We showed that body sizes of the intermediate consumers and energy partition between mesohabitats jointly determine the limits of species coexistence in multichannel food webs. Classic theory of apparent competition predicts that the prey resilient to the highest predation pressure prevails (Holt et al., 1994). Further extensions examining the combined roles of apparent and exploitative competition found that consumer coexistence requires a trade-off in the ability to dominate in each type of competition (Holt et al., 1994) and that habitat productivity drives the outcome (Chase, 1999; Leibold, 1996). That is, species dominating in exploitative competition should be gradually replaced by species resistant to predation as productivity increases, with coexistence possible at intermediate productivity levels (Leibold, 1996). This will often mean that small and large species will respectively dominate at low and high habitat productivity if predators cannot feed on large prey (Chase, 1999, 2003).

Consumers with larger relative body size were superior competitors in our model due to lower susceptibility to predation and critical resource density despite decreasing *per capita* growth and birth rates in larger individuals. Such a double population-level advantage does not always lead to competitive dominance. The 'double-handicapped loser' model of a diamond food web module (de Roos, 2020) showed that a consumer that is (1) an inferior exploitative competitor in the absence of predation and (2) more vulnerable to predation can exclude the superior competitor when exposed to predation due to the counterintuitive effects of size-dependent predation on the critical resource density required by each consumer population. In our case, additional mortality did not reverse the relationship between the relative body size and critical resource density of the consumer population (Figure 2d), and separate resources were thus required to keep the smaller consumers alive.

As a consequence, consumer coexistence in our model was primarily driven by the ratio of productivity in both linked mesohabitats when the two consumers were similarly sized and by productivity in the larger consumer's mesohabitat (i.e. similar to the findings by Chase (1999) and Leibold (1996)) when their sizes differed substantially. These conditions ensured sufficient productivity in each mesohabitat to meet the increased critical resource density requirements due to the predation pressure on vulnerable juveniles. We conclude that a 'symmetry in asymmetries' is required for consumer coexistence in multichannel food webs: asymmetry in body size, leading to different critical resource density at a given level of predation risk, must compensate for a mirror asymmetry in energy partitioning such as smaller consumers living in a more productive mesohabitat.

These combination of asymmetries occur frequently between pelagic and benthic mesohabitats in freshwater systems (Rooney et al., 2006). The pattern of (1) smaller organisms and high photosynthetic-driven productivity in pelagic mesohabitats and (2) larger organisms and low allochtonous productivity in benthic mesohabitat (Baird & Ulanowicz, 1989; Rooney et al., 2008) corresponds to the observations for $K_2 < K_1$ and $\beta < 1$ in our model (Figs. S3–S5). This implies that these multichannel food webs rely on the above compensatory asymmetries to ensure stable coexistence of apparent competitors in different food web channels (Rooney et al., 2006). Interestingly, our model also predicts stable coexistence if the larger organisms and lower productivity occur in the pelagic mesohabitat, that is, the observed coexistence patterns are not primarily driven by higher resource turnover rate in the pelagic mesohabitat ($\rho_2 > \rho_1$).

Emergent Allee effects, alternative stable states and catastrophic collapses

Increasing anthropogenic pressure on fish stocks through eutrophication and harvesting (Möllmann & Diekmann, 2012) has led to catastrophic declines of two thirds of freshwater and marine predatory fish, with an acceleration of 54% over the past 40 years (Christensen et al., 2014; Otto, 2018). While these declines can be reversible (Hutchings, 2000; Persson et al., 2007), they require disproportionately large efforts if the collapses associate with Allee effects that affect population resilience and recovery, promote alternative stable states in the system (van Kooten et al., 2005; Scheffer et al., 2001) and make the food webs vulnerable to sudden collapse (Gårdmark et al., 2015; Möllmann & Diekmann, 2012).

Here, we demonstrated that multichannel food webs can become disconnected not only by the loss of top predator but also by the loss of populations at intermediate trophic levels in response to increased productivity in the other mesohabitat, for example, due to eutrophication. Our results imply that multichannel food webs show the highest propensity for alternative stable states at highly unequal consumer body sizes and intermediate habitat productivity levels, which may guide future empirical studies on alternative stable states in such food webs. Intermediate levels of habitat productivity are also required for alternative stable states in the diamond and intraguild predation food web modules (Chase, 1999, 2003; Diehl & Feißel, 2000), suggesting that this pattern is independent of food web topology.

We did not observe alternative stable states affecting consumers via priority effects (Chase, 1999, 2003) as our model excludes exploitative competition. However, we identified other novel types of community transitions leading to the loss of the inferior consumer through an emergent Allee effect when (1) the top predator invades the system and the system shifts from separate consumer–resource pairs to a trophic chain, (2) increased or decreased productivity in one mesohabitat disrupts the energy balance and the system changes from a multichannel food web to a trophic chain and (3) cascading emergent Allee effects arise. In the latter case, we predict that the system can alternate between multiple stable states involving separate consumer–resource pairs, a trophic chain and the complete multichannel food web. This additional complexity may contribute to the limited evidence of alternative stable states on whole-ecosystem level (Schröder et al., 2005; but see Möllmann & Diekmann, 2012).

The emergent Allee effect in the top predator requires food- and size-dependent growth and size-dependent mortality of the consumers, but similar results can be obtained for size-structured predator population and predation risk given by the predator–prey body size ratio as long as the predation mortality induces competitive release in the prey (de Roos & Persson, 2002). The same mechanisms underpin the emergent Allee effects involving collapses of intermediate consumer populations, because they are caused by abrupt shifts in the critical resource density mediated by changes in predation mortality of vulnerable juveniles (Figure 2d). Although we have not run extensive simulations, we thus believe that our results do not critically depend on the stepwise predation mortality used for simplicity in (de Roos & Persson, 2002) and our model.

Conclusions and future directions

Our model showed that asymmetries in consumer body sizes and mesohabitat productivities can explain empirical data on multichannel food webs (McCann & Rooney, 2009; Rooney et al., 2006). We conclude that further studies exploring the links between the size scaling of individual vital rates and the dependence of critical resource density on consumer body size and predation pressure can provide mechanistic insights in the structure and functioning of multichannel food webs, including their propensity to sudden collapses due to emergent Allee effects. In particular, different size scaling of energy intake and expenditure can shift the competitive dominance towards adults or juveniles and lead to adult- or juvenile-driven consumer–resource cycles (Huss et al., 2013) rather than an equilibrium (as in our model), with all but unknown consequences for the structure and dynamics of multichannel food webs (but see Post et al., 2000). Detailed understanding of the role of individual and species traits such as body size in multichannel food webs could also help identify communities and species vulnerable to regime shifts (Gårdmark et al., 2015) and suggest possible restoration approaches.

DATA STATEMENT

No new data were used.

ACKNOWLEDGEMENTS

We thank Andrea Landeira-Dabarca and two anonymous reviewers for detailed comments that helped us improve the manuscript. This research was supported by the Grant Agency of the Czech Republic, project nr. 14-29857S.

AUTHORSHIP

DSB and SD designed the study. SD performed all numerical analyses with additional input from DSB. Both authors discussed the results and made suggestions for their presentation. SD wrote the first draft of the manuscript and DSB revised it.

PEER REVIEW

The peer review history for this article is available at https://publons.com/publon/10.1111/ele.13772.

OPEN RESEARCH BADGES

This article has earned an Open Materials badge for making publicly available the components of the research methodology needed to reproduce the reported procedure and analysis. All materials are available at: https://doi.org/10.5281/zenodo.4580494.

DATA AVAILABILITY

All code used in this study can be found in Zenodo (https://doi.org/10.5281/zenodo.4580494).

ORCID

Samuel Dijoux https://orcid.org/0000-0002-8086-7696
David S. Boukal https://orcid.org/0000-0001-8181-7458

REFERENCES

Abrams, P.A. & Rueffler, C. (2009) Coexistence and limiting similarity of consumer species competing for a linear array of resources. *Ecology*, 90, 812–822.

Andersen, K.H. & Beyer, J.E. (2006) Asymptotic size determines species abundance in the marine size spectrum. *American Naturalist*, 168, 54–61.

Baird, D. & Ulanowicz, R.E. (1989) The seasonal dynamics of the Chesapeake Bay ecosystem. *Ecological Monographs*, 59, 329–364.

Barnes, A.D., Jochum, M., Lefcheck, J.S., Eisenhauer, N., Scherber, C., O'Connor, M.I. et al. (2018) Energy flux: The link between multitrophic biodiversity and ecosystem functioning. *Trends in Ecology and Evolution*, 33, 186–197.

Beisner, B.E., Haydon, D.T. & Cuddington, K. (2003) Alternative stable states in ecology. *Frontiers in Ecology and the Environment*, 1, 376–382.

Scheffer, M. & van Nes, E.H. (2007) Shallow lakes theory revisited: Various alternative regimes driven by climate, nutrients, depth and lake size. *Hydrobiologia*, 584, 455–466.
Schindler, D. & Scheuerell, M. (2002) Habitat coupling in lake ecosystems. *Oikos*, 98, 177–189.
Schröder, A., Persson, L. & De Roos, A.M. (2005) Direct experimental evidence for alternative stable states: A review. *Oikos*, 110, 3–19.
van Kooten, T., De Roos, A.M. & Persson, L. (2005) Bistability and an Allee effect as emergent consequences of stage-specific predation. *Journal of Theoretical Biology*, 237, 67–74.
Wolkovich, E.M., Allesina, S., Cottingham, K.L., Moore, J.C., Sandin, S.A. & de Mazancourt, C. (2014) Linking the green and brown worlds: The prevalence and effect of multichannel feeding in food webs. *Ecology*, 95, 3376–3386.
Zou, K., Thébault, E., Lacroix, G. & Barot, S. (2016) Interactions between the green and brown food web determine ecosystem functioning. *Functional Ecology*, 30, 1454–1465.

SUPPORTING INFORMATION

Additional supporting information may be found online in the Supporting Information section.

How to cite this article: Dijoux S, Boukal DS. Community structure and collapses in multichannel food webs: Role of consumer body sizes and mesohabitat productivities. *Ecology Letters*. 2021;00:1–12. https://doi.org/10.1111/ele.13772

Supplementary information for

Community structure and collapses in multi-channel food webs: role of consumer body sizes and mesohabitat productivities

[Ecology Letters (2021), 24: 1607-1618]

Samuel Dijoux [a,b,*], David S. Boukal [a,b]

[a] Department of Ecosystem Biology, Faculty of Science, University of South Bohemia, Branišovská 1760, 370 05 České Budějovice, Czech Republic

[b] Czech Academy of Sciences, Biology Centre, Institute of Entomology, Branišovská 31, 370 05 České Budějovice, Czech Republic

E-mail addresses: dijoux.samuel@gmail.com (S. Dijoux); dboukal@prf.jcu.cz (D.S. Boukal)

Text S1. Full description of the food web model.

Text S2. Additional detailed results on emergent Allee effects.

Table S1. Individual state and population-level variables.

Table S2. Model parameters including the default values.

Table S3. Individual-level model equations of consumers.

Table S4. Equations of state dynamics.

Fig. S1. Dependence of the critical total carrying capacity (TCC) required for the top predator extinction (A) and invasion (B) thresholds on the PB ratio of resource partitioning and on consumer body size ratio.

Fig. S2. Resource substitutability in the system.

Fig. S3. Changes in community structure of the multi-channel system along productivity gradients, illustrated for multiple consumer size ratios.

Fig. S4. Changes in community structure of the multi-channel system along gradients of pelagic productivity and consumer size ratio.

Fig. S5. Changes in community structure of the multi-channel system along gradients of benthic productivity and consumer size ratio.

Fig. S6. Examples of community transitions in the multi-channel food web along the benthic resource productivity gradient.

Fig. S7. Examples of community transitions in the multi-channel food web along the pelagic resource productivity gradient.

Text S1. Full description of the food web model

We begin by focusing on the life histories of intermediate consumer populations. Individual consumers in both populations are born at length $l_{b,i}$, mature when reaching length $l_{j,i}$, and can reach the asymptotic length $l_{m,i}$ under unlimited food conditions. Consumer life histories are characterized by size- and resource-dependent feeding rates $I_i(R_i, l_i)$, growth rates $g_i(R_i, l_i)$ and fecundities $b_i(R_i, l_i)$ and size- and predator-dependent mortality rates $\mu_i(P, l_i)$, with $i = 1$ or 2. We use the same dynamic energy budget (DEB) model as in (de Roos & Persson 2002) to describe their individual size- and resource-dependent growth and reproduction. This so-called Kooijman-Metz model is a widely used DEB model that falls in the category of net production models, in which the ingested energy is first used to cover maintenance, a fixed fraction of the remainder is used for maturation and reproduction, and the rest for somatic growth (de Roos *et al.* 1990; Noonburg *et al.* 1998; Smallegange *et al.* 2017).

The rate of energy acquisition is assumed proportional to body surface (~ length^2), while maintenance is proportional to body weight (~ length^3). That is, ingestion rates of individual consumers with length l_i feeding on the respective basal resource R_i follow a type II functional response, $I_i(R_i, l_i) = I_m l_i^2 R_i/(R_h+R_i)$ with the proportionality constant I_m and half-saturation constant R_h. Given that maintenance increases faster with body size than the ingestion, individuals of both consumers follow a von Bertalanffy growth curve with resource-dependent growth rate and asymptotic size, $g_i(R_i, l_i) = k(l_{m,i} R_i/(R_h+R_i) - l_i)$, where k is the growth rate coefficient. They produce offspring after maturation at a *per capita* rate $b_i(R_i, l_i) = r_m l_i^2 R_i/(R_h+R_i)$, with a proportionality constant r_m. For simplicity, we assume in the code that the individuals only stop growing and reproducing but do not shrink or use energy reserves to cover maintenance costs when the food intake becomes insufficient (see (de Roos *et al.* 1990) for details); this simplification does not affect our results.

In addition to predation induced-mortality μ_p, individuals of both consumers die with the same size-independent background mortality rate μ_b. The top predators feed indiscriminately on vulnerable individuals from both consumer populations when present, following a Holling type II

functional response with constant attack rate a and handling time h. We assume constant conversion efficiency ϵ of ingested prey biomass to predator biomass and background mortality rate δ of the top predators.

References

Noonburg, E.G., Nisbet, R.M., McCauley, E., Gurney, W.S.C., Murdoch, W.W. & De Roos, A.M. (1998). Experimental testing of dynamic energy budget models. *Funct. Ecol.*, 12, 211–222.

de Roos, A.M., Metz, J.A.J., Evers, E. & Leipoldt, A. (1990). A size dependent predator-prey interaction: who pursues whom? *J. Math. Biol.*, 28, 609–643.

de Roos, A.M. & Persson, L. (2002). Size-dependent life-history traits promote catastrophic collapses of top predators. *Proc. Natl. Acad. Sci. U. S. A.*, 99, 12907–12912.

Smallegange, I.M., Caswell, H. & Toorians, M.E.M. (2017). Mechanistic description of population dynamics using dynamic energy budget theory incorporated into integral projection models. *Methods Ecol. Evol.*, 8, 146–154.

Text S2. Additional detailed results on emergent Allee effects

We varied body size of pelagic consumers while keeping the size of benthic consumers constant in our analyses. Thus, the range of environmental conditions giving rise to the emergent Allee effect in the benthic food chain (community state 3/6) was independent of β, while the other emergent Allee effects in the top predator (1/4 and 2/5) and the two-species Allee effect associated with the loss of the benthic consumer (2/4) became more common as β increased (Figs. 3B, 4B and S4; see also Fig. 5AD). Alternative stable states in which the top predator could gain access to the benthic consumers (community states 2/6, 3/6 and 2/5/6) were less common and limited to sufficiently small pelagic consumers living in a moderately productive mesohabitat (states 2/6 and 2/5/6 in Figs. 5C, S3A-F, S4FG and S5A-D) and to food webs with intermediate benthic productivity K_1 and pelagic productivity K_2 below the pelagic consumer persistence threshold (state 3/6 in Figs. 3B, S3 and S4FG). Finally, we found the emergent Allee effect in which the top predator drove the pelagic consumers to extinction (community state 5/6) only for very small pelagic consumers ($\beta < 0.5$, $l_j < 55$ mm) and a narrow range of moderate benthic productivity ($K_2 \approx 10^{-4}$ g.L^{-1}, Figs. 5CD, S3AB, S4FG, and S5).

Table S1. Individual state and population-level variables

Variable	Symbol	Unit
Consumer length	l_i	mm
Population density of consumers	c_i	mm^{-1}.L^{-1}
Resource biomass	R_i	g.L^{-1}
Top predator biomass	P	g.L^{-1}

Note: Subscript (i = 1 or 2) refers to the consumer or resource population in the respective mesohabitat

Table S2. Model parameters including the default values

Symbol	Default value	Unit	Description
$l_{b,2}$	7	mm	Length at birth of consumer C_2
$l_{v,1} = l_{v,2} = l_v$	27	mm	Predation vulnerability threshold
$l_{j,2}$	110	mm	Length at maturation of consumer C_2
$l_{m,2}$	300	mm	Asymptotic length of consumer C_2
ω	9×10^{-6}	$g.mm^{-3}$	Proportionality constant of the consumer length-weight relationship
I_m	10^{-4}	$g.day^{-1}.mm^{-2}$	Proportionality constant of the consumer functional response
$R_{h,1}$	1.5×10^{-5}	$g.L^{-1}$	Half-saturation constant or resource R_1
$R_{h,2}$	1.5×10^{-5}	$g.L^{-1}$	Half-saturation constant or resource R_2
k	0.006	day^{-1}	Von Bertalanffy growth rate coefficient
r_m	0.003	$day^{-1}.mm^{-2}$	Birth rate proportionality constant
μ_b	0.01	day^{-1}	Background mortality rate of consumers
K_1	3×10^{-4} / varied	$g.L^{-1}$	Carrying capacity of resource R_1
K_2	3×10^{-4} / varied	$g.L^{-1}$	Carrying capacity of resource R_2
ρ_1	0.1	day^{-1}	Flow-through rate of resource R_1
ρ_2	0.2	day^{-1}	Flow-through rate of resource R_2
a	5000	$L.day^{-1}$	Predator attack rate

h	0.1	day.g^{-1}	Predator handling time
ϵ	0.5	-	Food conversion efficiency
δ	0.01	day^{-1}	Predator mortality rate
β	1.2 / varied	-	Body size ratio between consumers C_1 and C_2

Table S3. Individual-level model equations of consumers

Subject	Equation	Equation no.
Length-weight relationship	$w = \omega l^3$	(S1)
Feeding rate	$I_i(R_i, l_i) = I_m l_i^2 R_i/(R_{h,i} + R_i)$	(S2)
Somatic growth rate	$g_i(R_i, l_i) = k\,(l_{m,i}\, R_i/(R_h+R_i) - l_i)$	(S3)
Per-capita birth rate	$b_i(R_i, l_i) = r_m l_i^2 R_i/(R_{h,i} + R_i)$	(S4)
Predation mortality rate	$\mu_P(P, l_i) = \begin{cases} \dfrac{aP}{1 + ah(C_{v,1} + C_{v,2})} & \text{if} \quad l_i \le l_v \\ 0 & \text{if} \quad l_i > l_v \end{cases}$	(S5)
Total mortality rate	$\mu_i(P, l_i) = \mu_b + \mu_P(P, l_i)$	(S6)

Note: Subscript (i = 1 or 2) refers to the consumer or resource population in the respective mesohabitat; see Eq (S10) for the biomasses of vulnerable consumers $C_{v,i}$ used in Eq (S5).

Table S4. Equations of state dynamics

Subject	Equation	Equation no.
Resource dynamics	$\frac{dR_i}{dt} = \rho_i (K_i - R_i) - \int_{l_{b,i}}^{l_{m,i}} I_i(R_i, l_i) c_i(t, l_i) dl$	(S7)
Population-level consumer birth rate	$B_i(t, R_i) = \int_{l_{j,i}}^{l_{m,i}} b_i(R_i, l_i) c_i(t, l_i) dl$	(S8)
Consumer size structure balance equation	$\frac{\partial c_i(t, l_i)}{\partial t} + \frac{\partial g_i(R_i, l_i) c_i(t, l_i)}{\partial l} = -\mu_i(P, l_i) c_i(t, l_i)$	(S9)
Biomass of vulnerable consumers	$C_{v,i} = \int_{l_{b,i}}^{l_v} \omega l_i^3 c_i(t, l_i) dl$	(S10)
Predator biomass dynamics	$\frac{dP}{dt} = (\epsilon \frac{a(C_{v,1} + C_{v,2})}{1 + ah(C_{v,1} + C_{v,2})} - \delta) P$	(S11)

Note: Subscript (i = 1 or 2) refers to the consumer or resource population in the respective mesohabitat.

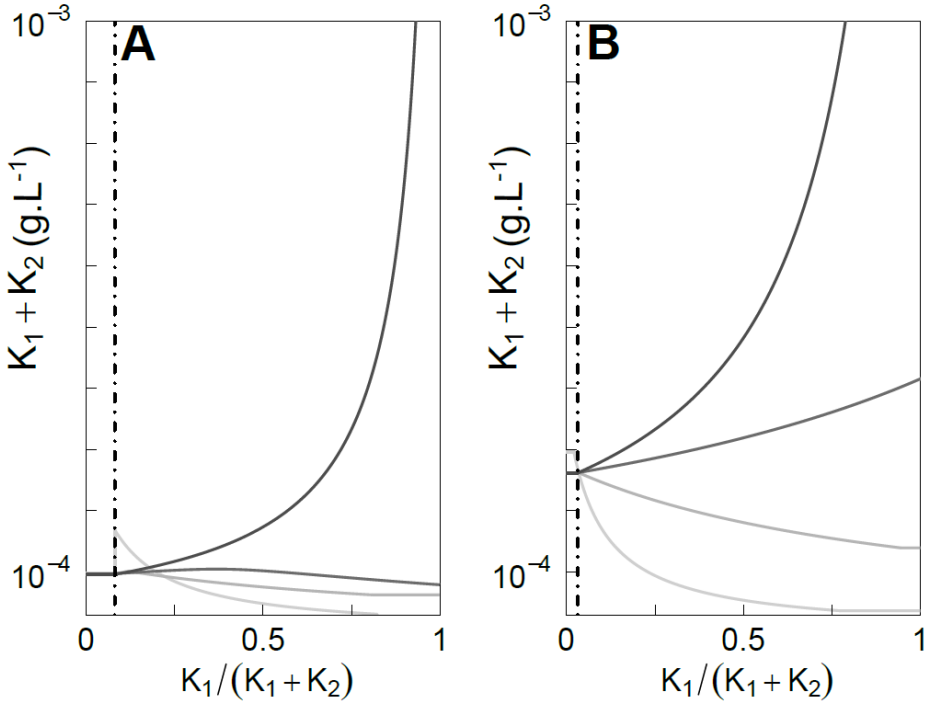

Fig. S1. Dependence of the critical total carrying capacity (TCC) required for the top predator extinction (A) and invasion (B) thresholds on the PB ratio of resource partitioning and on consumer body size ratio. Consumer body size ratios: β = 0.5, 1.0, 1.5 and 3.0 (light grey to black lines); other parameters as in Table S1. Dash-dotted lines = minimum proportion threshold below which predator extinction and invasion thresholds become independent from K_1.

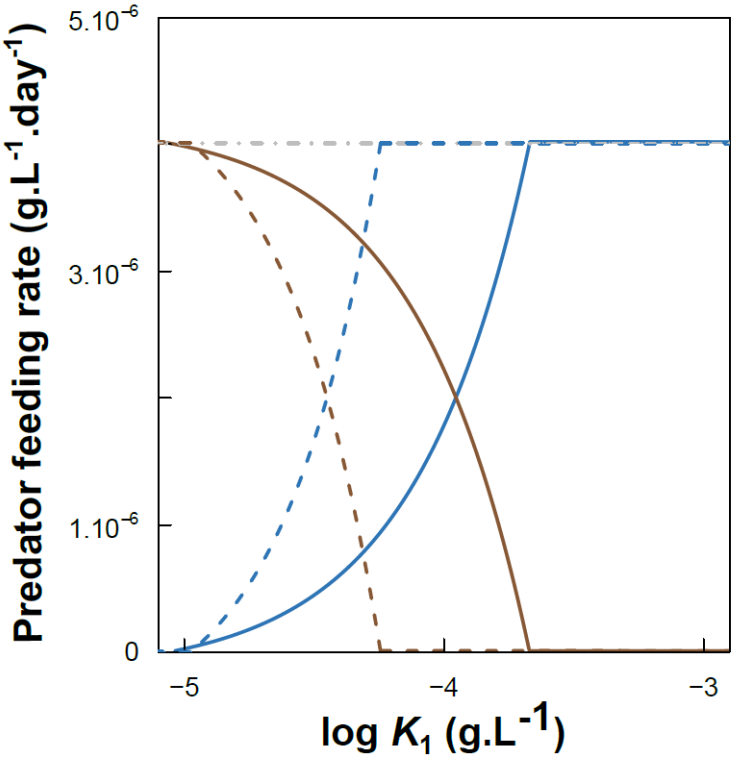

Fig. S2. Resource substitutability in the system. Contribution by pelagic (C_1, blue) and benthic (C_2, brown) consumers to predator feeding rate at predator invasion (solid lines) and collapse thresholds (dashed lines) along the pelagic productivity gradient for $\beta = 1.2$ (Fig. 3B). Other parameters as in Table S1. Dash-dotted grey line = total biomass intake of predators, ca. 4×10^{-6} g.L^{-1}.day^{-1}.

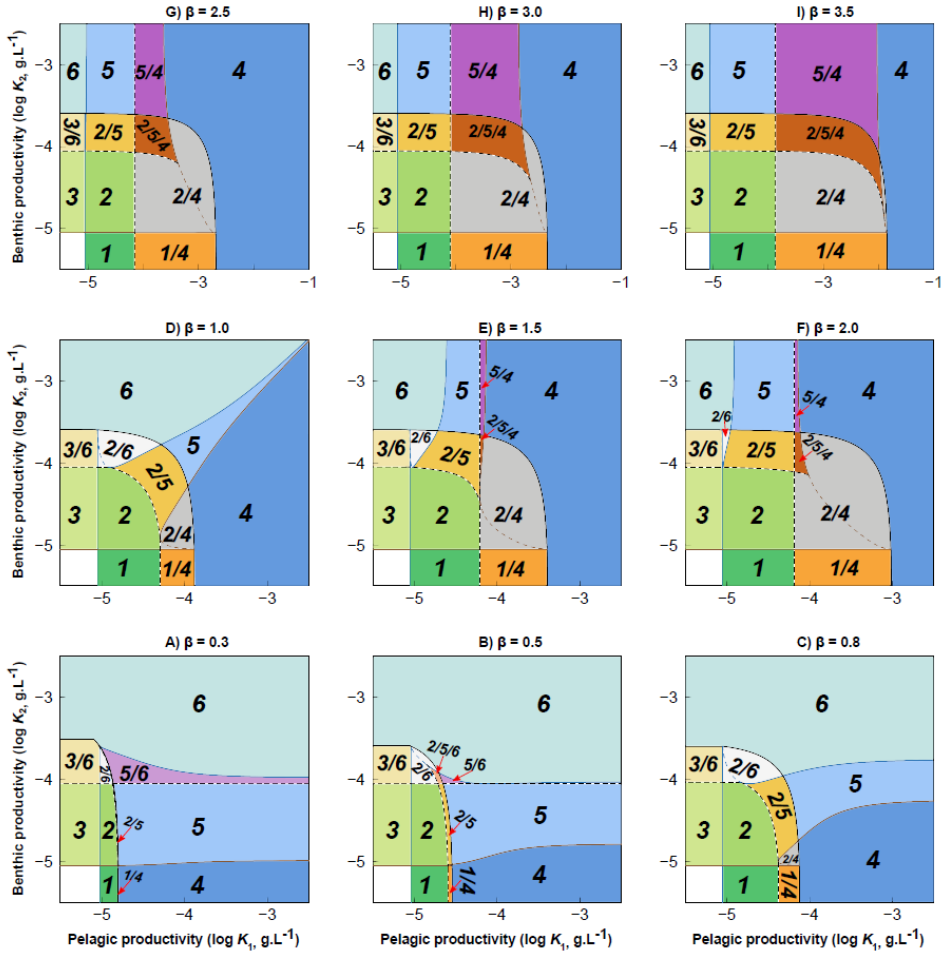

Fig. S3. Changes in community structure of the multi-channel system along productivity gradients, illustrated for multiple consumer size ratios. Community structures numbered as in Fig. 1; coexistence of all five species denoted by '5'. Consumer size ratios: pelagic consumers smaller than benthic ones (from A to C: β = 0.3, 0.5 and 0.8), (B) both consumers equally sized (D: β = 1.0), benthic consumers larger than pelagic ones (from E to I: β = 1.5, 2, 2.5, 3 and 3.5). Other parameters as in Table S1. Note the different scaling of the x axis in panels G–I.

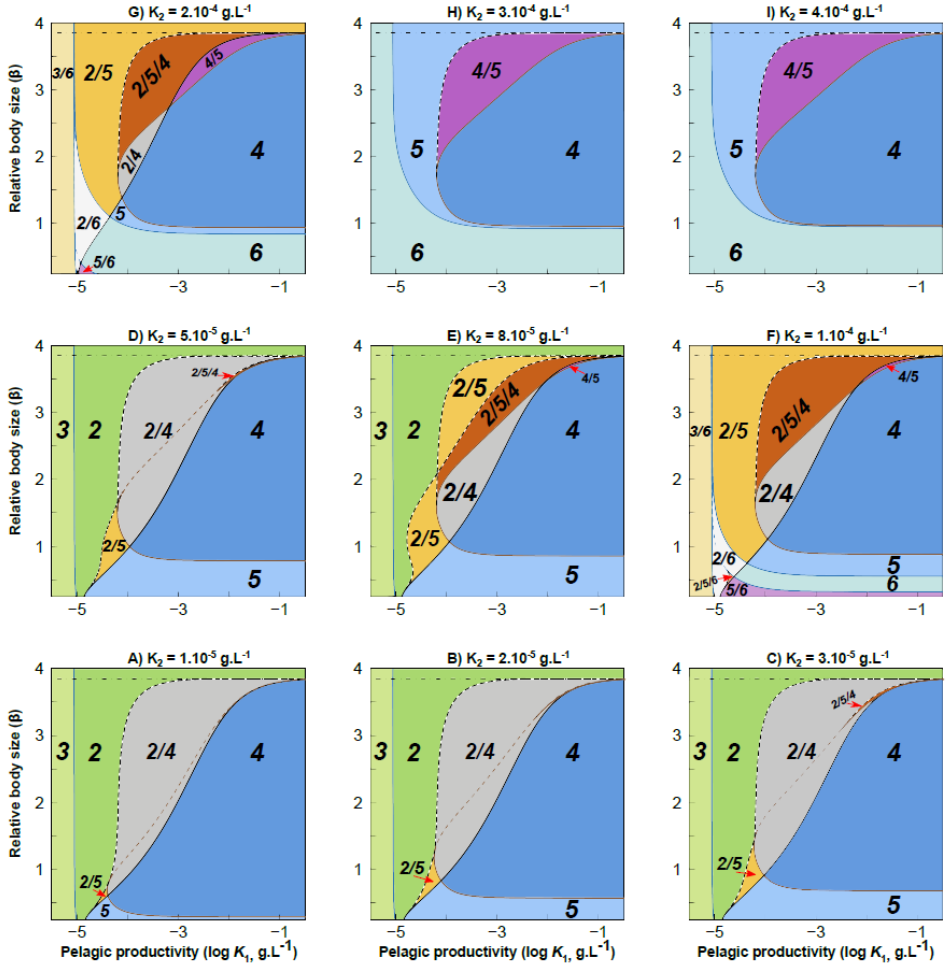

Fig. S4. Changes in community structure of the multi-channel system along gradients of pelagic productivity and consumer size ratio. Community structures numbered as in Fig. 1; coexistence of all five species denoted by '5'. Benthic resource carrying capacity: K_2 = 10^{-5} g.L^{-1} (A), 2×10^{-5} g.L^{-1} (B), 3×10^{-5} g.L^{-1} (C), 5×10^{-5} g.L^{-1} (D), 8×10^{-5} g.L^{-1} (E), 10^{-4} g.L^{-1} (F), 2×10^{-4} g.L^{-1} (G), 3×10^{-4} g.L^{-1} (H), and 4×10^{-4} g.L^{-1} (I). Other parameters as in Table S1. Dash-dotted line: predation vulnerability limit of the pelagic consumer.

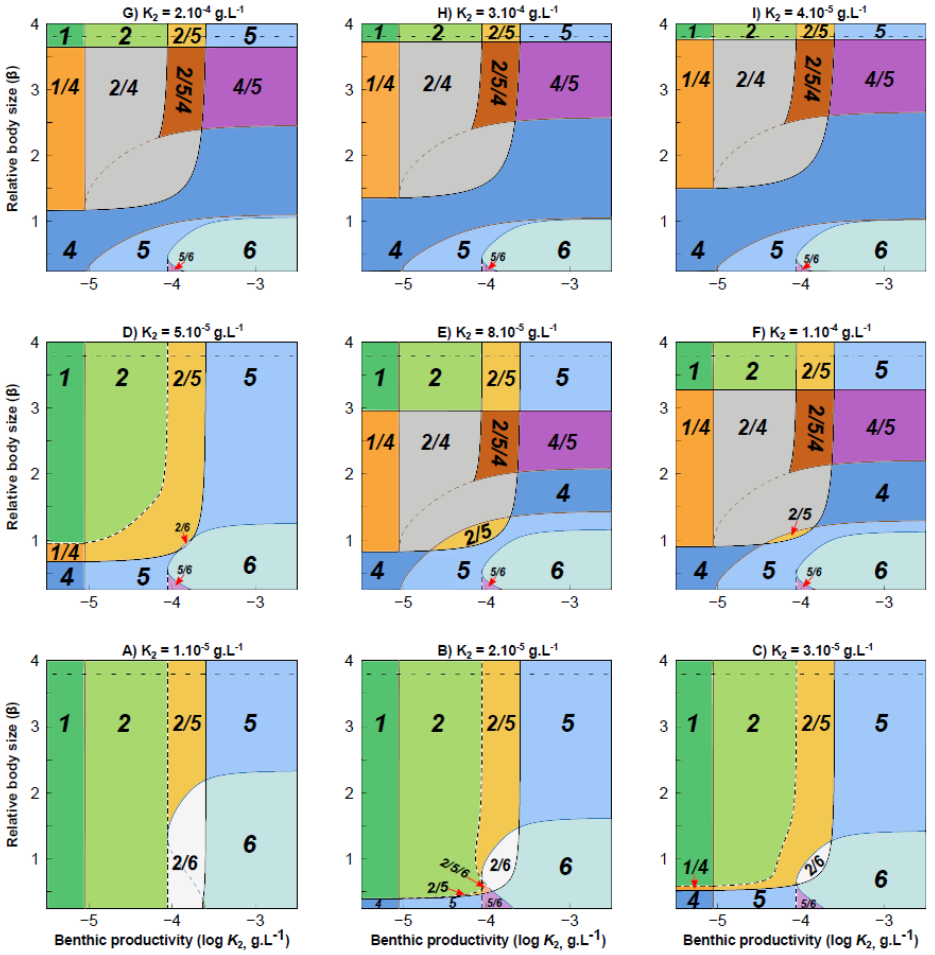

Fig. S5. Changes in community structure of the multi-channel system along gradients of benthic productivity and consumer size ratio. Community structures numbered as in Fig. 1; coexistence of all five species denoted by '5'. Pelagic resource carrying capacity: $K_1 = 10^{-5}$ g.L^{-1} (A), 2×10^{-5} g.L^{-1} (B), 3×10^{-5} g.L^{-1} (C), 5×10^{-5} g.L^{-1} (D), 8×10^{-5} g.L^{-1} (E), 10^{-4} g.L^{-1} (F), 2×10^{-4} g.L^{-1} (G), 3×10^{-4} g.L^{-1} (H), and 4×10^{-4} g.L^{-1} (I). Other parameters as in Table S1. Dash-dotted line: predation vulnerability limit of the pelagic consumer.

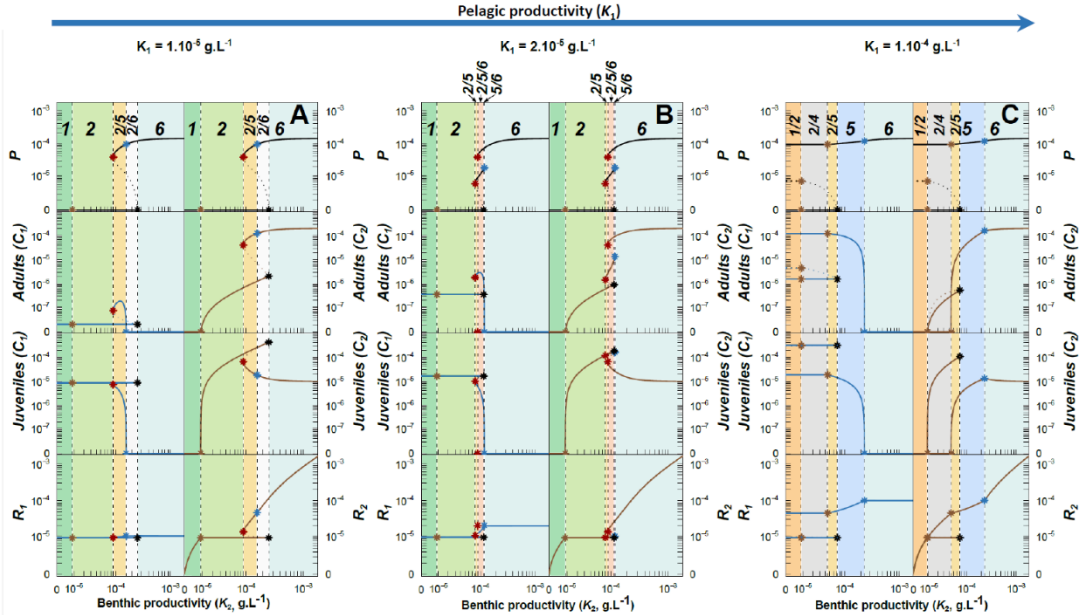

Fig. S6. Examples of community transitions in the multi-channel food web along the benthic resource productivity gradient. Parameter values: β = 0.5 (B), 1 (C) and 2 (A); K_2 = 10^{-5} g.L^{-1} (A), 2×10^{-5} g.L^{-1} (B), and 10^{-4} g.L^{-1} (C), i.e., pelagic resource productivity increasing from A to C. Other parameters as in Table S1. Top predator panel is duplicated to enable comparison within each mesohabitat. Solid lines = stable equilibria, dashed lines = unstable equilibria, dotted vertical lines = resource productivity thresholds separating different community structures; numbers refer to community states in Fig. 1. The examples include emergent Allee effects in the top predator (A–C), two species (top predator and a consumer, A and C), and an intermediate consumer (B), and a cascading emergent Allee effect (B). Scaling of axes as in Fig. 4; blue arrow above the panels illustrates the gradient of pelagic productivity.

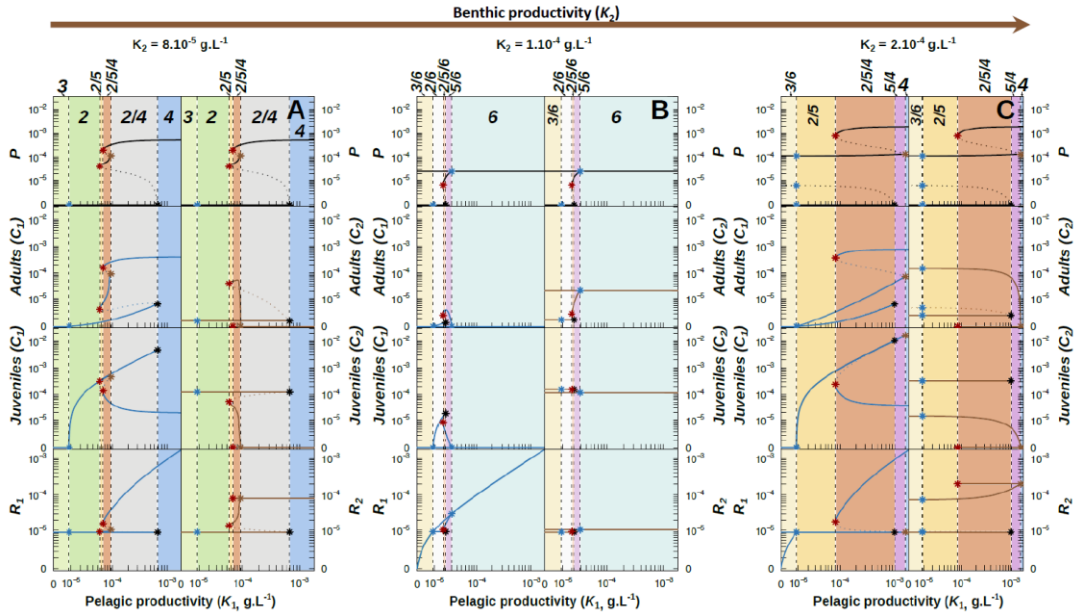

Fig. S7. Examples of community transitions in the multi-channel food web along the pelagic resource productivity gradient. Parameter values: β = 2.5 (A), 0.5 (B) and 3 (C); $K_1 = 8\times10^{-5}$ g.L^{-1} (A), 10^{-4} g.L^{-1} (B) and 2×10^{-4} g.L^{-1} (C), i.e., benthic resource productivity increasing from A to C. Other parameters as in Table S1. Top predator panel is duplicated to enable comparison within each mesohabitat. The examples include emergent Allee effects in the top predator (A–C), two species (top predator and one consumer, A and B) and intermediate consumer (B and C), and a cascading emergent Allee effect (A–C). Lines, arrows, community state numbers and scaling of axes as in Fig. S6; brown arrow above the panels illustrates the gradient of benthic productivity.

~ Chapter III ~

Temperature-dependent consumer growth rates, rather than temperature-size rule, determine the propensity for catastrophic collapses of top predators

[Manuscript]

Temperature-dependent consumer growth rates, rather than temperature-size rule, determine the propensity for catastrophic collapses of top predators

Authors: Samuel Dijoux[1,2,*], Aslak Smalås[3,4], Raul Primicerio[3], David S. Boukal[1,2,*]

Affiliations:
[1.]Department of Ecosystems Biology, Faculty of Science, University of South Bohemia, České Budějovice, Czech Republic.
[2.]Czech Academy of Sciences, Biology Centre, Institute of Entomology, České Budějovice, Czech Republic.
[3.]Department of Arctic and Marine Biology, Faculty of Bioscience, Fisheries and Economy, UiT, The Arctic University of Norway, Tromsø, Norway.
[4.]SNA-Skandinavisk naturoveråking AS (Scandinavian Nature-monitoring), Åkerblå Group, Tromsø, Norway.

E-mail addresses: dijous00@prf.jcu.cz (S. Dijoux); dboukal@prf.jcu.cz (D. S. Boukal).
[*] Corresponding author: dijous00@prf.jcu.cz; dboukal@prf.jcu.cz.

Author ORCID numbers: SD (0000-0002-8086-7696), AS (0000-0002-6316-2811), RP (0000-0002-1287-0164), DSB (0000-0001-8181-7458).

Short-running title: Temperature-dependent catastrophic collapses of top predators

Keywords: Alternative stable states; emergent Allee effect; trophic chain; temperature-size rule; predator-prey interaction; metabolic ecology; warming

Target journal: Proceedings of the Royal Society B / Ecology

Number of words in the abstract: 158 words
Number of words in the main text: 5545 words
Number of references: 54
Number of figures, tables and text boxes: 2 figures

Authorship statement: DSB and SD designed the study, SD performed the analyses. All authors discussed the results and made suggestions for their presentation. SD and DSB wrote the first draft of the manuscript, and all co-authors revised it.

Conflict of Interest Statement: The authors declare no conflict of interest.

Data statement: No new data were used in this study

Abstract

Warming climate affects aquatic ectotherms directly by altering individual vital rates and indirectly through changes in body size and environmental feedbacks. Body size of many aquatic ectotherms declines at higher temperatures, but little is known how these responses combine together on the community level. Community responses to environmental drivers can be abrupt, as exemplified by catastrophic collapses of top predators caused by size-structured trophic interactions. Here we model the structure and dynamics of a tri-trophic food chain with size- and temperature-dependent vital rates and species interactions to explore how direct kinetic effects of temperature and temperature-size rule (TSR) affect the community structure and its propensity to catastrophic collapses along resource productivity and temperature gradients. We find that the community structure and propensity to collapse are primarily driven by the direct kinetic effects of temperature on consumer growth and ingestion rates and predator feeding rate, while the impact of TSR in consumers and predators on community structure are limited.

Keywords: tri-trophic food chain; emergent Allee effects; body size reductions; size-dependent predation; community dynamics; metabolic ecology

Introduction

Species responses to environmental change underlie community responses to future global changes. Aquatic biota faces multiple anthropogenic stressors including the warming climate, habitat degradation, overharvesting, agricultural runoff, warming, and invasions (Sala et al. 2000; IPBES 2019). The precipitous decline in freshwater biodiversity, estimated to suffer a 76% decline since 1970 (McLellan et al. 2014), raises an alarm and urges us to develop better approaches to understand the emerging responses to environmental change from species level to the ecosystem scale (Young et al. 2016). In particular, the increasing global temperatures predicted to rise by 1.4-4.4°C by the end of the 21st century (IPCC 2022) will profoundly change the composition and structure of communities worldwide (Sala et al. 2000; Young et al. 2016).

Environmental productivity and temperature are two main drivers of the structure and dynamics of communities in aquatic ecosystems (Binzer et al. 2012, 2016). Habitat productivity, defined by the carrying capacity of primary producers, provides a measure of the system's ability to support elongated food webs (Oksanen et al. 1981; Fretwell 1987). Environmental change, however, can affect local habitat productivity, which in turn affects species at higher trophic levels in the food web. In particular, changes in prey biomass in response to habitat productivity can lead to non-linear phenomena in predator population such as the emergent Allee effect characterized by alternative stable states of the community structure (de Roos & Persson 2002; Lindmark et al. 2019; Dijoux & Boukal 2021) and trigger sudden ecosystem regime shifts (Scheffer et al. 2001). However, the impact of warming on these alternative stable states is not fully understood (Lindmark et al. 2019).

The impacts of rising temperatures in freshwater ecosystems are expected to be stronger than in terrestrial biota due to the dominance of ectotherm taxa (plankton, amphibians, insects, crustaceans, fishes) (Forster et al. 2012). Temperature drives the structure and persistence of communities through direct and indirect effects on individuals and species interactions (Yvon-Durocher et al. 2011; Sentis et al. 2017; Uszko et al. 2017; Lindmark et al. 2018, 2019; Boukal et al. 2019). Temperature directly

modulates ectotherm vital rates (growth, consumption, metabolism, and reproduction) that together define the species thermal niche within which the species can persist (Angilletta Jr. 2009). Key performance traits such as individual growth or reproduction are usually well described by unimodal thermal performance curves (TPCs) that reach a maximum value at an intermediate temperature and then drop sharply towards the upper thermal limit (Huey & Kingsolver 1989). This is because moderate warming directly enhances species performance rates, but metabolic demands typically increase faster than food intake with increasing temperature (Rall et al. 2010; Fussmann et al. 2014). Given their broad conceptual appeal, TPCs have been widely used in mechanistic models of organismal responses to the warming climate (e.g. Kearney & Porter (2006); Angert et al. (2011); Schulte et al. (2011)).

Together with the direct kinetic effects of rising temperatures on individual performance traits, the impacts of warming include species-specific changes in phenology and distributional shifts (Parmesan & Yohe 2003; Kingsolver & Huey 2008; Sunday et al. 2012). Warming also leads to declining body sizes in many ectotherms, especially in freshwater, although the proximate causes for this phenomenon are still being debated (Daufresne et al. 2009; Verberk et al. 2021; Wootton et al. 2022). It has been termed the 'temperature-size rule' (hereafter 'TSR') and recognized the 'third universal response to warming' (Gardner et al. 2011; Forster et al. 2012). These direct and indirect effect of warming on species responses and community structure have separately received considerable attention. Yet, little is known about their joint effects on community structure and stability. Many models explored the impacts of temperature-dependent species interactions on community composition (Vasseur & McCann 2005; Rall et al. 2010; Binzer et al. 2012, 2016) or included both temperature-dependent species interactions and TSR (Sentis et al. 2017). However, these studies typically used a biomass-based description of population dynamics and species interactions (e.g. Yodzis & Innes (1992)) and neglected population structure and ontogenetic variation in individual responses to temperature that can drive population and community responses to warming (Gårdmark & Huss 2020; Thunell et al. 2021). In particular, we do not know to what extent the effects of warming on

individual performance traits and TSR at different trophic levels lead to the same or different effects on the community structure, and which of these effects dominate when operating together.

To fill these knowledge gaps, we focus on how the joint effects of temperature and habitat productivity affect community structure of a tri-trophic chain. Warming can trigger regime shifts in size-structured populations (Ohlberger et al. 2011). A tri-trophic chain with size-structured population of the intermediate consumer exhibits an emergent Allee effects in the top predator that is gape limited and feeds only on sufficiently small consumer individuals (de Roos & Persson 2002). Here we aim to disentangle the direct kinetic effects of temperature-dependent vital rates and indirect effects of TSR on the structure of this community. Using a physiologically structured population model with size- and temperature-dependent vital rates and trophic interactions, we investigate how the temperature and size dependence of multiple processes that underpin the consumer life history (growth, development, and reproduction), predator functional response and predator metabolic loss contribute to the alternative stable states and community structure in response to warming. We also ask how TSRs in three different size thresholds characterizing consumers (size at maturation and maximum size) and predators (predation vulnerability size threshold) affect the outcome.

Methods

Community model

We extend the physiologically structured population model of a tri-trophic chain developed by de Roos & Persson (2002) to include temperature-dependent vital rates and TSR in the consumers and top predators. Following de Roos & Persson (2002), we assume that the community is composed of unstructured top predator and basal resource populations and a size-structured population of consumers characterized by their length l. We used the same dynamic budget model as in de Roos & Persson (2002) and Dijoux & Boukal (2021) for the consumer population (Text S1). Consumer individuals are born at length l_b, mature at length l_{mat} and can reach maximum length l_∞ under unlimited food conditions (Eq. S1, Table S3). They feed on the resource following a Holling type II functional response that scales with l^2 (Eq. S2) and follow a von-Bertalanffy growth curve (Eq. S3). Adult reproductive investment also scales proportionally to l^2 (Eq. S4). Maximum feeding rate, somatic growth rate and birth rate are assumed constant in the baseline scenario (Eq. S5; see below for rates modified by temperature dependence and TSR).

Top predators feed on juvenile consumers smaller than l_v (Eq. S6) and follow a Holling type II functional response (Eq. S7). Consumer mortality therefore consists of size-dependent predation mortality and constant natural mortality (Eq. S6); this pattern of mortality decreasing with size is characteristic for many aquatic taxa. Biomass loss rate of the predator is assumed constant in the baseline scenario (Eq. S8). We use parameters derived for perch (*Perca fluviatilis*) as the top predator, European roach (*Rutilus rutilus*) as the consumer and cladocerans (*Daphnia* sp.) as the resource to parameterise the model (de Roos & Persson 2002) and assume that these parameters pertain to the environmental temperature of 20°C.

Temperature dependent vital rates and temperature-size rule

We explore the direct and indirect effects of temperature on community structure and dynamics in two ways: (1) body size reductions of the

consumer or top predator species that indirectly affect the maturation, reproduction, and predation mortality rates of the consumer and biomass loss rate of the top predator, and (2) direct kinetic effects of temperature on the ingestion, growth, and birth rates of the consumer and on the functional response and biomass loss of the predator (hereafter referred to as consumer and top predator 'vital rates', respectively).

We apply the TSR using a length-specific reduction in l_{mat}, l_v and/or l_∞ of 5% .°C^{-1} (Fig. 1, Eq. S9); this value is based on the estimated mean mass-specific for aquatic ectotherms (Forster et al. 2012) and length-weight allometry of $W \sim l^3$ (Table S2). While TSR applied to l_{mat} and/or l_∞ mimics reduction in consumer size with warming, TSR applied to predation size threshold l_v mimics reduction in predator size with warming. This allows us to explore the consequences of predator-prey size mismatches (sensu Sentis et al. subm.) in this system.

We model temperature-dependent consumer ingestion, growth and birth rates (Eqs. S10-S12) as in by applying a Rosso function to the respective proportionality constants (Mallet et al. 1999; Smalås et al. 2020) (Eq. S13). The Rosso function describes a left-skewed, non-linear thermal performance curve (Fig. 1b). We set the lower and upper thermal boundaries at 5 and 25°C and use the same optimum temperature of 20°C for all three taxa. We implement temperature dependence of the predator functional response (Eq. S15) through the attack rate and handling time parameters as in (Uszko et al. 2017). Finally, we model temperature-dependent predator metabolic loss rate as in (Sentis et al. 2017; Dijoux et al. 2023) (Eq. S16), assuming the average mass of a 200 mm long predator (de Roos & Persson 2002).

Analyses

We model the tri-trophic food chain dynamics using Eqs S17-S21 (Table S4) and solve them numerically using the R package *PSPMAnalysis* version 0.3.9 (de Roos 2021) to track the system equilibria and detect thresholds associated with successful establishment of the intermediate

consumer and top predator and the collapse threshold of the top predator along temperature and habitat productivity gradients.

To disentangle the different effects of temperature on community structure, we explore multiple scenarios combining temperature-independent (Eqs. S1-S8) and temperature-dependent (Eqs. S9-S16) consumer and predator sizes and vital rates. Our seven main scenarios include: (1) body size and vital rates of the consumer and top predator are independent of temperature as in de Roos & Persson (2002) and Dijoux & Boukal (2021), (2) only vital rates of the consumer, including its functional response, depend on temperature, (3) only consumer size depends on temperature, (4) both vital rates and body size of the consumer depend on temperature, (5) only vital rates of the consumer and top predator, including their functional responses, depend on temperature, (6) only consumer and predator size depend on temperature, and (7) vital rates including the functional responses and body size of the consumer and top predator depend on temperature. That is, scenarios 2 and 5 explore the direct kinetic effects of temperature, scenarios 3 and 6 explore the indirect effects mediated by TSR, and scenarios 4 and 7 explore the combined direct and indirect effects. Scenarios 2–4 focus on the temperature effects on the consumer population, while scenarios 5–7 consider that the temperature affects both consumers and the top predator.

We first summarise the community structure along the productivity gradient in the absence of temperature dependence (Scenario 1). Next, we explore how the direct and indirect effects of TSR and temperature-dependent rates (i.e. vital rates of the consumer and predator and their trophic interaction) alter the habitat productivity thresholds that mark the changes in community structure. We begin with Scenarios 2–4 that consider only the temperature effects on the consumer population, and then compare the results for Scenarios 5–7 that consider the temperature effects on both consumer and top predator population. Some of these scenarios assume simultaneous temperature dependence of multiple model parameters. To gain further insight into the importance of individual processes, we also explore additional scenarios in which we consider only

one temperature-dependent process (or parameter) at a time and scenarios in which all but one process (or parameter) depend on temperature.

Results

Community structure along the productivity gradient

Community structure in the absence of temperature dependence (Scenario 1, dotted vertical lines at optimum temperature T_{opt} in Fig. 2; see also de Roos & Persson (2002)) changes with resource productivity. Consumers can invade and persist when the resource productivity exceeds the consumer invasion threshold of $K_C \sim 9\times10^{-6}$ g.L^{-1}. Their biomass increases with resource productivity (Fig. S1a) until the juvenile consumer biomass becomes high enough to sustain the top predator at its invasion threshold $K_P \sim 2.5\times10^{-4}$ g.L^{-1}. The system exhibits an emergent Allee effect for intermediate productivities ($K_A \sim 9\times10^{-5}$ g.L^{-1} $\leq K \leq K_P$) with two alternative stable states, consumer-resource and trophic chain equilibria, and the top predator population collapses abruptly when resource productivity drops below the persistence threshold K_A (Fig. S1a).

Effects of TSR and temperature-dependent rates in the consumers on community structure

The effects of temperature-dependent rates (Scenarios 2 and 5, Figs. 2a and 2d) and TSR (Scenarios 3 and 6, Figs. 2b and 2e) on the community structure differ strongly. When only the consumer vital rates vary with temperature (Scenario 2, Fig. 2a), consumer population persists within its thermal niche (~ 5–25 ºC) and above an invasion threshold $K_C(T)$ that is approximately constant within a large part of the consumer's thermal niche and increases sharply at temperatures approaching the lower or upper limit of the consumer's thermal niche (dotted line in Fig. 2a). This contrasts with the values of the invasion threshold $K_P(T)$ and the persistence threshold $K_A(T)$ of the top predator, which decrease as the temperature moves away from the optimum. The lowest habitat productivity values at which the top predators can invade and persist therefore occur close to the lower and

upper limit of the consumer's thermal niche (dashed and solid lines in Fig. 2a). A comparison of the effects of temperature-dependent consumer feeding, birth and growth rates when considered alone (Fig. S2a-c) reveals that the overall effect of temperature on community structure when only the consumer vital rates vary with temperature (Fig. 2a) is primarily driven by the temperature dependence of individual growth rate, while the temperature dependence of consumer feeding rate shapes the concave-down temperature dependence of the persistence threshold $K_A(T)$ of the top predator (Fig. 2a, S2a and S2c).

The results are much simpler when only the consumer body size varies with temperature due to TSR (Scenario 3, Fig. 2b). First, this scenario assumes no thermal viability limits for the consumer and hence also the top predator. Simultaneous reduction of the consumer maturation and maximum sizes with warming does not alter the consumer invasion threshold K_C, but leads to lower predator invasion threshold $K_P(T)$ and persistence threshold $K_A(T)$ with warming (Fig. 2b). Moreover, TSR in consumer maturation size and TSR in consumer asymptotic size alone lead to different temperature dependences of consumer invasion, predator invasion and predator extinction thresholds $K_C(T)$, $K_P(T)$ and $K_A(T)$ (Fig. S3bc). Warming-induced smaller size at maturation of the consumer leads to markedly lower habitat productivity thresholds $K_C(T)$, $K_P(T)$ and $K_A(T)$ at higher temperatures (Fig. S3b), while all three productivity thresholds increase with warming when TSR affects only consumer asymptotic size, and the increases are less steep (Fig. S3c). Additionally, TSR affecting both maturation size and asymptotic size of the consumer leads to very similar predator invasion and extinction thresholds $K_P(T)$ and $K_A(T)$ at any given temperature, suggesting that consumer maturation size is the main driver of predator persistence in the system (Figs. 2b and S3bd).

Finally, the joint effects of temperature-dependent consumer rates and TSR in consumer maturation size and asymptotic size on the community structure (Scenario 4, Fig. 2a) are nearly identical to those of Scenario 2 (Fig. 2c). This means that the effects of temperature on community structure arise primarily through the varying consumer vital rates, and especially the somatic growth rate.

Effects of TSR and temperature-dependent rates in top predators on community structure

To disentangle the effects of TSR and temperature-dependent rates in top predators on the community structure, we compare the results of Scenarios 5–7 that consider the temperature effects on both consumer and top predator populations (Fig. 2d-f) to those of Scenarios 2–4 in which the predator rates and body size are kept constant (Fig. 2a-c). By definition, considering the temperature dependence of vital rates and TSR in the top predator has no effect on the consumer invasion threshold (dotted lines in Fig. 2) and only alters the predator invasions and extinction thresholds $K_P(T)$ and $K_A(T)$.

When temperature only affects the vital rates in the top predator, the productivity-dependent invasion and extinction thresholds of the top predator $K_P(T)$ and $K_A(T)$ are concave down along the temperature gradient, reaching their minima at the optimum temperature T_{opt} (Fig. S2e). For temperature-dependent consumer and predator rates (Scenario 5), the contribution of the temperature dependence in the top predator to the overall result depends on the system temperature. At temperatures above the optimum T_{opt}, the influence of consumer growth rates on predator invasion and extinction boundaries is stronger than the influence of the predator foraging efficiency (Figs. 2ad and S2ce). This contrasts with temperatures below the optimum ($T < T_{\mathrm{opt}}$), at which the inclusion of temperature-dependent functional response and biomass loss of the top predator leads to much higher invasion and extinction thresholds of the top predator $K_P(T)$ and $K_A(T)$, especially at temperatures near the lower limit of the thermal window of both species (Figs. 2ad). This is caused by slower consumer population growth and decrease in predation efficiency, which must be compensated by a much higher system productivity.

TSR in both consumer and the top predator leads to increasing predator invasions and extinction thresholds $K_P(T)$ and $K_A(T)$ with warming (Scenario 6, Fig. 2e), but the rate of increase is lower than the rate of decrease when TSR affects only consumers (Scenario 3, see Fig. 2b). This

is because warming-induced reduction in predation size threshold l_v, corresponding to TSR only in the top predator, leads to a smaller range of juvenile consumers vulnerable to predation that must be compensated by increased habitat productivity and hence higher predator invasion and extinction thresholds $K_P(T)$ and $K_A(T)$ with warming (Fig. S3a). Interestingly, this effect of decreased predation threshold on the predator invasion and extinction thresholds $K_P(T)$ and $K_A(T)$ is offset by the reduction in consumer size at maturation (Fig. S3e), but further enhanced by the reduction of consumer asymptotic size (Fig. S3f) with warming.

Finally, the joint effect of temperature-dependent rates and TSR in the top predator and consumer on the community structure (Scenario 7, Fig. 2f) confirms that the effects of temperature on community structure arises primarily through the varying vital rates of both consumer and the top predator. As in Scenario 5 with only temperature-dependent vital rates, the predator invasion and extinction thresholds $K_P(T)$ and $K_A(T)$ depend on both consumer and predator vital rates when temperatures are below the optimum ($T < T_{opt}$), but are primarily driven by the vital rates of the consumer when temperatures are above the optimum (compare Figs. 2f and 2c).

Effects of warming on community structure

The effects of warming on community structure depends on the initial temperature, habitat productivity and the type of temperature dependence included in the model (Fig. S1). Some of the effects are rather counterintuitive, as illustrated in an example in which both vital rates and body size of the consumer depend on temperature (Scenario 4, Fig. 2c), habitat productivity is at an intermediate level ($K = 1.3\times10^{-4}$ g.L^{-1}) and temperature increases from 5°C to 30°C (Fig. S1b). In this case, warming triggers community transitions from a system with only the resource present at low temperatures (below ~ 8°C) to a stable tri-trophic food chain at ~8–12.5°C, followed by the tri-trophic chain with alternative stable states (with the potential collapse of the top predator, e.g. if predator mortality increased or if habitat productivity decreased as in Fig. S1a) at

~12.5–23°C, a stable tri-trophic chain at ~23–25°C, and finally a collapse to the system with only the resource present at high temperatures above ~25°C (Fig. S1b).

In other cases, increasing temperatures (up to the upper thermal limit) have the same qualitative effect on the community structure as increasing habitat productivity, e.g. when all vital rates including the functional responses and body size of both the consumer and top predator depend on temperature (Scenario 7, Fig. 2f), habitat productivity is at an intermediate level ($K = 1.3\times10^{-4}$ g.L^{-1}) and temperature increases from 5°C to 30°C (Fig. S1c). In this case, the system transitions from resource-only equilibrium below ~ 7°C to a consumer-resource system at ~7–15°C, followed by the tri-trophic chain with alternative stable states at ~7–24°C and a stable tri-trophic chain at ~24–25°C and ultimately the collapse to the resource-only equilibrium at temperatures above ~25°C (Fig. S1c). This example also illustrates that the predators may require a finely tuned interplay between habitat productivity and warming to temperatures close to but below the upper limit of the thermal window to invade the system, although they may be present at substantially colder temperatures once they become established. This contrasts with the effect of increased habitat productivity: there is no upper limit on habitat productivity above which the top predator would collapse.

Discussion

Our modelling study integrates multiple responses of organisms to warming by considering the direct and indirect effects of warming on the vital rates and body sizes of different species in a size-structured tri-trophic food chain. Previous theoretical studies have shown that warming can induce regime shifts in size-structured consumer-resource dynamics (Ohlberger et al. 2011) and simplify more complex food webs (O'Gorman et al. 2019). In particular, warming may lead to extinction of the top predator in food chains (Binzer et al. 2012; Sentis et al. 2017; Lindmark et al. 2019), but also in a simple size-structured intraguild predation community (Thunell et al. 2021).

Here we show that temperature-dependent vital rates and TSRs affect community structure differently. Their effects are dominated by temperature-dependent consumer growth rates above optimal temperature and consumer growth rates and predator vital rates below optimal temperature. This suggests that TSRs in consumer and predator populations play only a minor role in community responses to warming, at least in some systems. Importantly, our results show that the population responses of top predators to warming, at least at temperatures close or above the optimum, can be determined primarily by responses at lower trophic levels. This means that interspecific interactions must be considered when predicting future species responses to warming (Ohlberger et al. 2011; Lindmark et al. 2019).

The effects of temperature and habitat productivity on community structure

We have found that the effects of temperature and habitat productivity on community structure within the consumer thermal range vary markedly depending on the underlying mechanisms captured by our Scenarios 1–7. The most important temperature-dependent process driving our results is the balance between biomass loss and gain of the top predator. The biomass gain depends crucially on the temperature-dependent biomass flux from the vulnerable juvenile consumers to the top predator, which in turn is determined by the temperature-dependent birth and growth rates of the consumers, and on the temperature dependence of the functional response parameters of the top predator. That is, our results are similar to the warming-induced loss of cultivation leading to an intraguild predator collapse at higher temperatures in an intraguild predation system (Thunell et al. 2021), although the underlying mechanisms are not identical.

If we consider temperature-dependent vital rates in the consumer but not in the top predator in our tri-trophic food chain model, this only affects the biomass gain of the top predator. In this case, the thresholds $K_P(T)$ and $K_A(T)$ of habitat productivity required for successful invasion and persistence of the top predator are highest at the optimal temperature,

where consumers grow fastest and spend the least time exposed to predation. The threshold habitat productivity required for predator invasion, $K_P(T)$, therefore decreases at temperatures further from the optimum, as the somatic growth rate of the consumers is slower, making the juvenile consumers more vulnerable to predation. On the other hand, the persistence threshold $K_A(T)$ appears to be primarily determined by the temperature dependence of the consumer ingestion rate. We hypothesise that these different relationships are due to the 'cultivation effect' of the top predators (de Roos & Persson 2002; de Roos et al. 2003): an established predator population can efficiently prey on the small juveniles and shifts the stage structure of the consumer population in favour of the adults. The density-dependent feedbacks mediated by the consumer ingestion rate and resource depletion then determine the persistence threshold of the top predator.

The inclusion of temperature-dependent vital rates in the top predator significantly changes the results at colder temperatures ($T < 15$°C), but not at temperatures around or above the optimum. We attribute the much higher thresholds of habitat productivity required for predator invasion and persistence at low temperatures to the much lower feeding rates of the top predators combined with the much lower consumer vital rates. The reduced consumer performance at high temperatures is partially compensated by increased predation rates, so that the invasion and persistence thresholds of the top predator are only slightly higher compared to the scenarios with temperature-dependent vital rates restricted to the consumer population. Given the ubiquitous effects of temperature on ectotherm individuals (Brown et al. 2004), we consider these results to be closest to what we should expect in natural tri-trophic chains with gape limited top predators (Van Leeuwen et al. 2008; Gårdmark et al. 2015).

The effect of TSR on community structure: the importance of being specific

Body sizes and body size ratios of interacting species play an important role in invasion success and persistence of top predators along temperature

and productivity gradients (de Roos & Persson 2002; Brose et al. 2012; Dijoux et al. subm.). In general, current theory predicts that populations composed of smaller individuals can withstand greater nutrient limitation and warmer temperatures before suffering from a metabolic meltdown (Binzer et al. 2012, 2016; Sentis et al. 2017; Dijoux et al. 2023). Invasion success of the top predator in a tri-trophic food chain is maximised across temperature and productivity gradients by a large size asymmetry between adjacent trophic levels, with similarly sized consumer and resource species and a large body size ratio between the top predator and intermediate consumer species (Dijoux et al. subm.). Body size may also determine competitive ability in apparent competition, which can explain the observed asymmetries in body size spectra and habitat productivity in pelagic and benthic habitats in multi-channel food webs (Rooney & McCann 2012; Dijoux & Boukal 2021). All these results suggest that TSR may play an important role in structuring communities along habitat productivity gradients (Sentis et al. 2017). Surprisingly, we found here that the effects of TSR on the structure and stability of the tri-trophic food chain with a size-structured population of the intermediate consumer are dwarfed by the temperature effects on vital rates.

Despite the limited role of TSR in the consumer and top predator for the invasion and persistence thresholds of the top predator population along temperature gradients in our tri-trophic food chain, we found that the TSR in consumer size at maturation and asymptotic size lead to qualitatively different temperature dependencies of minimum resource requirements for the consumer population. Fewer resources are required to maintain the consumer population when individuals mature at smaller sizes under warming while growing to the same asymptotic size. The opposite outcome is observed when their asymptotic size, but not maturation size, decreases with temperature. We attribute these differences to changes in the juvenile-to-adult biomass ratio, which alters the strength of density dependence in the consumer population (de Roos & Persson 2013).

We also showed that the habitat productivity thresholds for invasion and persistence of the top predator depend on TSR in both consumers and the top predator. The invasion and persistence thresholds always decrease with

warming when the predator size, and thus the predation vulnerability window of the consumer, is constant, while the consumer maturation size decreases with warming. We explain this result by a reduced delay in maturation of invulnerable juvenile consumers, which leads to a faster turnover of the consumer population and thus to better feeding conditions for the top predator (de Roos & Persson 2002).

On the other hand, invasion and persistence thresholds of the top predator in our model always increase with warming when TSR occurs in the predator or when TSR results in lower asymptotic size, but not size at maturation, in the consumer. In both cases, the biomass of vulnerable juvenile consumers decreases with warming because a smaller size range of consumers becomes vulnerable to predation or because the consumer birth rate decreases as adult consumers do not grow as large at higher temperatures. Finally, a concurrent TSR in the top predator and consumer maturation size has a negligible effect on invasion and persistence thresholds, as the effects of the reduced predation vulnerability window on the intake rate of the top predator are almost entirely offset by the reduced delay in maturation of invulnerable juvenile consumers.

These results complement previous findings by Sentis et al. (2017), who showed that the effects of TSRs on the persistence and stability of a simple tri-trophic food chain vary predictably with the direction and magnitude of the TSR and with the trophic level of the species exhibiting the TSR. Our results extend them further, as Sentis et al. (2017) used only a biomass-based model that did not account for stage-dependent interactions and size-dependent predation risk among the intermediate consumers. Although we only considered one type of TSR relationship, namely declining body size with warming with the average TSR slope for aquatic ectotherms, our results highlight another new and important aspect. TSR is usually defined for size at maturation (Atkinson 1994), but a similar relationship could be envisaged for asymptotic size, which can be much larger than size at maturation in many taxa with indeterminate growth, such as most fish (McDowall 1994). The relationship between TSRs in size at maturation and in asymptotic size is driven by the temperature dependence of reproductive investment, which itself can be optimised in response to

different temperatures (Thunell et al. 2022), suggesting that the magnitude of these two TSR responses may differ. Since we have examined both extremes where one of the sizes does not depend on temperature, any realistic responses are likely to lie between the three possibilities we have covered (Fig. S3bcd).

The effects of warming on catastrophic collapses of top predators

Tri-trophic food chains, intraguild predation modules and multi-channel food webs with size-dependent mortality and resource dependent consumer growth are characterised by their propensity for emergent Allee effects. That is, a small change in the environmental conditions can lead to a catastrophic collapse in the predator population associated with abrupt changes in its prey size structure (de Roos & Persson 2002; Thunell et al. 2021) or to a collapse of an intermediate consumer population after a successful invasion of the top predator in a multi-channel food web (Dijoux & Boukal 2021). These abrupt collapses have been associated with decreasing habitat productivity (de Roos & Persson 2002; Dijoux & Boukal 2021) and increasing predator mortality (de Roos & Persson 2002) and increasing temperature (Lindmark et al. 2019; Thunell et al. 2021).
Our results provide new insights in the propensity of tri-trophic chains for emergent Allee effects and catastrophic collapses of the top predators. We show that the hysteresis, i.e. the difference between habitat productivity thresholds separating the invasion and persistence thresholds of the top predator, is largest at the optimum temperatures and always decreases away from the optimum. The propensity for catastrophic collapses will therefore increase with future warming if the initial temperature is well below the optimum, but it will decrease as the temperature approaches the upper thermal limit of the consumers and predators, as in Uszko et al. (2017), Lindmark et al. (2019), and Thunell et al. (2021). In addition, our results confirm that warming may destabilise the community by triggering the bistability as in Lindmark et al. (2019) and similar to Thunell et al. (2021). This outcome is most common when both consumer and predator vital rates depend on temperature. However, warming may also have the opposite effect and stabilise the dynamics when only the consumer vital

rates depend on temperature. The latter outcome is unexpected and occurs only very rarely in our results when both consumer and predator vital rates depend on temperature (e.g. in Fig. S4a). However, it becomes more common when only the consumer vital rates depend on temperature.

Conclusions

Body size and temperature are two universal currencies that determine many ecological processes from individuals to entire communities (Brown *et al.* 2004). Using a tri-trophic food chain with temperature- and size-dependent interactions, we show that a detailed understanding of the temperature and size dependence of vital rates and life histories is needed to better predict future community responses to global change, including the propensity for catastrophic collapses of the top predators. Most importantly, we found that the direct and indirect effects of warming on species and species interactions can have very different consequences for community structure. Our results also suggest that warming can either increase or decrease the propensity of top predator populations to abrupt collapses. Surprisingly, we found limited evidence for the importance of the temperature-size rule on community structure and stability. Our results point to promising avenues for future research, such as the development of more mechanistic models that examine the role of temperature and size dependence of life histories (Ohlberger et al. 2011) across multiple taxa and trophic levels, including e.g. asymmetric thermal responses in interacting populations (Dell et al. 2014), in community responses to warming.

References

Angert, A.L., Sheth, S.N. & Paul, J.R. (2011). Incorporating population-level variation in thermal performance into predictions of geographic range shifts. *Integr Comp Biol*, 51, 733–750.

Angilletta Jr., M.J. (2009). *Thermal Adaptation: A Theoretical and Empirical Synthesis*. Oxford University Press.

Atkinson, D. (1994). Temperature and Organism Size-A Biological Law for Ectotherms? *Adv Ecol Res*, 25, 1–58.

Binzer, A., Guill, C., Brose, U. & Rall, B.C. (2012). The dynamics of food chains under climate change and nutrient enrichment. *Philos T Roy Soc B*, 367, 2935–2944.

Binzer, A., Guill, C., Rall, B.C. & Brose, U. (2016). Interactive effects of warming, eutrophication and size structure: Impacts on biodiversity and food-web structure. *Glob Chang Biol*, 22, 220–227.

Boukal, D.S., Bideault, A., Carreira, B.M. & Sentis, A. (2019). Species interactions under climate change: connecting kinetic effects of temperature on individuals to community dynamics. *Curr Opin Insect Sci*, 35, 88–95.

Brose, U., Dunne, J.A., Montoya, J.M., Petchey, O.L., Schneider, F.D. & Jacob, U. (2012). Climate change in size-structured ecosystems. *Philos T Roy Soc B*, 367, 2903–2912.

Brown, J.H., Gillooly, J.F., Allen, A.P., Savage, V.M. & West, G.B. (2004). Toward a Metabolic Theory of Ecology. *Ecology*, 85, 1771–1789.

Daufresne, M., Lengfellner, K. & Sommer, U. (2009). Global warming benefits the small in aquatic ecosystems. *P Natl Acad Sci USA*, 106, 12788–93.

Dell, A.I., Pawar, S. & Savage, V.M. (2014). Temperature dependence of trophic interactions are driven by asymmetry of species responses and foraging strategy. *J Anim Ecol*, 83, 70–84.

Dijoux, S. & Boukal, D.S. (2021). Community structure and collapses in multichannel food webs: Role of consumer body sizes and mesohabitat productivities. *Ecol Lett*, 24, 1607–1618.

Dijoux, S., Pichon, N.A., Sentis, A. & Boukal, D.S. (2023). Body size and trophic position determine the outcomes of species invasions along temperature and productivity gradients. *Authorea*.

Forster, J., Hirst, A.G. & Atkinson, D. (2012). Warming-induced reductions in body size are greater in aquatic than terrestrial species. *P Natl Acad Sci USA*, 109, 19310–14.

Fretwell, S.D. (1987). Food chain dynamics: the central theory of ecology? *Oikos*, 50, 291–301.

Fussmann, K.E., Schwarzmüller, F., Brose, U., Jousset, A. & Rall, B.C. (2014). Ecological stability in response to warming. *Nat Clim Chang*, 4, 206–210.

Gårdmark, A., Casini, M., Huss, M., van Leeuwen, A., Hjelm, J., Persson, L., *et al.* (2015). Regime shifts in exploited marine food webs: Detecting mechanisms underlying alternative stable states using size-structured community dynamics theory. *Philos T Roy Soc B*, 370, 1–10.

Gårdmark, A. & Huss, M. (2020). Individual variation and interactions explain food web responses to global warming: Emergent warming effects on food webs. *Philos T Roy Soc B*, 375.

Gardner, J.L., Peters, A., Kearney, M.R., Joseph, L. & Heinsohn, R. (2011). Declining body size: A third universal response to warming? *Trends Ecol Evol*, 26 (6), 285–291.

Huey, R.B. & Kingsolver, J.G. (1989). Evolution of thermal sensitivity of ectotherm performance. *Trends Ecol Evol*, 4, 131–135.

IPBES. (2019). *Global assessment report of the Intergovernmental Science-Policy Platform on Biodiversity and Ecosystem Services*. E. S. Brondizio, J. Settele, S. Díaz, and H. T. Ngo (editors)

IPCC. (2022). *Climate Change 2022: Impacts, Adaptation and Vulnerability. Contribution of Working Group II to the Sixth Assessment Report of the Intergovernmental Panel on Climate Change*. Cambridge University Press.

Kearney, M. & Porter, W.P. (2006). Ecologists have already started rebuilding community ecology from functional traits. *Trends Ecol Evol*, 21, 481–482.

Kingsolver, J.G. & Huey, R.B. (2008). Size, temperature, and fitness: three rules. *Evol Ecol Res*, 10, 251–268.

Van Leeuwen, A., De Roos, A.M. & Persson, L. (2008). How cod shapes its world. *J Sea Res*, 60, 89–104.

Lindmark, M., Huss, M., Ohlberger, J. & Gårdmark, A. (2018). Temperature-dependent body size effects determine population responses to climate warming. *Ecol Lett*, 21, 181–189.

Lindmark, M., Ohlberger, J., Huss, M. & Gårdmark, A. (2019). Size-based ecological interactions drive food web responses to climate warming. *Ecol Lett*, 22, 778–786.

Mallet, J.P., Charles, S., Persat, H. & Auger, P. (1999). Growth modelling in accordance with daily water temperature in European grayling (Thymallus thymallus L.). *Can J Fish Aquat Sci*, 56, 994–1000.

McDowall, R.M. (1994). On size and growth in freshwater fish. *Ecol Freshw Fish*, 3, 67–79.

McLellan, R., Iyengar, L., Jeffries, B. & Oerlemans Natasja. (2014). *Living Planet Report 2014: Species and spaces, people and places*. WWF International.

O'Gorman, E.J., Petchey, O.L., Faulkner, K.J., Gallo, B., Gordon, T.A.C., Neto-Cerejeira, J., *et al.* (2019). A simple model predicts how warming simplifies wild food webs. *Nat Clim Chang*.

Ohlberger, J., Edeline, E., Vøllestad, L.A., Stenseth, N.C. & Claessen, D. (2011). Temperature-driven regime shifts in the dynamics of size-structured populations. *Am Nat*, 177, 211–223.

Oksanen, L., Fretwell, S.D., Arruda, J., Niemela, P. & Niemelä, P. (1981). Exploitation ecosystems in gradients of primary productivity. *Am Nat*, 118, 240–261.

Parmesan, C. & Yohe, G. (2003). A globally coherent fingerprint of climate change impacts across natural systems. *Nature*, 421, 37–42.

Rall, B.C., Vucic-Pestic, O., Ehnes, R.B., EmmersoN, M. & Brose, U. (2010). Temperature, predator-prey interaction strength and population stability. *Glob Chang Biol*, 16, 2145–2157.

Rooney, N. & McCann, K.S. (2012). Integrating food web diversity, structure and stability. *Trends Ecol Evol*, 27, 40–45.

de Roos, A.M. (2021). PSPManalysis: Steady-state and bifurcation analysis of physiologically structured population models. *Methods Ecol Evol*, 12, 383–390.

de Roos, A.M. & Persson, L. (2002). Size-dependent life-history traits promote catastrophic collapses of top predators. *P Natl Acad Sci USA*, 99, 12907–12912.

de Roos, A.M. & Persson, L. (2013). *Population and Community Ecology of Ontogenetic Development*. Princeton University Press.

de Roos, A.M., Persson, L. & McCauley, E. (2003). The influence of size-dependent life-history traits on the structure and dynamics of populations and communities. *Ecol Lett*, 6, 473–487.

Sala, O.E., Chapin, F.S., Armesto, J.J., Berlow, E., Bloomfield, J., Dirzo, R., *et al.* (2000). Global Biodiversity Scenarios for the Year 2100. *Science (1979)*, 287, 1770–1774.

Scheffer, M., Carpenter, S., Foley, J.A., Folke, C. & Walker, B. (2001). Catastrophic shifts in ecosystems. *Nature*, 413, 591–596.

Schulte, P.M., Healy, T.M. & Fangue, N.A. (2011). Thermal performance curves, phenotypic plasticity, and the time scales of temperature exposure. *Integr Comp Biol*, 51, 691–702.

Sentis, A., Binzer, A. & Boukal, D.S. (2017). Temperature-size responses alter food chain persistence across environmental gradients. *Ecol Lett*, 20, 852–862.

Smalås, A., Strøm, J.F., Amundsen, P.A., Dieckmann, U. & Primicerio, R. (2020). Climate warming is predicted to enhance the negative effects of harvesting on high-latitude lake fish. *J Appl Ecol*, 57, 270–282.

Sunday, J.M., Bates, A.E. & Dulvy, N.K. (2012). Thermal tolerance and the global redistribution of animals. *Nat Clim Chang*, 2, 686–690.

Thunell, V., Gårdmark, A., Huss, M. & Vindenes, Y. (2022). Optimal energy allocation trade-off driven by size-dependent physiological and demographic responses to warming. *Ecology*, 104 (4): e3967.

Thunell, V., Lindmark, M., Huss, M. & Gårdmark, A. (2021). Effects of warming on intraguild predator communities with ontogenetic diet shifts. *Am Nat*, 198, 706–718.

Uszko, W., Diehl, S., Englund, G. & Amarasekare, P. (2017). Effects of warming on predator-prey interactions - A resource-based approach and a theoretical synthesis. *Ecol Lett*, 20, 513–523.

Vasseur, D.A. & McCann, K.S. (2005). A mechanistic approach for modeling temperature dependent consumer resource dynamics. *Am Nat*, 166, 184–198.

Verberk, W.C.E.P., Atkinson, D., Hoefnagel, K.N., Hirst, A.G., Horne, C.R. & Siepel, H. (2021). Shrinking body sizes in response to warming: explanations for the temperature–size rule with special emphasis on the role of oxygen. *Biol Rev*, 96, 247–268.

Wootton, H.F., Morrongiello, J.R., Schmitt, T. & Audzijonyte, A. (2022). Smaller adult fish size in warmer water is not explained by elevated metabolism. *Ecol Lett*, 25, 1177–1188.

Yodzis, P. & Innes, S. (1992). Body Size and Consumer-Resource Dynamics. *Am Nat*, 139, 1151–1175.

Young, H.S., McCauley, D.J., Galetti, M. & Dirzo, R. (2016). Patterns, Causes, and Consequences of Anthropocene Defaunation. *Annu Rev Ecol Evol S*, 47, 333–358.

Yvon-Durocher, G., Montoya, J.M., Trimmer, M. & Woodward, G. (2011). Warming alters the size spectrum and shifts the distribution of biomass in freshwater ecosystems. *Glob Chang Biol*, 17, 1681–1694.

Figure legends

Fig. 1. Temperature dependence of consumer sizes (a) and vital rates (b) and overview of the size-structured tri-trophic chain (c). (a) TSR in consumers can affect their vulnerability to predation (l_v, dotted line), size at maturation (l_{mat}, dashed line) and maximum size (l_∞, solid line). (b) Temperature dependent vital rates of consumers; T_{min} and T_{max} refer to the lower and upper limit of the thermal range, while T_{opt} denotes the optimal temperature. (c) Summary of the main processes driving the tri-trophic chain dynamics; orange arrows indicate possible size reductions under warming that influence consumer life history.

Fig. 2. Effects of TSR and temperature-dependent vital rates on the community structure along habitat productivity and temperature gradients. Each panel shows different scenario: (a, d) temperature-dependent rates only (Scenarios 2 and 5), (b, e) TSR only (Scenarios 3 and 6), (c, f) TSR and temperature-dependent rates (Scenarios 4 and 7) in either (a-c) consumer traits only, or in (d-f) both consumer and predator traits. TSR implemented in consumer maturation size l_{mat} and maximum size l_∞ (b, c), and in l_{mat}, l_∞ and maximum size l_v exposed to predation (e, f). Temperature-dependent rates include consumer growth, ingestion and birth rates (a, c) and consumer growth, ingestion and birth rates and predator functional response and metabolic loss rate (d, f). Colours refer to the community structure: resource-only equilibrium (light green), consumer-resource equilibrium (CR, ochre), trophic chain equilibrium (PCR, dark red), and alternative stable state (PCR/CR, orange). Dotted lines = consumer invasion threshold; solid line = top predator invasion threshold; dashed line = predator persistence threshold. T_{opt} = optimum temperature of consumer and predator traits.

Figures

Fig. 1

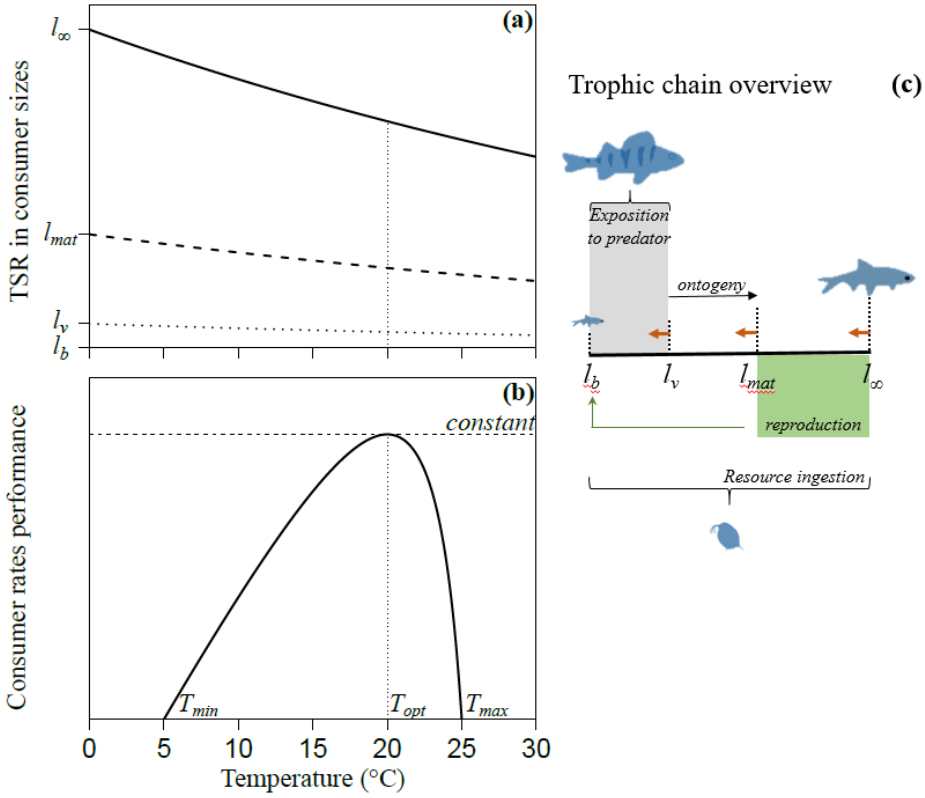

Fig. 2.

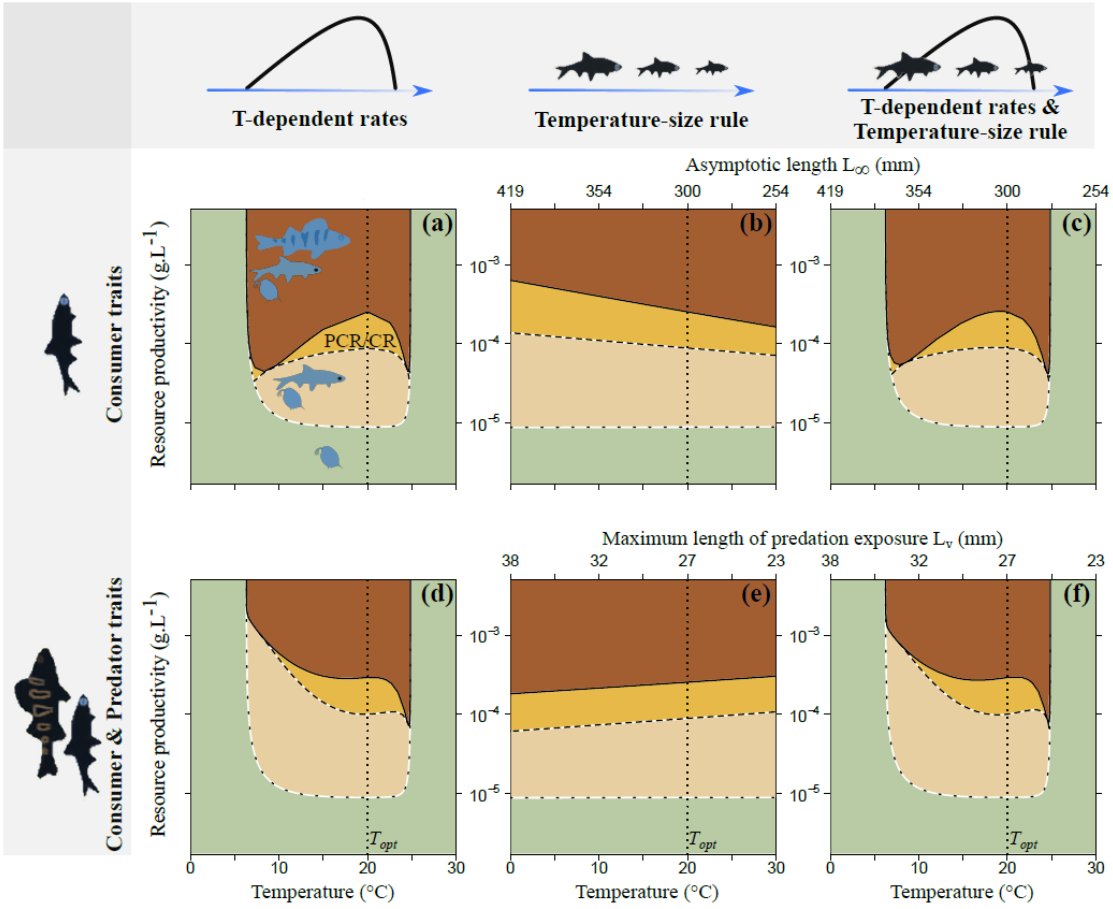
T-dependent rates
Temperature-size rule
T-dependent rates & Temperature-size rule
Asymptotic length L_∞ (mm)
419
354
300
254
Consumer traits
Resource productivity (g.L^{-1})
(a)
(b)
(c)
PCR
CR
10^{-3}
10^{-4}
10^{-5}
Maximum length of predation exposure L_v (mm)
38
32
27
23
Consumer & Predator traits
(d)
(e)
(f)
T_{opt}
0
10
20
30
Temperature (°C)

Supplementary information for

Temperature-dependent consumer growth rates, rather than temperature-size rule, determine the propensity for catastrophic collapses of top predators

Authors: Samuel Dijoux[1,2,*], Aslak Smalås[3,4], Raul Primicerio[3], David S. Boukal[1,2]

[1.] Department of Ecosystems Biology, Faculty of Science, University of South Bohemia. Branišovská 1760, 370 05 České Budějovice, Czech Republic.

[2.] Czech Academy of Sciences, Biology Centre, Institute of Entomology, Branišovská 31, 370 05 České Budějovice, Czech Republic.

[3.] Department of Arctic and Marine Biology, Faculty of Bioscience, Fisheries and Economy, UiT, The Arctic University of Norway, Breivikia, Tromsø, Norway.

[4.]SNA-Skandinavisk naturoveråking AS (Scandinavian Nature-monitoring), Åkerblå Group, Tromsø, Norway.

[*]E-mail addresses: dijous00@prf.jcu.cz (S. Dijoux); dboukal@prf.jcu.cz (D. S. Boukal).

This supplementary material contains the following texts, tables and figures:

Text S1. Dynamic energy budget model of consumer life history

Table S1. Individual state and population-level variables

Table S2. Model parameters

Table S3. Equations of temperature-independent and temperature-dependent consumer and predator traits and vital rates

Table S4. Equations of state dynamics

Fig. S1. Community transitions in the trophic chain along habitat productivity gradient and temperature gradient.

Fig. S2. Influence of TSR on community structure along gradients of temperature and habitat productivity

Fig. S3. Influence of temperature-dependent vital rates on community structure along gradients of temperature and habitat productivity

Fig. S4. Influence of TSR and temperature-dependent vital rates in community structure along gradients of temperature and habitat productivity when all but one model component change

Text S1. Dynamic energy budget model of consumer life history

We use the same dynamic energy budget (DEB) model as in (de Roos & Persson 2002, Dijoux and Boukal 2021) to describe how individual size- and resource-dependent growth and reproduction vary with temperature. This so-called Kooijman-Metz model is a widely used DEB model that falls in the category of net production models, in which the ingested energy is first used to cover maintenance, a fixed fraction of the remainder is used for maturation and reproduction, and the rest for somatic growth (de Roos *et al.* 1990; Noonburg *et al.* 1998; Smallegange *et al.* 2017).

Individual consumers are born at length l_b, exposed to predation until reaching length l_v, mature when reaching length l_{mat}, and can reach the maximum length l_∞ under unlimited food conditions. Consumer life histories are characterized by size-, resource- and temperature-dependent feeding rate, growth rate and fecundity rate and size-, predator- and temperature-dependent mortality rate (Table S3). The rate of energy acquisition is assumed proportional to body surface ($\sim l^2$), while maintenance is proportional to body weight ($\sim l^3$). That is, ingestion rates $I(l, R, T)$ of individual consumers with length l feeding on the respective basal resource R follow a type II functional response (Eqs. S2 and S10). Given that maintenance increases faster with body size than the ingestion, consumer individuals follow a von Bertalanffy growth curve with resource- and temperature-dependent growth rate and asymptotic size $G(l, R, T)$ (Eqs. S3 and S11). They produce offspring after maturation at a *per capita* rate $b(l, R, T)$ that is proportional to l^2 (Eqs. S4 and S12). For simplicity, we assume that the individuals stop growing and reproducing but do not shrink or use energy reserves to cover maintenance costs when the food intake becomes insufficient (see (de Roos *et al.* 1990) for details). In addition to predation mortality, individual consumers die with the same size-independent background mortality rate μ_b (Eqs. S6 and S14). Top predators feed indiscriminately on vulnerable juvenile consumer individuals when present, following a Holling type II functional response f (Eqs. S7 and S15), and may face an additional temperature- and size-dependent metabolic mass loss in addition to constant background

mortality (Eqs. S8 and S16). We assume constant conversion efficiency ϵ of ingested prey biomass to predator biomass.

Table S1. Individual state and population-level variables

Variable	Symbol	Unit
Consumer length	l	mm
Population density of consumers	c	$mm^{-1}.L^{-1}$
Resource biomass	R	$g.L^{-1}$
Top predator biomass	P	$g.L^{-1}$

Table S2. Model parameters

Subject	Description	Symbol	Default value	Unit
Environment	Temperature	T	20	°C
	Normalisation temperature (=equal to 20°C)	T_{20}	293.15	K
	Converting factor from Celsius to Kelvin	T_0	273.15	K
	Boltzmann constant	k	8.617×10^{-5}	$eV.K^{-1}$
Resource	Carrying capacity	K_R	5×10^{-4}	$g.L^{-1}$
	Renewal rate	ρ	0.1	day^{-1}
Consumer	Length-weight allometric coefficient	a	9×10^{-6}	$g.mm^{-3}$
	Length-weight allometric exponent	b	3	-
	Length at birth	l_b	7	mm
	Predation vulnerability threshold	l_v	27	mm
	Length at maturation	l_{mat}	110	mm
	Asymptotic length	l_∞	300	mm
	Ingestion rate coefficient	I_{max}	10^{-4}	$g.day^{-1}.mm^{-2}$

	Half-saturation constant	R_h	1.5×10^{-5}	$g.L^{-1}$
	von Bertalanffy growth rate	G_{max}	6×10^{3}	day^{-1}
	Birth rate coefficient	B_{max}	3×10^{3}	$day^{-1}.mm^{-2}$
	Background mortality rate	μ_b	0.01	day^{-1}
Predator	Body length	L_P	200	mm
	Attack rate	A_P	5000	$L.day^{-1}$
	Handling time	H_P	0.1	$day.g^{-1}$
	Food conversion efficiency	ϵ	0.5	-
	Biomass loss rate	δ_P	0.01	day^{-1}
	Intercept of metabolic loss rate	I_δ	-16.54	-
	Allometric exponent of metabolic loss rate	S_δ	-0.31	-
	Activation energy of metabolic loss	E_δ	-0.69	$eV.K^{-1}$
Consumer / predator	Lower temperature threshold for vital rates	T_{min}	5	°C
	Optimal temperature for vital rates	T_{opt}	20	°C
	Upper temperature threshold for vital rates	T_{max}	25	°C
	TSR slope	β	-0.05	$(°C)^{-1}$

Table S3. Equations of temperature-independent and temperature-dependent consumer and predator traits and vital rates. Temperature-dependent and temperature-independent variants of the same parameter or rate always in the same row.

Population	Subject	Temperature independent	Eq.	Temperature dependent	Eq.
Consumer	Size threshold $l_i(T)$ (i = v, mat, ∞ or P)	$l_i(T) = l_i$	(S1)	$l_i(T) = l_i e^{\frac{\beta(T-T_{opt})}{b}}$	(S9)
	Feeding rate $I(l,R,T)$	$I(l,R,T) = I_{max}\, l^2 \frac{R}{R_h+R}$	(S2)	$I(l,R,T) = I(T)\, l^2 \frac{R}{R_h+R}$	(S10)
	Somatic growth rate $g(l,R,T)$	$g(l,R,T) = G_{max}\left(l_\infty \frac{R}{R_h+R} - l\right)$	(S3)	$g(l,R,T) = G(T)\left(l_\infty \frac{R}{R_h+R} - l\right)$	(S11)
	Per-capita birth rate $b(l,R,T)$	$b(l,R,T) = \begin{cases} 0 & \text{if } l \le l_{mat} \\ B_{max} \frac{R\, l^2}{R_h+R} & \text{if } l > l_{mat} \end{cases}$	(S4)	$b(l,R,T) = \begin{cases} 0 & \text{if } l \le l_{mat} \\ B(T) \frac{R\, l^2}{R_h+R} & \text{if } l > l_{mat} \end{cases}$	(S12)
	Proportionality constants $\Phi(T)$ (Φ = I, B or G)	$\Phi(T) = \Phi_{max}$	(S5)	$\Phi(T) = \Phi_{max} \frac{(T-T_{min})(T-T_{max})}{(T-T_{min})(T-T_{max}) - (T-T_{opt})^2}$	(S13)
	Mortality rate $\mu(l,C_v,P,T)$	$\mu(l,C_v,P,T) = \begin{cases} \mu_b + f(C_v)P & \text{if } l \le l_v \\ \mu_b & \text{if } l > l_v \end{cases}$	(S6)	$\mu(l,C_v,P,T) = \begin{cases} \mu_b + f(C_v,T)P & \text{if } l \le l_v \\ \mu_b & \text{if } l > l_v \end{cases}$	(S14)
Predator	Functional response $f(C_v,T)$	$f(C_v,T) = \frac{A_P}{1 + A_P H_P C_v}$	(S7)	$f(C_v,T) = \frac{A_P(T)}{1+A_P(T)H_P(T)C_v}$ with $A_P(T) = A_P \frac{(T-T_{opt})^2}{2(T_{max}-T_{min})}$, $H_P(T) = H_P \frac{(T-T_{opt})^2}{4(T_{max}-T_{min})^2}$	(S15)
	Biomass loss rate $\delta(T,L_P)$	$\delta(T,L_P) = \delta_P$	(S8)	$\delta(T,L_P) = \delta_P + e^{I_\delta} \left(a\, L_P^b\right)^{S_\delta} e^{E_\delta \frac{T_{opt}-T}{k\,T\,T_{opt}}}$	(S16)

Table S4. Equations of state dynamics

Subject	Equation	Equation no.
Resource dynamics	$\frac{dR}{dt} = \rho(K_R - R) - \int_{l_b}^{l_\infty} I(l,R,T)c(t,l)dl$	(S17)
Population-level consumer birth rate	$B(t,R,T) = \int_{l_{mat}}^{l_\infty} b(l,R,T)c(t,l)dl$	(S18)
Consumer size structure balance equation	$\frac{\partial c(t,l)}{\partial t} + \frac{\partial g(\,l,R,T)c(t,l)}{\partial l} = -\mu(l,C_v,P,T)c(t,l)$	(S19)
Biomass of vulnerable consumers	$C_v = \int_{l_b}^{l_v} a l^b c(t,l)dl$	(S20)
Predator biomass dynamics	$\frac{dP}{dt} = \big(\epsilon\, f(C_v,T)C_v - \delta(T,L_P)\big)P$	(S21)

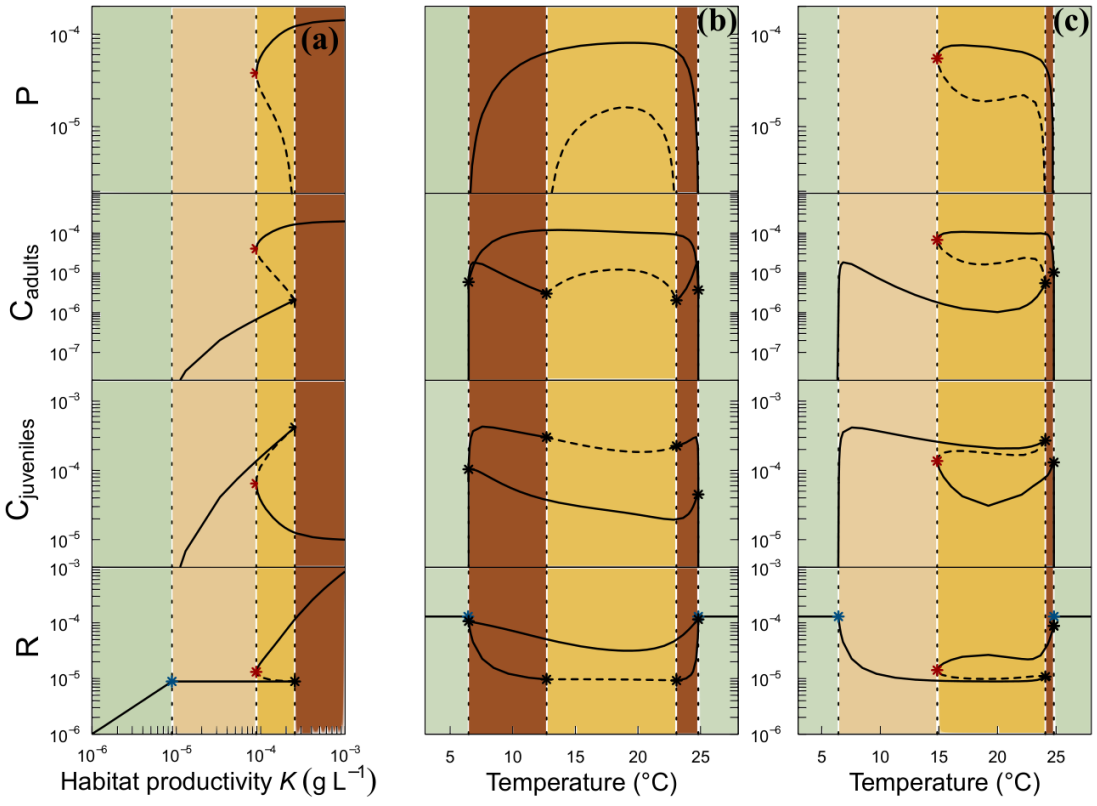

Fig. S1. Community transitions in the trophic chain along gradients of habitat productivity and temperature. (a) Transitions observed in Fig. 2 at the optimal temperature (T = 20°C) in all scenarios, (b and c) transitions at constant habitat productivity (K = 1.3 10^{-4} g.L^{-1}) with temperature-dependent rates and TSR in consumers (b, Scenario 4) and in consumers and predators (c, Scenario 7). Solid lines = stable equilibria, dashed lines = unstable equilibria, dotted vertical lines = threshold resource productivities (a) and temperatures (b-c). Colours as in Fig. 2.

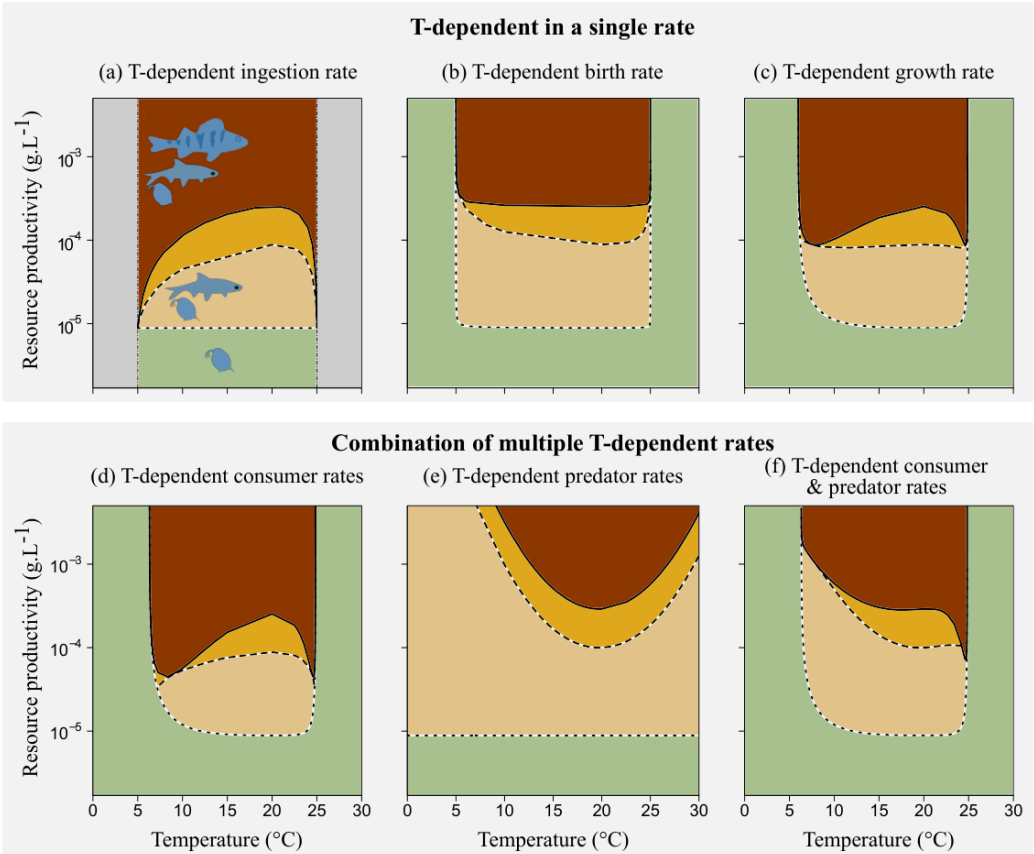

Fig. S2. Effects of temperature-dependent rates on community structure along gradients of temperature and habitat productivity. Temperature dependence limited to (a-c) one rate, (d-e) multiple rates or (f) all rates simultaneously. Legend as in Fig 2.

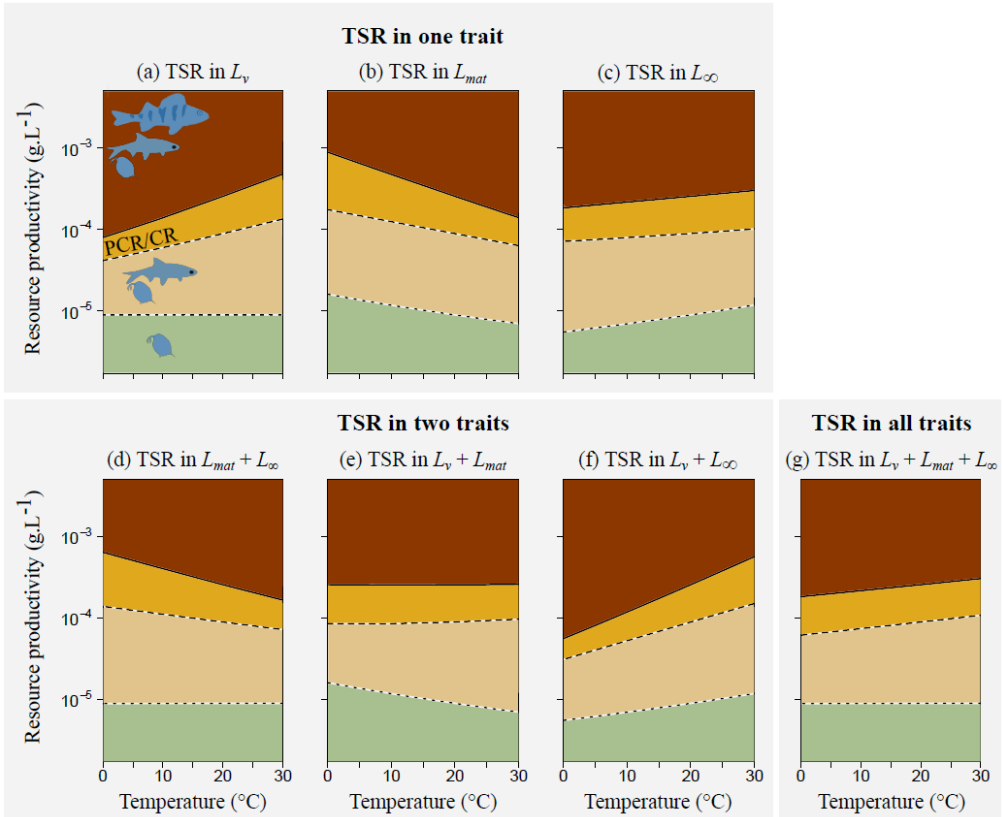

Fig. S3. Effect of TSR on community structure along gradients of temperature and habitat productivity. TSR affects (a-c) one measure of body size, (d-f) two measures of body size, or (g) all three measures of body size. Colours, line types and community structure as in Fig. 2.

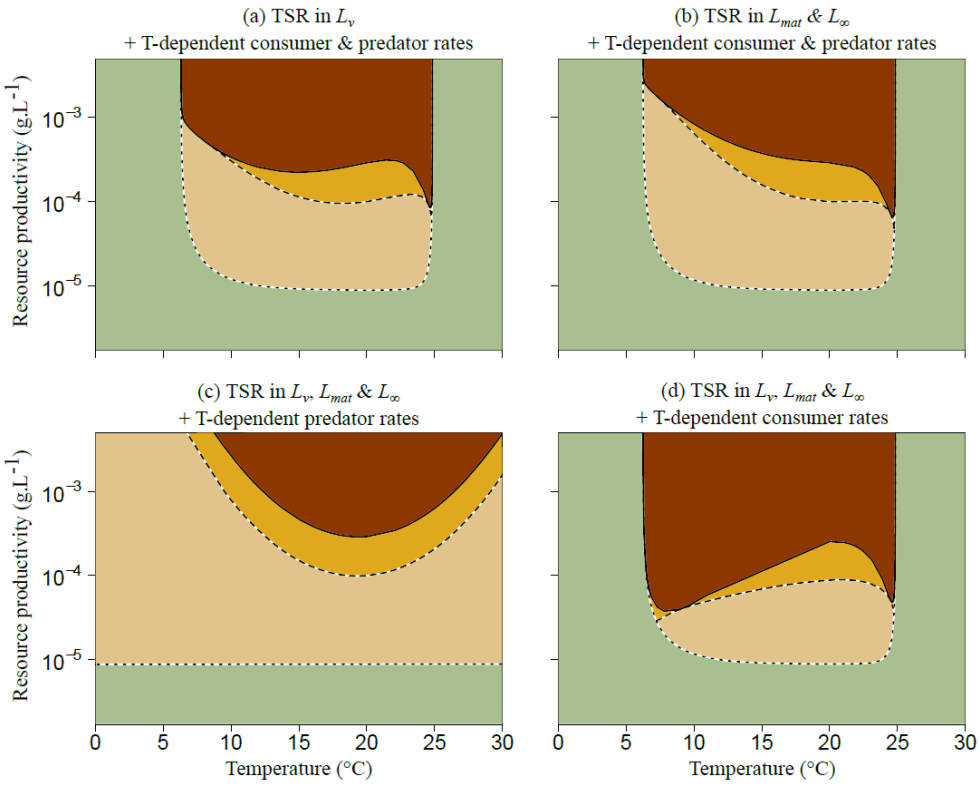

Fig. S4. Combined effects of TSR and temperature-dependent rates in community structure along gradients of temperature and habitat productivity. TSR affects all consumer and predator sizes and rates except one. Exclusion of: (a) consumer TSR (l_{mat} and l_∞); (b) top predator TSR (through l_v); (c) temperature-dependent consumer rates; (d) temperature-dependent predator rates. Legend as in Fig. 2.

~Summary~

~ Summary ~

Environmental stressors influence the structure and stability of size-structured communities in freshwaters through direct and indirect interactions ranging from individual physiology to the community scale. This thesis aimed to explore how communities respond to environmental drivers by accounting for species traits (body size, trophic position, life histories, and species thermal niche) and responses to abiotic drivers at the community scale. I used bioenergetic and physiologically structured population models to explain empirically observed phenomena and to provide tools that can be used by theoreticians, empiricists, and field ecologists to link individual-level responses to global patterns observed at community scale.

Chapter I dealt with how communities respond to species invasions under the joint influence of warming and nutrient enrichment. Using bioenergetic models accounting for the interactions between temperature, nutrients, and body mass at species levels, this study synthesized all interactions formed between resident and invading species and provides robust predictions on how future invasions will affect communities subjected to abiotic drivers. Using well-known rules of species coexistence and exclusion, I showed how body size and trophic position determine the fate of species invasions. Notably, I predict that smaller species will be the most likely to succeed and invade communities in warmer, nutrient-limited environments, while large predators will be more likely to succeed in cold and nutrient enriched systems. At the community scale, the synthesis of the changes induced by invading species on community structure and stability enabled me to test the diversity-stability relationship, to explore the conditions in which invading species lead to negative, neutral, or positive changes in the community, and to understand whether these changes were mitigating or amplifying the actions of abiotic drivers. I demonstrated that while invasions (of small competing consumers) could magnify the destabilizing actions of nutrient enrichment on the community, other invasions could either mitigate nutrient enrichment directly through a rescue effect or by

dampening population oscillations, or act indirectly through niche occupancy, which helps restore the loss in ecosystem functions due to species extinctions.

Chapters II and III dealt with the structure and dynamics of size-structured communities along environmental gradients. They accounted for species life histories and the feedback effects between community and individual responses. **Chapter II** focused on the joint effect of mesohabitat productivities and consumer body size on the structure of multichannel food webs. It showed that asymmetries in consumer sizes and mesohabitat productivities can explain patterns of ecosystem stability that were previously observed in empirical studies but their mechanisms were not fully understood. I demonstrate that the stability of freshwater communities relies on the compensation effect of both types of asymmetries, with small pelagic consumer inhabiting more productive systems compared to larger benthic consumer living off more limited resources. In the absence of such compensation effects, the interaction between these asymmetries leads to a sudden collapse of the top predator or the less resilient intermediate species. This enabled me to identify new, previously unknown types of emergent Allee effects, such as the *cascading emergent Allee effect* that involves a simultaneous collapse of several species in the community. This study also highlights that the rising pressure on freshwater habitats can lead to previously unexpected disruptions of food webs including the energy pathways between mesohabitats, with potentially severe consequences for freshwater ecosystems.

Chapter III extended some of the findings in Chapter II in the trophic chain and dealt with the direct and indirect influences of temperature on a tri-trophic chain. By exploring multiple scenarios accounting for temperature-induced size reductions in consumers and predators and temperature-dependent species performance, I showed that different types of species responses to warming lead to different community structure at a larger scale. However, when these different responses are considered together, the resulting community structure is primarily driven by temperature-dependent consumer growth and ingestion rates and to some

extent also predator foraging efficiency. This highlights that community-level responses to abiotic drivers are not a simple sum of species-level responses, and that species-level responses may be dominated by one process. I also observed that, while the emergent Allee effect in the predator is driven by food dependency, temperature can alter species performance and prevent the emergent Allee effect when the species operate further away from their thermal optimum. My findings imply that warming alone can trigger or prevent catastrophic collapses of the top predator, thereby adding another previously overlooked phenomenon to the long list of potential consequences of climate change on freshwater ecosystems.

Take-home messages and future directions

Overall, my research in this thesis aimed to demonstrate the importance of considering species traits (body size, performance of vital rates, trophic position, diet) and life histories to investigate the influences of environmental changes on species responses and their feedback actions on the environment. Accounting for species traits can improve our prediction of the future effects of climate change across ecosystems and to develop appropriate conservation measures. Predictions from trophic modules can be useful for empiricists as they simplify redundant species interactions observed at the large community scale. This thesis also highlights that known principle of species coexistence and exclusion in food webs (e.g.., R* and P* rules, cascading effect) determine community responses to environmental changes and species invasions (Chapter I).

Accounting for species physiology in models (through physiologically structured population models) notably enlarges our perceptions of food webs from a network of constant interacting species into something more variable and dynamic. Classical views of food webs consider species interactions as constant. However, individuals of the same species perceive the environment very differently as they grow. They can escape predation pressure by reaching a non-vulnerable size (as in Chapters II and III) or by shifting to a new habitat (through ontogenetic niche shift). Other trophic interactions (exploitative and apparent competition, omnivory) also depend on species traits and habitat use.

Exploring the consequences of habitat linkage through ontogenetic niche shifts and predator mobility offers interesting avenues for future research to investigate the different impacts of species invasions, temperature, and nutrient availability in multichannel food webs. Given the common phenomenon of thermal stratification in many standing waters, pelagic species are subject to (on average) warmer temperatures compared to benthic species. These asymmetries in temperature across mesohabitats may play an important role together with resource productivity in the stability of multichannel food webs by influencing the energy turnover rate and energy transfer to higher trophic positions. For example, future

warming may disrupt the survival of larger species in the benthic habitat. Another interesting avenue of potentially interesting future research lies in the exploration of the consequences of different size and temperature scaling of key vital rates such as energy intake and expenditure. In my thesis, I assumed that they have the same allometric slope. Deviating from this assumption can disrupt the competitive abilities of individuals during ontogeny, which can in turn affect how population dynamics and species interactions respond to changes in temperature or habitat productivity.

In the absence of detailed data about life histories for many species, bioenergetic models are needed to investigate unexplored complex phenomena. One of the current challenges is to understand how community diversity, structure and stability respond to additional stressors such as microplastics, pesticides and pharmaceutical molecules. Accumulation of these pollutants in the highest trophic position, accelerated by warming, could disrupt the community through cascading effects. Likewise, the interactions between the downsizing effect (caused by size-selective harvesting of the largest species and individuals) and warming-induced species reduction is currently unexplored, with unknown consequences for life history evolution, population dynamics and community change. One could expect that the loss of top predators and largest size classes in the system can make the community more prone to collapses, including those triggered in multichannel food webs due to the loss of highest mobile species.

The complex nature of human impacts on current ecosystems, together with the rich behaviour observed in food web models of freshwater communities, means that modelling of food webs will continue to provide important insight into the functioning of contemporary freshwater ecosystems.

~ Curriculum vitae ~

~ Author's curriculum vitae ~

Name	M.Sc. Samuel Dijoux
Date of Birth	July 11th, 1990
Nationality	French
Address	Žižkova tř. 223/9, 370 01 České Budějovice, Czech Republic
Tel	+420 774 257 941
E-mail:	dijoux.samuel@gmail.com

Education

2016-present

Ph.D. in Ecosystem Biology: University of South Bohemia in České Budějovice, Faculty of Science
Stability and dynamics of size-structured freshwater communities along environmental gradients. (Supervisor: David Boukal)

2013-2015

M.Sc. in Ecology, *Modelling of Ecological Systems*
University of Paul Sabatier in Toulouse, Faculty of Science

2011-2013

B.Sc. in Biology, *Biology of organisms, populations and ecosystems,* University of Paul Sabatier in Toulouse, Faculty of Science

Work experience

2020-present	Strategies of freshwater organisms for a warming world: from individual to community perspectives (GAČR 21-29169S). Position: technician
2017-2019	Freshwater ectotherms under climate change: the role of phenotypic plasticity in life histories and trophic interactions (GAČR 17-15480S). Position: technician

Research Fellowships

2019	IRSTEA, Dr. A. Sentis (Aix-en-Provence) (1 months).
2018-2019	Arctic University of Norway (Tromsø, Norway), Prof. R. Primicerio (2 months).

Undergraduate Research Internships

2015	Exploitative and apparent competition in physiologically structured populations. (Supervisor: David Boukal, 6 months)
2014	Differential reproduction and population dynamics in a human Pyrenean population. (Supervisor: Morgane Gibert, 4 months)
2013	Influences of Propranolol on mice in a Fear conditioning context (Supervisor: Pascal Roullet, 1 month)
2012-2013	Valorization of the Rival's and Fournier's Herbarium (Supervisor: Valérie Trichon, 4 months)
2012	Cartography and evaluation of the aquatic macrophyte in the Tarn and Garonne streams (supervisor: Arnaud Elger, 7 weeks)

Author details on Scopus

Number of publications in peer-review journals with IF:	2
Total citations/self-citation excluded:	14/13
h-index:	2

Online presence

ORCID 0000-0002-8086-7696

Google Scholar
https://scholar.google.com/citations?user=VmDlsZEAAAAJ&hl=en

Researchgate
https://www.researchgate.net/profile/Samuel-Dijoux

Github
https://github.com/Samuel-Dijoux

Peer-reviewed publication with impact factor (IF)

Published

Brown, Joel; Mennicken, Sophie; Massante, Jhonny; **Dijoux, Samuel;** Telea, Alexandrea; Benedek, Ana; Götzenberger, Lars; Májeková, Maria; Leps, Jan; Šmilauer, Petr; Hrček, Jan; de Bello, Francesco (2019). A novel method to predict dark diversity using unconstrained ordination analysis. *Journal of Vegetation Science* 30 : 610-619. DOI: 10.1111/jvs.12757.

Dijoux, Samuel; and Boukal, David. S. (2021), Community structure and collapses in multichannel food webs: Role of consumer body sizes and mesohabitat productivities. *Ecology Letters*, 24: 1607-1618. DOI: 10.1111/ele.13772.

Submitted or in preparation

Dijoux, Samuel; Pichon, Noémie A.; Sentis, Arnaud; Boukal David S. (2023), Body size and trophic position determine the outcomes of species invasions along temperature and productivity gradients. Manuscript submitted to *Ecology Letters*.

Dijoux, Samuel; Smalås, Aslak; Primicerio, Raul; Boukal, David S. (2023), Temperature-dependent consumer growth rates, rather than temperature-size rule, determine the propensity for catastrophic collapses of top predators at suboptimal temperatures. Manuscript in preparation.

International conferences

Invited talk

2022 **Dijoux, Samuel**; Boukal, David S. Community structure and collapses in multichannel food web.
(8th ČSPE conference, Brno, Czechia, 7-9/9/2022)
(Invited talk for the Vojtěch Jarošík 2021 student competition)

Dijoux, Samuel; Boukal, David S. Community structure and collapses in multichannel food web.
(36th Congress of the International Society of Limnology, Berlin, Germany, 7-10/08/2022) (Plenary student speaker for the winning award of the Brian Moss 2022 student competition)

Conference talk

2022 Boukal, David S.; **Dijoux, Samuel**; Pichon, Noémie A.; Sentis, Arnaud. Global change and species invasions in simple communities: a modelling study.
(8th ČSPE conference, Brno, Czechia, 7-9/9/2022)

2021 **Dijoux, Samuel**; Pichon, Noémie A.; Sentis, Arnaud; Boukal, David. Invasions in simple food webs along environmental and size structure gradients: insights on

exploitative competition. (Virtual SMB 2021 Annual meeting, 13-17/06/2021)

2019 **Dijoux, Samuel**; Pichon, Noémie; Sentis, Arnaud; Boukal, David. Species invasions and food web structure under climate changes. (*BES Annual meeting*, Belfast, Northern Ireland, 13-16/12/2019)

Dijoux, Samuel; Boukal, David. Relative body size and habitat productivities jointly drive trophic energetic flows: insights on a size- dependent freshwater food web and apparent competition.
(*6th FBFW*, Tihany, Hungary, 11/04/2019)

Conference poster

2021 **Dijoux, Samuel**; Boukal, David. 'Symmetry in asymmetries' of body sizes and productivities drives consumer coexistence in multi-channel food webs. (Virtual SMB 2021 Annual meeting, 13-17/06/2021)

2017 **Dijoux, Samuel**; Boukal, David. Relative consumer body size and habitat productivities jointly drive apparent competition in a tri-trophic food web.
(*BES Annual meeting*, Ghent, Belgium, 11-14/12/2017)

Dijoux, Samuel; Boukal, David. Influence of body size and habitat productivities on trophic energetic flows: insights on a size-dependent freshwater food web and apparent competition. (*5th FBFW*, České Budějovice, Czechia, 9-13/04/2017)

International workshops

Presentation

2020 **Dijoux, Samuel**. Aquatic Insect Lab: Unravelling the responses of aquatic macroinvertebrates facing multiple

	stressors from local to global scales (*3rd Virtual Career day*, webinar)
2019	**Dijoux, Samuel**. Size-structured models of food web modules, first insights. (*Freshwater food web Workshop*, České Budějovice, Czechia)
2017	**Dijoux, Samuel**. Food web modelling workshop. Tips to read, understand and build simple food web population dynamics models. (*5th FBFW*, České Budějovice, Czechia)

Participation

2021	BC Introductory mentoring workshop (České Budějovice, Czechia)
2016	Climefish workshop: Modelling of freshwater fisheries (České Budějovice, Czechia)
	CERES ENS|PNL Summer School: Modelling Environmental Resilience (Paris, France)

Organization

Organizing member of the *5th FreshBlood for FreshWater* conference (České Budějovice, Czechia, 2017)

International seminars

2019	**Dijoux, Samuel**. Structure of freshwater food webs under global changes: insights from two modelling approaches. (*IRSTEA*, Aix-en-Provence, France)
2018	**Dijoux, Samuel**. Trait-based modelling in freshwater ecosystems. (*Arctic University of Norway*, Tromsø)
2017-2021	**Dijoux, Samuel**. Trait-based models of the dynamics of invertebrate communities in freshwaters (Annual KBE Ph.D. students seminar)

Awards

The following mentioned awards have been attributed for the publication: **Dijoux S.,** Boukal D. (2021): Community structure and collapses in multichannel food webs: Role of consumer body sizes and mesohabitat productivities. *Ecology Letters*, 24: 1607-1618.

2022	1st rank winner of the Brian Moss Student competition 2022, awarded by the International Limnological Society.
	3rd rank winner of the Vojtěch Jarošík Award for the 2021 competition for an excellent student publication in ecology, awarded by the Czech Society of Ecology.
2021	Award for the best fully published first author publication of the PhD student in 2021, awarded by the Director of the Entomology Institute, Czech Academy of Science.

e-mail address: dijoux.samuel@gmail.com

Stability and dynamics of size-structured freshwater communities along environmental gradients
Ph.D. Thesis Series, 2023, No. 4.

Printed in the Czech Republic by Typodesign
Edition of 30 copies

University of South Bohemia in České Budějovice
Faculty of Science
Branišovská 1760
CZ-37005 České Budějovice, Czech Republic

Phone: +420 387 776 201
www.prf.jcu.cz, email: sekret-fpr@prf.jcu.cz